UiT The Arctic University of Norway

Faculty of Health Sciences, Department of Clinical Medicine

Circle of Willis variants and cerebrovascular health:

Representations, prevalences, functions and related consequences

Incomplete anatomy and changes to flow appear to induce more unfavourable health outcomes

Lars Bakke Hindenes

A dissertation for the degree of Philosophiae Doctor - July 2021

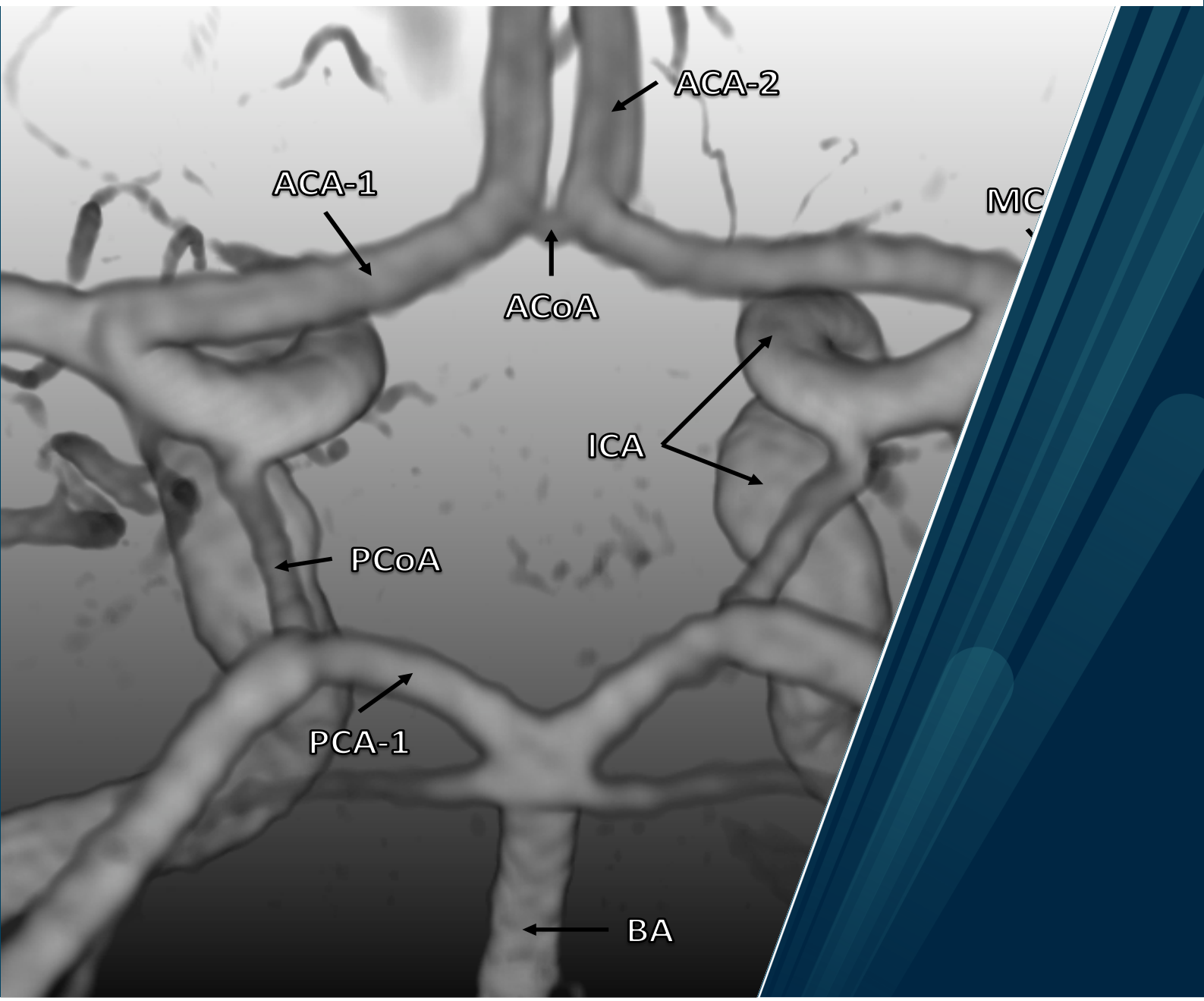

Table of Contents

List of Figures

List of Tables

Acknowledgements

First and foremost, I would like to thank my closest family and especially my mother for the support, patience and understanding for the duration of this work. Without her support I would likely never have finished this degree due to financial circumstances induced by a "neat" cocktail of a pandemic, policies and national labour laws.

Second, I would like to thank my primary supervisor and principal investigator of this project for making this project possible by, among many other things, providing invaluable feedback on the work with the original research and finishing this thesis.

Third, I would like to thank my co-authors of our articles for providing the necessary algorithmic, medical and clinical insight and feedback.

List of papers

Paper I: Hindenes, L.B., Håberg, A.K., Johnsen, L.H., Mathiesen, E.B., Robben, D., Vangberg, T.R. Variations in the Circle of Willis in a large population sample using 3D TOF angiography: The Tromsø Study. *PLoS ONE*, 2020;15(11):e0241373.

Paper II: Hindenes, L.B., Håberg, A.K., Johnsen, L.H., Mathiesen, E.B., Vangberg, T.R. An incomplete Circle of Willis is not a risk factor for white matter hyperintensities: The Tromsø Study. *Journal of the Neurological Sciences*, 2021;420:117268.

Paper III: Hindenes, L.B., Ingebrigtsen, T, Isaksen, J.G., Håberg, A.K., Johnsen, L.H., Herder, M., Mathiesen, E.B., Vangberg, T.R. Incomplete Circle of Willis variants associated with increased odds of intracranial aneurysms in a cross-sectional population-based study: The Tromsø study. Submitted as a manuscript to be published.

List of abbreviations

CoW = Circle of Willis

WMH = white matter hyperintensities

DWMH = deep white matter hyperintensities

PWMH = periventricular white matter hyperintensities

IA = intracranial aneurysm

ACA = anterior cerebral artery

ACoA = anterior communicating artery

PCoA = posterior communicating artery

PCA = posterior cerebral artery

MCA = middle cerebral artery

ICA = internal carotid artery

BA = basilar artery

MRI = magnetic resonance imaging

TOF = time-of-flight

RF = radio frequency

TE = time to echo

TR = time to repeat

TI = inversion time

FLASH = fast low angle shot

GRAPPA = generalised autocalibrating partially parallel acquisition

FOV = field of view

CT = computed tomography

Abstract

Background: The Circle of Willis (CoW) is a circular structure of arteries in which most of the blood flowing to our brains pass through. The structure has primarily been regarded as important for its ability to redistribute blood flow in case of acute arterial occlusion, but may also have a role in dampening the pressure gradient in cerebral blood flow. The CoW anatomy also varies considerably, where its segments can be missing or thinner than normal, and therefore appears as a risk factor for cerebrovascular health.

Objectives: To describe and report (**I**) the observed CoW variants and anatomy, and also examine the incomplete CoW variants' associations to (**II**) white matter hyperintensities (WMH) and (**III**) saccular intracranial aneurysms (IA) compared to the complete CoW variant.

Methods: Participants were invited from The Seventh Tromsø Study of which 1878 underwent magnetic resonance imaging. From the scans, CoW variants were semi-automatically classified. Likewise, WMH was automatically segmented and IAs were manually ascertained by radiologists.

Results: The complete CoW is not very prevalent in participants older than 40 years old, and our findings suggest that the CoW becomes more incomplete with older age. Furthermore, incomplete CoW variants were not associated with increased WMH volume compared to the complete CoW variant. Incomplete CoW variants were associated increased odds of IA presence compared to the complete CoW variant.

Conclusion: The results indicate that a complete CoW variant is not common in adults and elderly, which may have unfortunate consequences when incomplete CoW variants are associated with increased prevalence of IAs. Fortunately, not all results imply unfavourable

outcomes, but further study of the CoW changes and possible effects of the variants over time are required.

1 Introduction

The overarching goal of this thesis was to determine whether an incomplete Circle of Willis (CoW) might be detrimental for brain health in the general population. To achieve this, we first needed to establish prevalence estimates of incomplete CoW variants. We then used these estimates to examine whether incomplete CoW variants were associated with two adverse health outcomes, white matter hyperintensities (WMH) and intracranial aneurysms (IA).

1.1 The Circle of Willis

The CoW is a roughly circular structure consisting of several arteries located right beneath the brain. The structure has its name from Thomas Willis, born in England 1621, who was the first to provide a complete description of the CoW and also indicated an understanding of the CoW's function in a clinical context (Molnár, 2021; Uston, 2005). Since before Willis' days and until today, studies have and continue to examine the CoW's morphology and how it may affect the brain's health.

Usually, the three main arteries that provides most of the blood flow to the brain, anastomose (i.e. join) forming the CoW. The blood flowing through the CoW is then distributed via arteries branching from the CoW to different regions of the brain, and the CoW is therefore regarded as a central component of the brain's cerebrovasculature. Similar blood distributive structures as the CoW in humans are also found in other animals, e.g. dogs, sheep, goats and rabbits (Kapoor et al., 2003), and the general CoW anatomy is seen across multiple classes of animals, including fish, reptiles and birds (Fenrich et al., 2021). However, this thesis will only concern the human CoW anatomy.

Interestingly, the CoW exhibits considerable variation in its anatomy across individuals. The so called “textbook” or complete CoW anatomy is visualised in **Figure 1**. Despite naming it as such, the complete CoW variant can be quite rare, with a reported prevalence as low as 7% (Wijesinghe et al., 2020) and usually not much higher than 45% (Forgo et al., 2018) depending on the type of study and sample demographic. The arteries that constitutes the CoW are the anterior cerebral artery (ACA), anterior communicating artery (ACoA), posterior communicating artery (PCoA) and the posterior cerebral artery (PCA) (**Figure 1**). More specifically, parts of the internal carotid arteries (ICA) are also part of the circle, and technically only the proximal portion of the ACA and PCA is part of circle since they have distal parts that extend beyond the circular structure of the CoW. At last, the end of the basilar artery (BA), that splits into the two proximal PCAs, is also effectively part of the circular arrangement of segments.

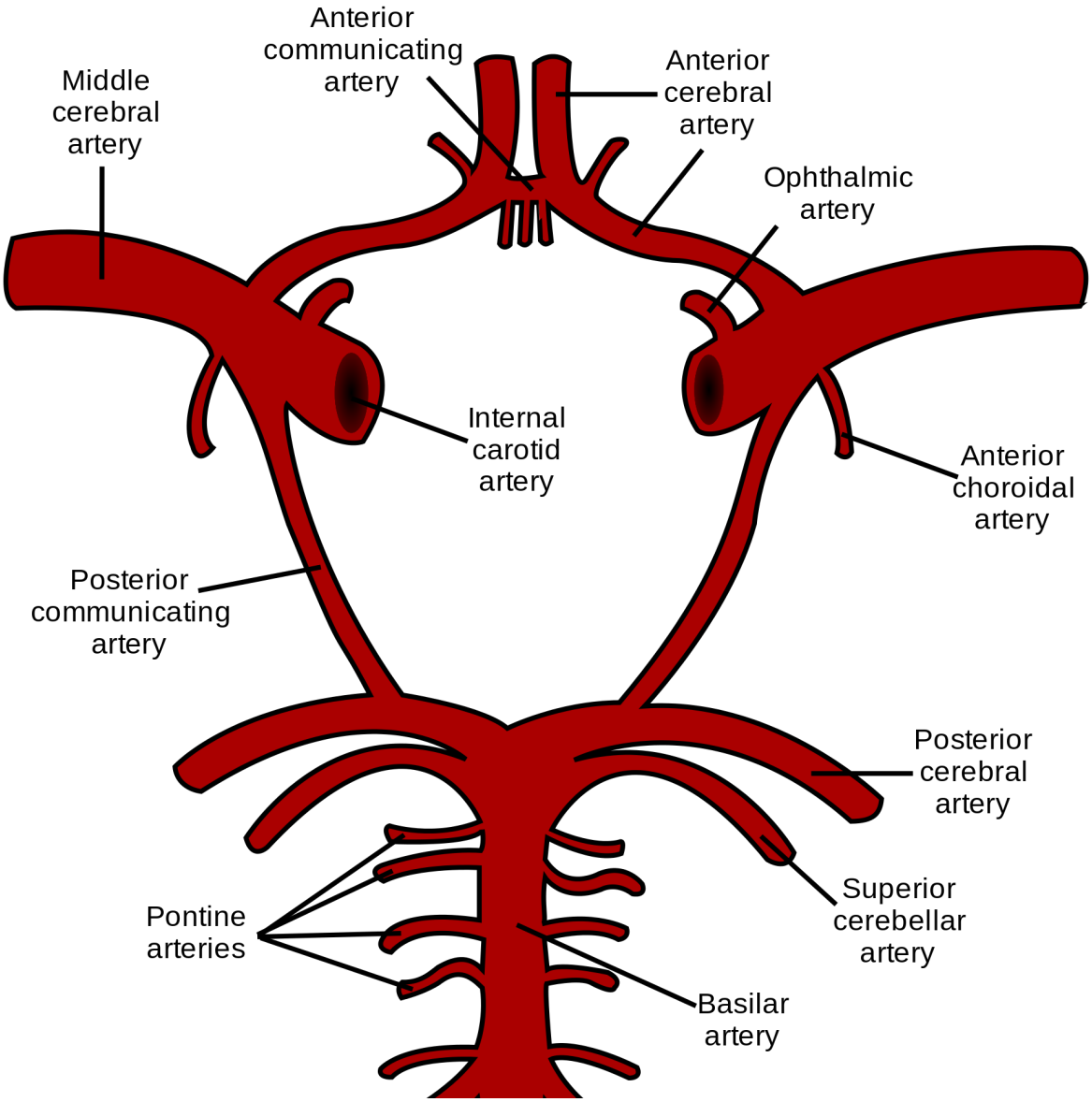

Figure 1. *The «textbook» or complete Circle of Willis anatomy. (Public domain image from Wikipedia).*

1.1.1 What is the purpose of the Circle of Willis?

The traditional assumption is that the CoW is important for its ability to provide collateral flow (Fenrich et al., 2021), i.e. the capacity or ability to compensate for reduced flow in a feeding artery via redistribution of blood throughout the circle. However, recent studies have argued that the collateral flow function is not the only function or consequence of the CoW (Fenrich et al., 2021; Vrselja et al., 2014). One study argues that the CoW acts as a pressure dissipating system protecting the cerebrovascular system from haemodynamic stress (Vrselja

et al., 2014). Furthermore, as argued in Fenrich et al. (Fenrich et al., 2021), the pressure dissipation system function by Vrselja et al. (Vrselja et al., 2014) needs experimental validation. Still, they both agree that the traditional assumption of the CoW anatomy is not satisfactory in the context of evolutionary pressure (Fenrich et al., 2021; Vrselja et al., 2014). For example, to paraphrase them both, it is dubious to assume that the evolution of the CoW anatomy has any foresight to accommodate modern diseases such as atherosclerosis that usually becomes prevalent in later stages of human life after the point of procreation.

However, one cannot dismiss the importance of collateral flow in the CoW, because it is useful in determining risk of ischemia in the brain. Still, considering the additional interpretation, it is not unlikely that the CoW has at least two different, but not necessarily mutually exclusive, functions or consequences that affect the brains' cerebrovascular health.

1.1.2 Anatomical variations in the Circle of Willis

As mentioned, the CoW anatomy varies considerably, and it is not unusual for a study to find more than 25 unique CoW variants (Coulier, 2021; Qiu et al., 2015). Variations in the CoW anatomy can include, but is not limited to, hypoplastic or missing segments, bifurcation or fenestration of arteries, presence or persistence of prenatal arteries, or growth of additional arteries that the majority of CoW variants do not have. Furthermore, length, tortuosity and diameter of the same arteries also vary within an individual and between individuals (**Figure 2**), and the average diameter of arteries in the CoW is also different (El-Barhoun et al., 2009; Krabbe-Hartkamp et al., 1998). Dimmick et al. (Dimmick and Faulder, 2009) describes a multitude of CoW variations, exemplifying the aforementioned variations in the CoW.

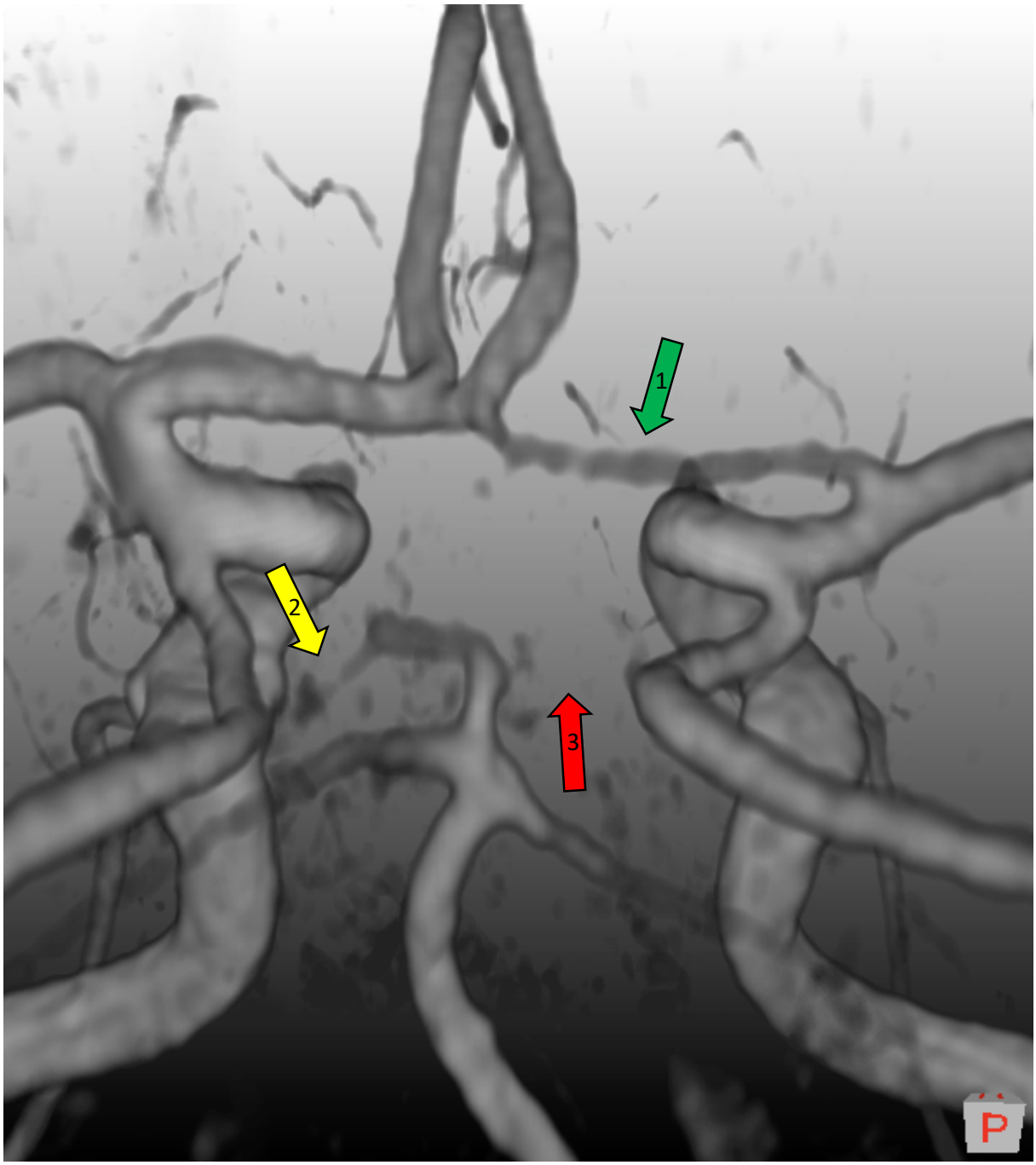

Figure 2. *Example of an incomplete and asymmetric Circle of Willis variant. According to our classification rules presented later: 1 = plastic anterior cerebral artery, 2 = hypoplastic posterior cerebral artery, 3 = not visible or missing posterior cerebral artery. Figure reused from* ***Paper I****.*

Some studies also describe many ACoA fenestrations (Ozaki et al., 1977; Qiu et al., 2015) which are more easily observed during autopsies than in medical images, see **Figure 3** for examples.

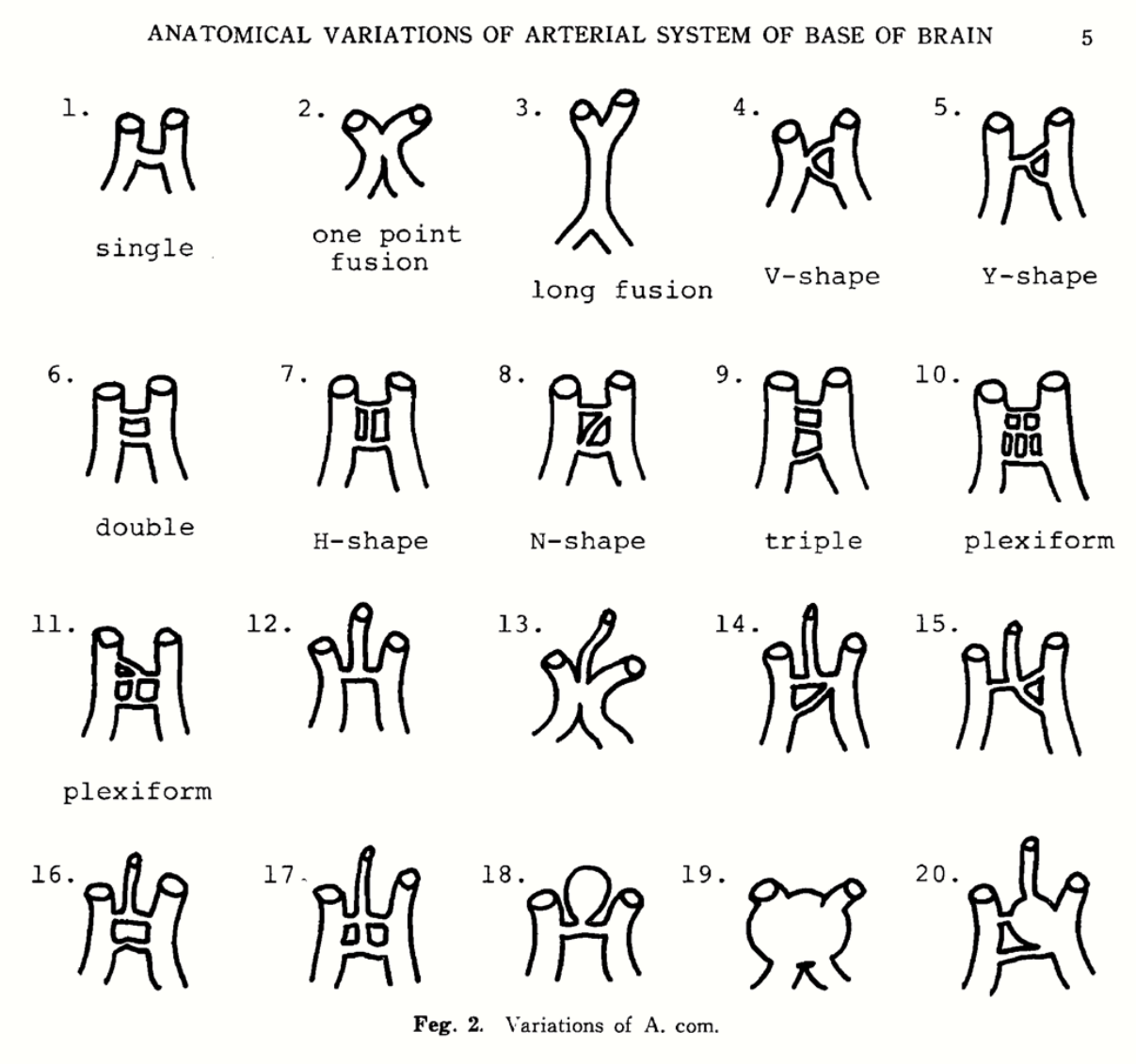

Feg. 2. Variations of A. com.

Figure 3. *Illustration of multiple anterior communicating artery (i.e. A. com. or ACoA) variations from 153 autopsy cases by Ozaki et al.* (Ozaki et al., 1977). *Paper available through Kyoto University Research Information Repository (KURENAI), and original journal is presumably discontinued after no matches with the journal name "Nihon Geka Hokan" in PubMed after the year 2000.*

1.1.3 Classifying the anatomical variation

Considering the anatomical variability, classifying the CoW anatomy appears as a daunting task. Fortunately, the classification can be simplified. However, due to such varying CoW anatomy, studies have developed multiple different practices for classifying and reporting the CoW anatomy which are far from uniform. Usually the classification consist of determining

whether arteries are present or absent using either a diameter threshold (Krabbe-Hartkamp et al., 1998) or relative comparisons of artery diameters (Horikoshi et al., 2002; Qiu et al., 2015). It is also common to not distinguishing between an artery defined either as hypoplastic or absent, and sometimes studies choose to omit classification of some arteries (Horikoshi et al., 2002). Considering multiple variants of an artery as one is also done due to the large number of unique intra segment variations (**Figure 3**). Furthermore, merging multiple different arteries in the CoW to one group category describing larger parts of the CoW anatomy is also possible (van der Grond et al., 2004; van Seeters et al., 2015).

Even though exact comparison of the reported CoW variants is difficult due to varying classifications, it is still possible to find some common ground between studies. Unfortunately, additional layers of heterogeneity and biases are introduced when studies use different ways of studying the CoW, which we will return to shortly. One possible solution capable of eliminating part of the heterogeneity with previous studies is to use advanced automatic artery segmentation and classification software (Robben et al., 2016, 2013), because such software have inherent flexibility from using continuous data. Access to such software would be immensely helpful, as classifying the CoW anatomy quickly becomes very work intensive even though only a simple binary classification is used. There is also the issue of inter- and intra-rater biases when manually classifying the CoW anatomy, which would also become less of a problem when using software that automates more of the classification process. Therefore, employing such automated software whenever possible for such tedious and time-expensive tasks are overall the preferred or viable option, at least in studies with larger sets of data.

1.2 Ways of studying the Circle of Willis

In order to ascertain the CoW anatomy, one first needs to observe and measure the segments. The three most common methods for doing this is via magnetic resonance imaging (MRI), computed tomography (CT), or post mortem dissections. The different methods have specific strengths, weaknesses and use cases.

1.2.1 Magnetic resonance imaging

There are three MRI methods commonly used for arterial imaging (see Appendix A for MRI fundamentals). These are time-of-flight (TOF) imaging, contrast-based magnetic resonance angiography (MRA) and 4D flow MRI (Dunås et al., 2017). All these techniques have the benefit of being able to image the CoW anatomy in vivo. However, due to these techniques' reliance on blood flow, they cannot capture the vessel wall and consequently underestimate the artery diameter compared to other methods (Krabbe-Hartkamp et al., 1998), making comparison with some studies more difficult. This reliance on flow may also make hypoplastic arteries appear as invisible in low flow or net zero flow cases. Although contrast-based MRA may be more robust to low-flow conditions (El-Barhoun et al., 2009), the contrast agent introduces an invasive element that is problematic in many research applications. Among the other non-invasive techniques, TOF specifically also has another limitation due to reliance on unsaturated blood flow to produce signals. Loss of signals will then occur when the flow is parallel to the imaging plane. Oppositely, flow that are perpendicular to the image slices will have the strongest signals.

1.2.2 Computed tomography imaging

Compared to MR, CT is able to capture the vessel wall (Klimek-Piotrowska et al., 2013; Li et al., 2011) and can be used on individuals with contraindications for MRI; e.g. ferromagnetic

implants. However, CT is inherently invasive due to the need of a contrast agent for angiography and the use of ionising radiation (i.e. X-ray), which also makes CT unfit for some studies due to ethical concerns.

1.2.3 Dissection

Dissection is considered the gold standard for studying the CoW, because it is currently the only way to derive exact measures of the CoW anatomy. However, a considerable weakness with this method is that repeated measurements over time are impossible. Furthermore, dissection studies may introduce age or disease biases. Studying the CoW anatomy via dissection is also more laborious than other methods, since the specimens have to be handled physically and not just virtually (Eftekhar et al., 2006; Iqbal, 2013; Kapoor et al., 2008).

1.3 Possible adverse health consequences from incomplete Circle of Willis anatomy?

Can an incomplete CoW have adverse health consequences? This is not inconceivable as many incomplete CoW variants have poor collateral function. Indeed, patient studies show that incomplete CoW variants are associated with hyperintense spots in the brain's white matter, so called WMH (Chuang et al., 2011; Ryan et al., 2015; Saba et al., 2015), which is further associated with adverse outcomes (Wardlaw et al., 2015). Incomplete CoW variants are also related to future ischemic strokes (van Seeters et al., 2015) and associated with elevated blood pressure (Warnert et al., 2016). Furthermore, parts of the vascular anatomy in CoW variants are also associated with elevated haemodynamic stress and altered flow conditions (Alnaes et al., 2007; Ingebrigtsen et al., 2004; Nixon et al., 2010), which may result in additional attrition for the cerebrovascular system; e.g. aneurysm development or atherosclerosis (Pascalau et al., 2018). Lastly, flow territories in the brain are shown to be

different for different CoW variations (van Laar et al., 2006), complicating the process of understanding adverse outcomes potentially related to poor collateral flow.

In this thesis however, I will focus on two possible adverse health outcomes of incomplete CoW variants, namely WMH and IA. The former will primarily reflect on the ability of the CoW anatomy to provide sufficient blood supply to the brain, while the latter reflects on how the CoW anatomy may alter cerebral haemodynamic; e.g. blood flow and subsequent distribution of stress.

1.3.1 White matter hyperintensities

WMH are diagnosed with MRI or CT, although MRI is the preferred modality. It is called WMH due to how WMH manifests in the white matter in the brain as hyperintense regions in T2-weighted MR images (Wardlaw et al., 2015). Furthermore, WMH is referred to as an intermediary marker of cerebral small vessel disease that is detrimental to cerebrovascular health. What exactly causes WMH and how WMH affects brain functions are still not yet fully uncovered (Wardlaw et al., 2015). However, a histology study reports signs of hypoxia in WMH (Fernando et al., 2006) suggesting that hypoperfusion could be a trigger. This is also supported by the tendency of WMH to occur in watershed regions of cerebral white matter. Excessive amounts of WMH are shown to be associated with cognitive decline (Murray et al., 2010; Silbert et al., 2008), vascular dementia (Barber et al., 1999; Román et al., 2002) and Alzheimer's disease (Barber et al., 1999; Provenzano et al., 2013).

Currently, the amount of WMH is best explained by older age (de Leeuw et al., 2001; Nyquist et al., 2015; van Dijk et al., 2008) and to a lesser extent by other risk factors such as hypertension, smoking, and diabetes (Vangberg et al., 2019; Wardlaw et al., 2014). In fact, a majority of people older than 60 years has WMH (de Leeuw et al., 2001), but some individuals may still have minimal or no WMH despite being much older than 60 years old.

Furthermore, WMH can be partitioned into regions that may be differently associated with risk factors (Griffanti et al., 2018; ten Dam et al., 2007) and genetics (Armstrong et al., 2020). Examples of commonly used regions are deep WMH (DWMH) farther from the ventricles in the brain, and periventricular WMH (PWMH) closer to or bordering the ventricles (Griffanti et al., 2018). This grouping is based on evidence that they have different aetiology, but similar to the CoW classification, it has been criticised as arbitrary since there is no single definite way to separate DWMH and PWMH among WMH (Griffanti et al., 2018).

1.3.2 Circle of Willis and white matter hyperintensities

Studies on the relationship between the CoW anatomy and WMH prevalence report deviating results. Most studies however, show that incomplete CoW variants are associated with increased WMH volume (Chuang et al., 2011; Ye et al., 2019) or higher Fazekas scoring of WMH (Ryan et al., 2015). Also, a higher number of missing arteries in the CoW is associated with increasing WMH volume (Saba et al., 2017, 2015). Somewhat confusingly it has also been reported that an incomplete posterior variant is associated with decreased WMH volume (van der Grond et al., 2004). There are also studies that do not find any association between incomplete CoW variants and WMH (Del Brutto and Lama, 2015; Li et al., 2015).

Most of the cited studies, except Del Brutto and Lama (Del Brutto and Lama, 2015), were performed in patients, most with either atherosclerosis or carotid artery stenosis, such that it is unclear to what extent these findings apply to a broader population. Despite some diverging results, incomplete CoW anatomy appear to be associated with increased WMH in patients. However, in a population of generally healthy individuals it is unclear if an incomplete CoW may pose a risk for WMH.

1.3.3 Saccular intracranial aneurysms

Incomplete CoW variants are also associated with presence of IA, which may lead to lethal subarachnoid haemorrhages (Brisman et al., 2006). In general, aneurysms can take more than one form, but here we only consider saccular IA since they are more common and with a unique pathophysiology. In a general population the prevalence of saccular IA is around 1.8% - 7.0% (Cras et al., 2020; Li et al., 2013; Müller et al., 2013; Vernooij et al., 2007; Vlak et al., 2011). According to a review study, 50% - 80% of IAs do not rupture (Brisman et al., 2006). However, those that do rupture have a median fatality rate at 44.4%, and up to 20% cannot live independently afterwards (Nieuwkamp et al., 2009).

Although not everything about the development of IA is fully understood, modifiable factors (e.g. smoking and hypertension) (Cras et al., 2020; Songsaeng et al., 2010), and vascular features (e.g. suboptimal bifurcation angles) or haemodynamic stress (Alnaes et al., 2007; Ingebrigtsen et al., 2004; Nixon et al., 2010) are IA risk factors. IAs also tend to develop more often at some locations than others (e.g. bifurcations) (Brisman et al., 2006; Nixon et al., 2010). The primary cause of IA development is the continued weakening of the arterial wall due to haemodynamic forces, which gradually results in development of saccular IA (Brisman et al., 2006). Vascular features, such as straighter in-flow angles into the aneurysm (Skodvin et al., 2019), along with smoking and hypertension (Isaksen et al., 2002; Lindekleiv et al., 2012) also increase risk of IA rupture, indicating that a better understanding of risk factors for presence or development of IA may also help preventing IA rupture.

1.3.4 Circle of Willis anatomy and intracranial aneurysms

Among known risk factors, vascular features and haemodynamic stress are aspects which may be affected by the CoW anatomy. Two previous simulation studies in the haemodynamic of the CoW support this by showing high wall shear stress at frequent IA locations in the CoW

(Alnaes et al., 2007) and changes in direction and magnitude of blood flow when only one CoW segment from complete CoW variants in turn are coded as missing (Mukherjee et al., 2018).

To my knowledge, only two studies have explicitly examined the co-occurrence of incomplete CoW variants and presence of IA. These studies found an association between CoW anatomy and the location the IA (Horikoshi et al., 2002; Kayembe et al., 1984). Similar to the risk factors for IA rupture, such as smoking and hypertension (Isaksen et al., 2002; Lindekleiv et al., 2012), studies also report associations between incomplete CoW variants and IA rupture (Lazzaro et al., 2012; Stojanović et al., 2019). It therefore appears that incomplete CoW variants may be a risk factor for IA development as well as for rupture of IA.

1.4 Objectives and hypotheses

The overall objective in this thesis was to examine whether incomplete CoW variants might be associated with two adverse health outcomes, WMH and IA. Based on the literature, we hypothesised that incomplete CoW variants would be associated with increased WMH volumes and increased odds of IA prevalence. To explore these hypotheses, we first had to assess the anatomical variations in the CoW (**Paper I**) before we could pursue the two primary objectives:

1. In **Paper I**, the objective was to describe and report the different CoW variants and anatomy observed.
2. In **Paper II**, the objective was to examine whether incomplete CoW variants were associated with increased WMH volume compared to the complete CoW variants.

3. In **Paper III**, the objective was to examine whether incomplete CoW variants were associated with increased odds of IA presence compared to the complete CoW variants, or presence of IA at specific location.

2 Materials and methods

2.1 Study population and The Tromsø Study

The baseline population sample used in all three papers, described in **Paper I**, consisted of 1864 participants from a subset of The Seventh Tromsø Study (Njølstad et al., 2016). These 1864 participants all had the necessary scans to be eligible for inclusion in the three studies in this thesis.

The Seventh Tromsø Study is part of a larger initiative named The Tromsø Study. The Tromsø Study was started in 1974 (Jacobsen et al., 2012) in an attempt to address high cardiovascular mortality in Northern Norway. The Tromsø Study invites residents of Tromsø municipality to participate. From one or more visits, The Tromsø Study then collects a wide range of quantitative and qualitative questionnaire data from participants, which can be combined with more specific sub-studies that collect other types of data. The MR study in The Seventh Tromsø Study and the overarching project of this thesis is an example of such a sub-study in The Tromsø Study.

2.2 Magnetic resonance imaging protocols

Participants were scanned at the University Hospital North Norway with the same 3T Siemens Skyra MR scanner (Siemens Healthcare, Erlangen, Germany) equipped with a 64-channel head coil, but in 39 examinations a slightly larger 20-channel head coil had to be used to accommodate those participants' head. For all scan series, slice prescription was automatically aligned to a standardized brain atlas to ensure consistent slice prescription across examinations (van der Kouwe et al., 2005). The total scan time per participant for the scan protocol (**Table 1**) was 22 minutes.

Table 1. *Key parameters in the MRI protocol.*

MRI sequence	Image resolution (mm)[#]	Slice orientation	TR (ms)	TE (ms)	TI (ms)	Flip-angle	Slice thickness (mm)	FOV (mm)
T1w	1 x 1 x 1	Saggital	2300	4.21	996	9	1.0	256 x 256
FLAIR	1 x 1 x 1	Saggital	5000	388	1800	Var.	1.0	256 x 256
TOF	0.3 x 0.3 x 0.5	Axial	21	3.43	3.43	18	0.5	200 x 181
SWI	0.6 x 0.6 x 1.6	Axial	28	20	-	15	1.6	220 x 220

All imaging was performed on the same 3T Siemens Skyra MR scanner (Siemens Healthcare, Erlangen, Germany) equipped with a 64-channel head coil. T1w = T1 weighted, FLAIR = fluid-attenuated inversion recovery, TOF = time-of-flight, SWI = susceptibility weighted images, TR = repletion time, TE = echo time, TI = inversion time, FOV = field of view. # = left-right x posterior-anterior x feet-head.

2.2.1 T1w and FLAIR scans

T1-weighted (T1w) images were acquired with a 3D magnetization prepared rapid acquisition gradient-echo (MPRAGE) sequence. T2-weighted fluid-attenuated inversion recovery (FLAIR) images were acquired with a 3D turbo spin echo sequence with variable flip angle. The T1w and FLAIR scans were acquired sagittally with 1 mm isotropic resolution using a generalised autocalibrating partially parallel acquisition (GRAPPA) parallel imaging acceleration factor 2.

2.2.2 TOF scans

TOF angiography scans were acquired with a 3D transversal fast low angle shot (FLASH) sequence with flow compensation GRAPPA parallel imaging acceleration factor 3, and 7 slabs with 40 slices each. Reconstructed image resolution was 0.3 x 0.3 x 0.5 mm.

2.2.3 SWI scans

Susceptibility weighted images (SWI) were acquired transversally with a GRAPPA parallel imaging acceleration factor 3. Reconstructed image resolution was 0.6 x 0.6 x 1.6 mm. The SWI scans were not used in this thesis.

2.3 Imaging and representing the Circle of Willis

In this thesis we used the TOF magnetic resonance angiography images to study the CoW anatomy. Due to limitations with this technique, it is necessary to clarify aspects of the interpretation of the images and how it affected the CoW classification.

2.3.1 Suitable Circle of Willis representations

A substantial portion of the work in this thesis was put into creating, coding and defining suitable data representations of the CoW, which can then be used to classify the CoW anatomy with minimal loss of information (**Figure 4**). We looked at representations in the literature for inspiration, and in the end, we defined representations for **Paper I**, **Paper II** and **Paper III** that we deemed suitable.

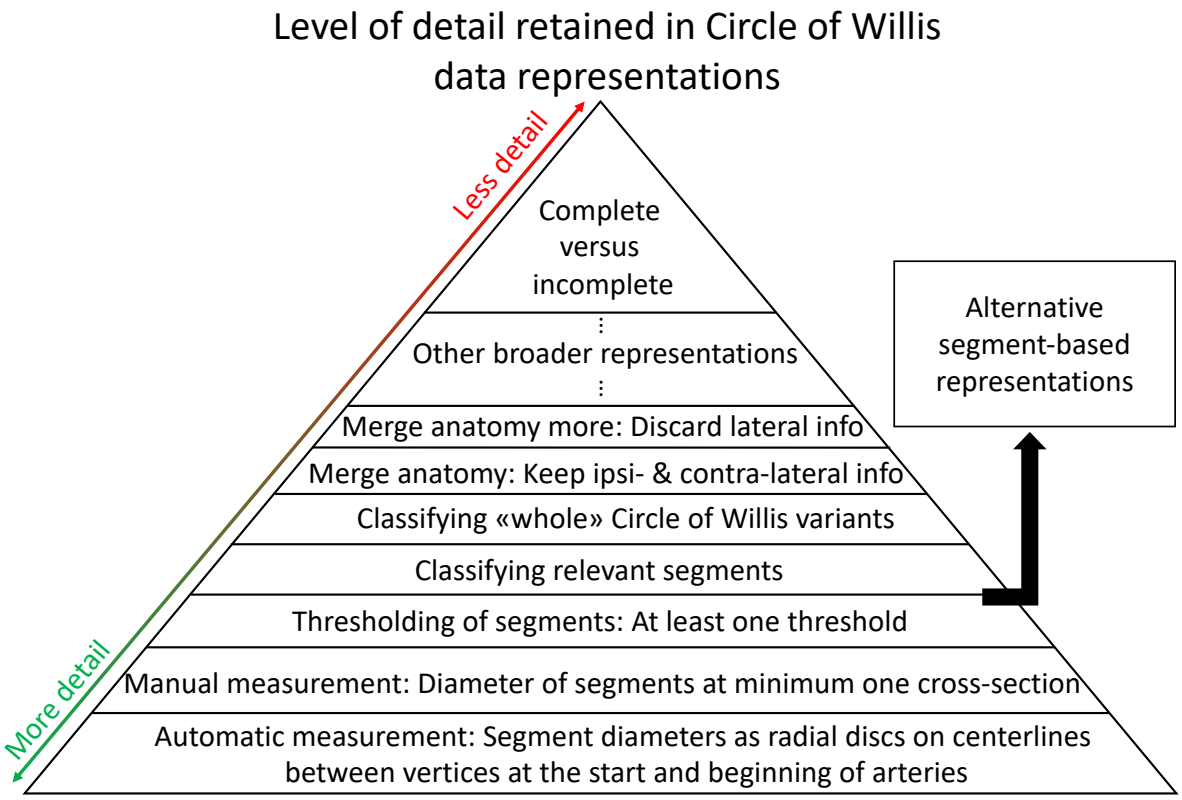

Figure 4. *Illustration of the hierarchical "detail retention" relationship of different stages of measuring, classifying and representing the Circle of Willis anatomy. More detail indicates that more information about the Circle of Willis is retained, while less detail indicates the opposite. Additional levels could also be added in between the presented levels where deemed informative.*

Initially, we wanted to represent the CoW anatomy in terms of edges and vertices in either directed or undirected graphs with radial discs along the edges or centrelines to continuously measure the diameters of segments in the CoW anatomy. This turned out to be too ambitious as the automatic classification software we attempted to use (Robben et al., 2016, 2013) did not sufficiently find the arteries in the CoW, even after training the software with in-house data.

After this attempt, we considered categorical CoW representations inspired by previous MRA studies on the CoW anatomy I found particularly relevant (Horikoshi et al., 2002; Krabbe-Hartkamp et al., 1998; Qiu et al., 2015). It was then natural to consider unique and whole CoW anatomies as a unique nominal category, as many, but not all, did before us. The

complete CoW variant with no missing segments was then considered the obvious reference variant, as the complete CoW have better collateral flow than incomplete variants. Even though this type of representation is often used, without further specifying which segments are classified as either present or hypoplastic and missing in this representation, the representation is inconsistently interpretable in terms of the level of detail embedded. Another weakness of such a representation is that it does not readily present information about how often subsets of segments across CoW variants are missing or hypoplastic. As such, we were compelled to define a more detailed representation underlying this holistic CoW representation.

To avoid occluding possibly crucial information, each segment considered in the CoW anatomy were then explicitly regarded as missing or present in our data. This required a diameter threshold to separate the missing and present segments from each other; which we will come back to. Additional practical applications of this segment-wise representation included the possibility to represent the CoW in terms of segment-by-segment dependent conditional probabilities. Similar practical use of the holistic representation was also possible, for instance in merging left- and right side or anterior and posterior parts of the CoW, to create more general or broader CoW representations.

2.3.2 Segments of interest and necessary simplifications

In the segment-wise representation, we chose a baseline of 12 segments that in most cases were relevant for describing the in- and out-flow of the CoW and collateral ability of the CoW anatomy (**Figure 5**). The first five artery segments, representing the in- and out flow were: The right and left ICA, BA, and the right and left middle cerebral artery (MCA). The last seven segments make up the CoW and were: The right and left proximal ACA, ACoA, right and left PCoA, and right and left proximal PCA.

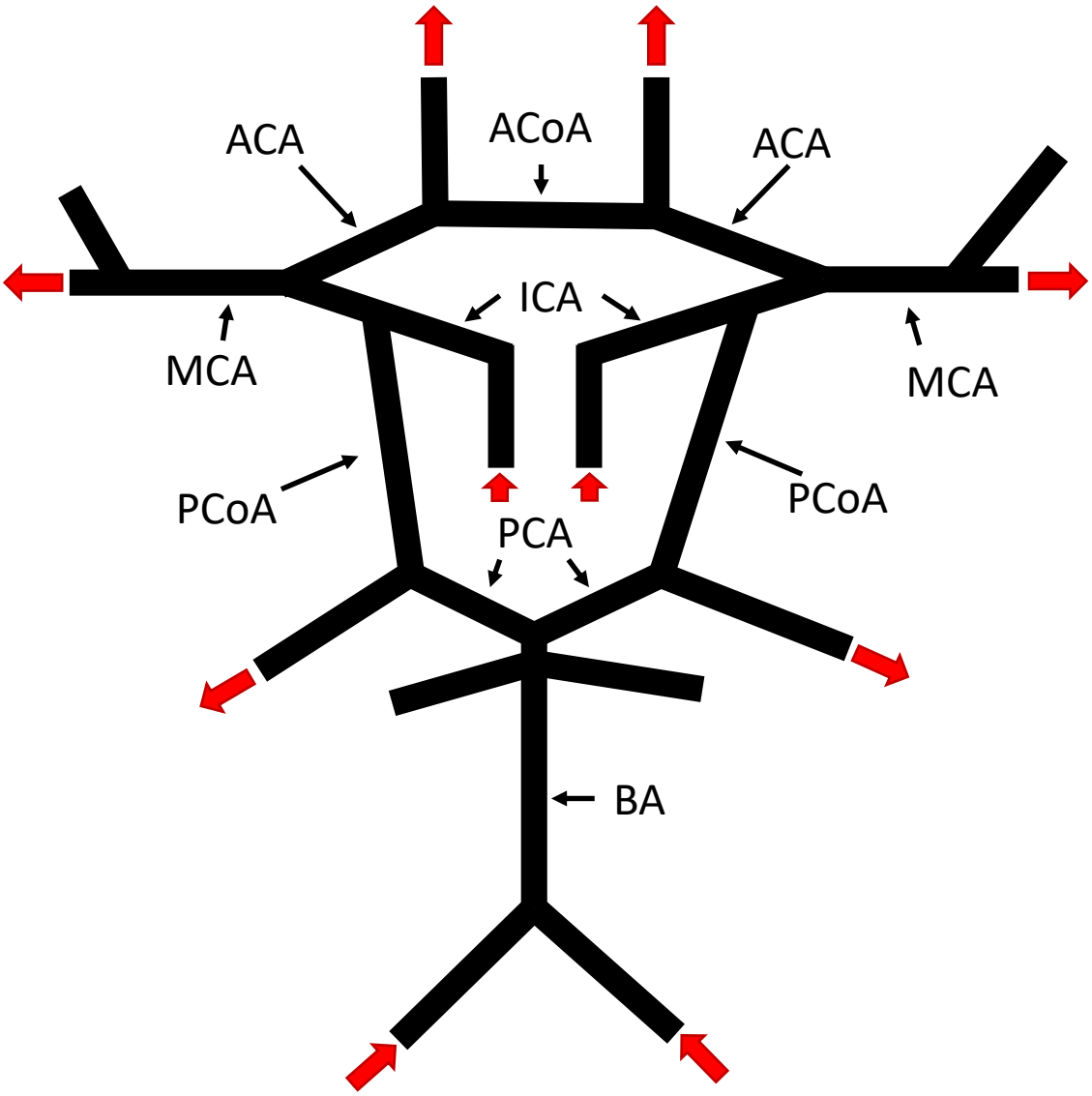

Figure 5. *Illustration of the 12 segments of interest in the Circle of Willis. Thick and red arrows denote the typical flow direction relative to the Circle of Willis. Abbreviations: ACA = proximal anterior cerebral artery, ACoA = anterior communicating artery, MCA = middle cerebral artery, ICA = internal carotid artery, PCoA = posterior communicating artery, PCA = posterior cerebral artery, BA = basilar artery.*

Despite including these 12 segments to represent essential aspects of the CoW anatomy, they were still insufficient to represent all possible variations in or near the CoW. Besides the 12 segments there are additional artery segments which did not make it into our representations, because they were too many and also too rare to warrant inclusion in quantitative studies that initially focused on the collateral ability of the CoW. Some of these extremely rare segments (Dimmick and Faulder, 2009; Hakim et al., 2018) have poorly or ill-defined possible

consequences for the collateral flow in the CoW as they appear upstream or downstream of the circle, e.g. the persistent trigeminal artery. Furthermore, certain segments may develop substantially different from a single tubular segment, e.g. one or multiple fenestration in segments may occur. The problem with segment fenestration in imaging is that it affects the visibility of any segment for the worse. Specifically, fenestrated segments with small diameter may most likely be classified as missing, even though they could have been regarded as present if no fenestration was present; e.g. two segments with diameter around 0.5 mm each have less cross-sectional area for blood to flow through compared to one segment with 1 mm diameter. Simplifications, such as choosing the 12 segments, or rather general study design choices are therefore important to remember when studies discuss how CoW variants were classified and why certain CoW segments and their properties were considered included rather than those other segments or properties.

2.3.3 Classification of segments

Since we used discrete representations of the CoW we required at least one diameter threshold. To justify selecting a specific threshold, without only referring to previous studies where a 0.8 mm (El-Barhoun et al., 2009; Krabbe-Hartkamp et al., 1998) or a 1.0 mm (Eftekhar et al., 2006; Kapoor et al., 2008; Klimek-Piotrowska et al., 2016) threshold were often used, we need to establish what was clearly visible in our images.

Initial testing with a 0.8 mm diameter threshold revealed that segments with discernible diameters at around 0.8 mm were difficult to consistently differentiate from the background noise. However, with a 1.0 mm diameter threshold we were able to consistently differentiate segments from the background noise. As such, by using this 1.0 mm threshold we also eliminated some uncertainty in our classification. Another strength of using the 1.0 mm diameter criterion was how segment diameters measured as larger than or equal to 1.0 mm in

the 2D viewer consistently translated to continuously visible arteries in the 3D image viewer (**Figure 2**); i.e. where the 2D and 3D viewer were part of the software we used for classification. The last important criterion for classifying segments constituting the circle in the CoW as present and not absent, was making sure they were connected to the other arteries they "normally" would be connected with; similar to criterion number two by Kapoor et al. (Kapoor et al., 2008). The posterior CoW variant "(k)" in Qiu et al. is an excellent example of when this last criterion is important to enforce classification uniformity (**Figure 6**) (Qiu et al., 2015); i.e. no direct collateral pathway between ipsilateral ICA and proximal PCA imply an ipsilaterally missing PCoA. Using (1) the quantitative diameter criterion, (2) the qualitative continuity criterion and at last (3) making sure arteries actually fulfilled the circle properly, the CoW representations we have constructed should portray CoW anatomy, and also the collateral ability of the CoW, better than the previous literature based on non-contrast MRA techniques.

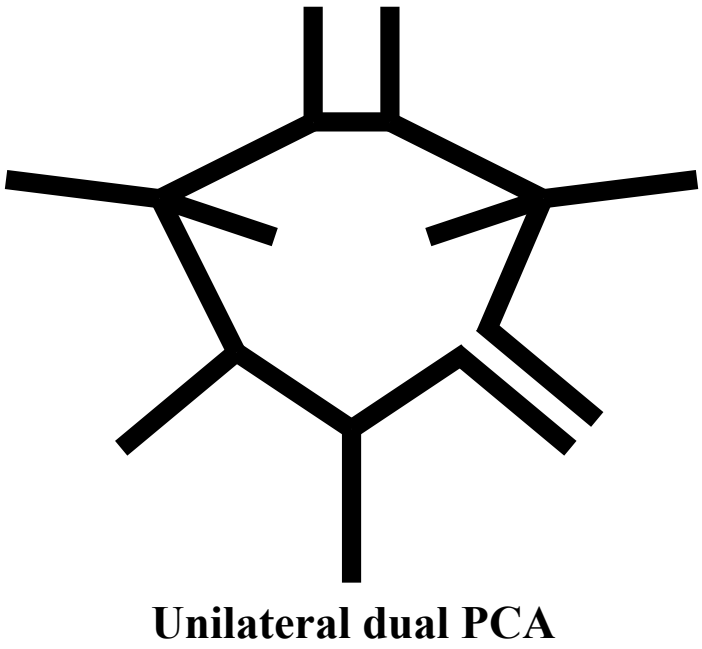

Figure 6. *Schematic illustration of the "(k)"/Unilateral dual PCA variant observed 29 times in Qiu et al., which highlights the importance of the third classification rule when prioritising collateral flow. A Circle of Willis exhibiting*

*the unilateral dual PCA variant was therefore according to rule three considered as missing a posterior communicating artery. PCA = posterior cerebral artery. Figure reused from **Paper I** supplementary.*

2.4 Imaging processing and validation

In **Paper I** and **Paper II** we used software to automatize parts of the CoW classification and the WMH segmentation.

2.4.1 Semi-automatic MeVisLab software

To make the classification of the CoW more efficient and less prone to errors, I created a semi-automatic segmentation program (**Figure 7**) in MeVisLab (v3.0.1) to speed up the process. The program automatically loaded new cases and had buttons for each segment in the CoW allowing for rapid rating of which segments were present or missing.

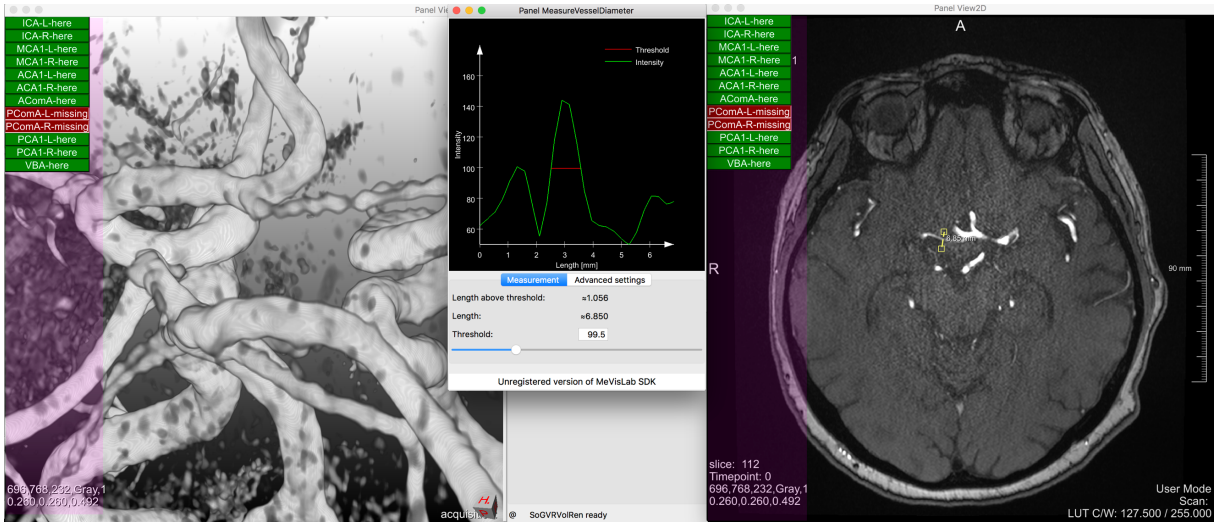

***Figure 7.** Screenshot of the semi-automatic classification for one brain. Here we can see the 3D viewer, 2D viewer where we measure the right proximal anterior cerebral artery which is just above 1.0 mm depending on how the threshold is selected relative to the background noise.*

Furthermore, the program included a 2D viewer and a 3D viewer showing the TOF image that was loaded. The 3D viewer allowed for free rotation, maximum intensity projection or 3D rendering (the preferred option) of the CoW anatomy. Simultaneously, the 2D viewer allowed

one to scroll through the 2D slices of the TOF image and measure the diameter of the segments that were seen as questionably thin in the 3D viewer. The aforementioned binary buttons were shown in both the 3D viewer and 2D viewer, but only clickable in the 2D viewer as we measured diameters in this program window. The program code, consisting of MeVisLab graphical elements, Python and R code, can at the time of publishing this thesis be found in a repository on GitHub called "cowtypemevis_gui" (URL: https://github.com/labhstats/cowtypemevis_gui) alongside some description of how it is used. Using all this with our CoW representation we classified the CoW anatomy fairly quickly. Although some cases took longer than others, depending on the complexity of the anatomy. The whole sample of 1864 images took approximately 10 effective working days. For a random subset of 100 TOF images we calculated intra and inter rater accuracy, which was 79% (**Figure 8**) and 82% (**Figure 9**), respectively.

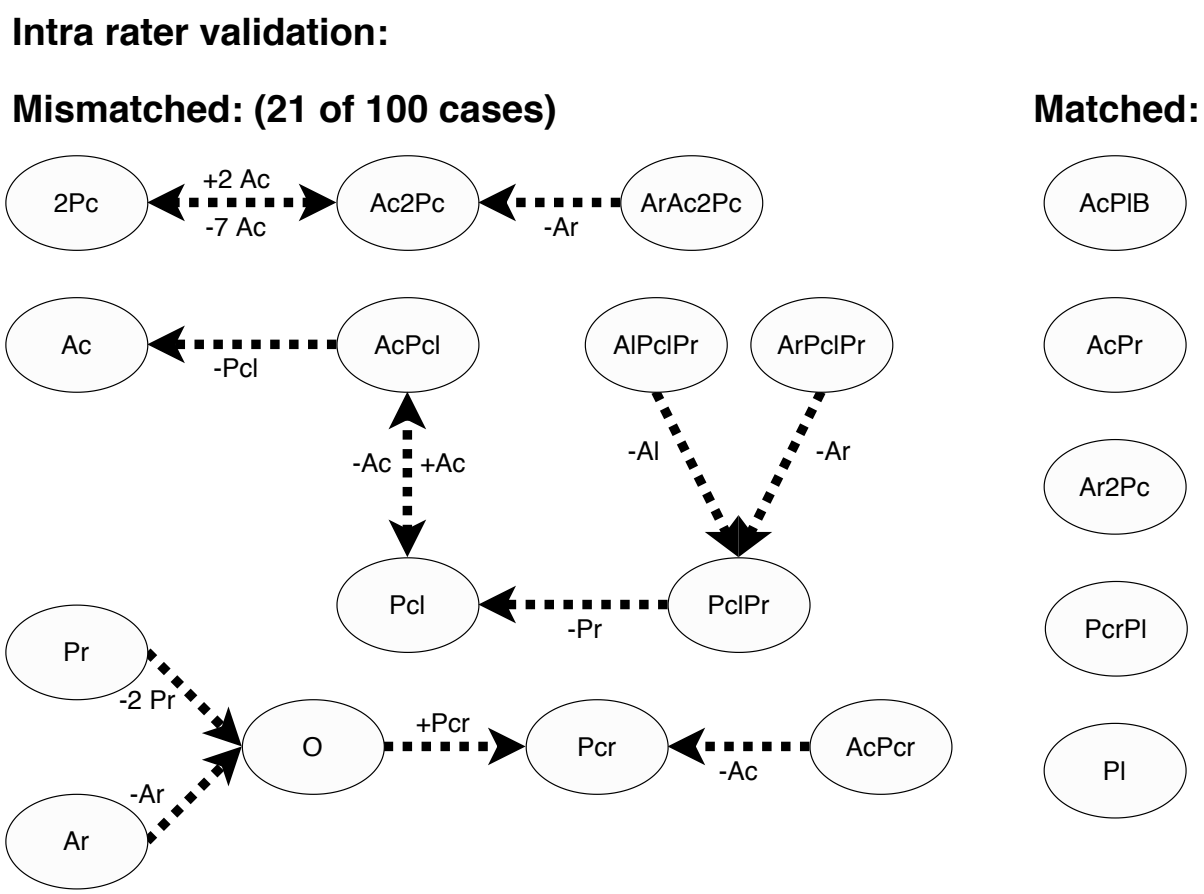

Figure 8. *Intra rater validation accuracy, showing which Circle of Willis variants that were misclassified as which. Each capital letter, followed by possible lateralisation (i.e. "l" or "r"), denote which segment that is missing or hypoplastic in each variant. A "2" prefix denotes that both left and right-side segment is missing or hypoplastic. O = complete variant, Ac = anterior communicating artery, A = anterior cerebral artery, Pc = posterior communicating artery, P = posterior cerebral artery, B = basilar artery. Figure reused from* ***Paper I*** *supplementary.*

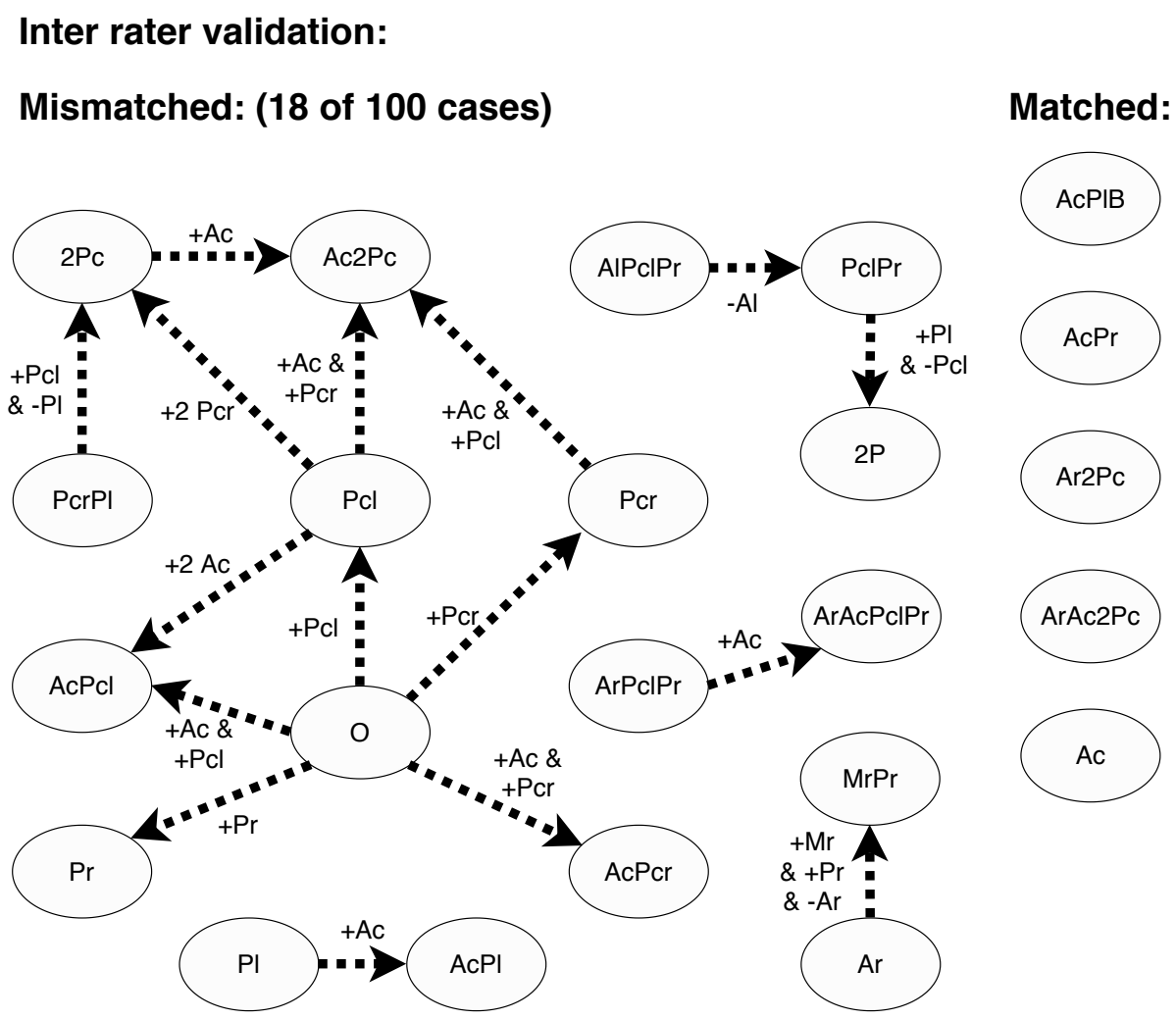

Figure 9. *Inter rater validation accuracy, showing which Circle of Willis variants that were misclassified as which. Each capital letter, followed by possible lateralisation (i.e. "l" or "r"), denote which segment that is missing or hypoplastic in each variant. A "2" prefix denotes that both left and right-side segment is missing or hypoplastic. O = complete variant, Ac = anterior communicating artery, A = anterior cerebral artery, Pc = posterior communicating artery, P = posterior cerebral artery, B = basilar artery, M = middle cerebral artery. Figure reused from* ***Paper I*** *supplementary.*

2.4.2 UNET segmentation algorithm

To estimate WMH volumes efficiently and unbiased in **Paper II**, we used an open source fully convolutional neural network (UNET architecture) algorithm (Li et al., 2018) to segment the WMH. The algorithm we used was the best performer in the WMH Segmentation Challenge MICCAI 2017 (Kuijf et al., 2019). We also added additional post processing steps to reduce false positives errors (i.e. using grey matter mask to remove false positives in grey matter), and the final pipeline was validated on a subset of 30 cases that had acceptable similarity coefficients, or DICE scores, that was on average 0.519 (**Figure 10**). Note that since the DICE score is sensitive to smaller volumes, the seemingly poor similarity scores were relatively acceptable.

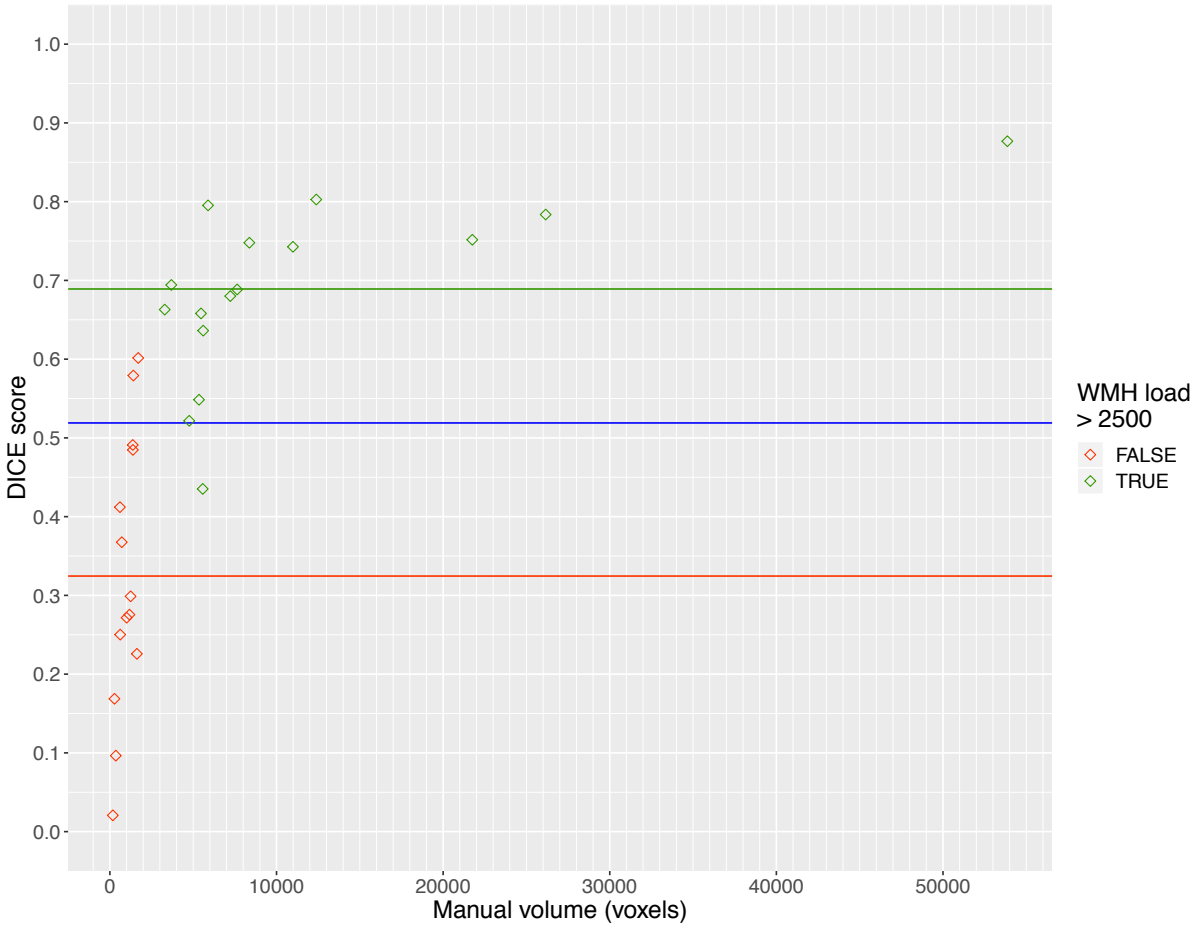

Figure 10. *Validation of white matter hyperintensities (WMH) segmentation algorithm. Figure reused from* ***Paper II****.*

Segmented WMH was then divided into DWMH and PWMH by a 10 mm rule (Griffanti et al., 2018) using dilated ventricle masks for defining the set of PWMH. Both T1w and FLAIR were used to manually check for segmentation errors. In the manual screening and validation, the FLAIR scans were mainly used to determine WMH, while using T1w scans as controls.

2.5 Methodological considerations when creating Circle of Willis representations for imaging studies

As mentioned, a substantial amount of work went into creating the CoW representations used in this thesis. Furthermore, no way of representing CoW variants are necessarily wrong depending on the context in which anatomical representations are used. This section will therefore address some relevant methodological considerations regarding the design of the CoW representations used in this thesis.

2.5.1 Which parts of cerebrovascular system to include for classification and subsequent analysis?

Ideally, the whole cerebro-vasculature should be considered included, and then simplified to whatever representation is necessary with respect to specific statistical assumptions or requirements, however this was not viable. As such, selecting common segments in the CoW and fitting them into a basic, uniform and "applicable" or flexible framework (i.e. compared to previous studies) seemed the most appropriate.

Omission of segments' lateralisation is an example of a simplification we used. However, it is not without possible flaws. Although the CoW anatomy itself is theoretically expected to be

fairly symmetrical, the practical surroundings of the CoW may make such simplifications somewhat erroneous.

Furthermore, the degree of comparison one wish to enable with previous and future studies, also affects how much of the vasculature one should include and how one should select at least one diameter threshold. For example, we have consciously chosen a level of detail, with the classification criteria, that is possible to generalise and then compare to previous prevalence studies. For instance, we successfully compared our material in **Paper I** with another TOF MRA study by Qiu et al. (Qiu et al., 2015) using a CoW representation that retained less details than ours.

Obviously, there are many aspects that will affect an appropriate level of detail for representing the CoW. Arguably, due to the absence of readily available automatic segmentation or classification software, which in theory should retain the most detail about the CoW (**Figure 4**), the pre-emptive methodological considerations presented in this thesis should continue to prove relevant when manual measurements and classification are done as there are bias and time issues associated with doing it more than once. The automatic measurements and classification have on the contrary the luxury of applying thresholds after quantifying the CoW anatomy without rater bias and more than enough diameter estimates per segment. In theory though, with many enough manual diameter measurements per segment, the manual approach can asymptotically converge to the standards of automatic software measurements.

2.5.2 Defining segments as missing or hypoplastic: Semantic issue

The distinction between missing and hypoplastic arteries has been a thorny issue. We often used the word missing instead of hypoplastic, when stating whether a segment was not seen on the TOF images or less than 1 mm in diameter. The scrutiny we received from others

presumably stemmed from a dichotomy between contexts in which one may study the CoW anatomy.

In the context of a surgery or in vitro studies, one is able to physically check that an in vivo invisible segment is hypoplastic and not missing. However, in an in vivo study, one is unable to physically check that arteries not seen on an image is truly missing or just hypoplastic. The need for distinguishing between hypoplastic and missing arteries then seemingly becomes an issue of adhering to semantical norms stemming from in vitro studies or clinical cases, which is not necessarily applicable for in vivo studies.

Consequently, I believe this scrutiny of the choice of words is not an issue in the context of our work based on in-vivo imaging where we also used one dichotomising diameter threshold. The persisting problem of in-vivo imaging not being able to distinguish between hypoplastic and missing arteries is undeniable, and it is this exact weakness of in-vivo TOF studies that enable the use of such simplified jargon with implied superposition of the two states of segments.

2.5.3 Pooling missing and hypoplastic segments: Statistical issue

Another related concern we encountered in the early stages of designing CoW representations is that one should not necessarily statistically merge the two distinct concepts of a missing and a hypoplastic segment; i.e. a segment rated as missing is combined into the same category of a segment rated as hypoplastic. Although, when prioritising to represent the collateral ability in the CoW from images in cross-sectional studies, it introduces less friction between the merged categories to merge these two rather than merging hypoplastic segments with present ones. The main argument is that both the concept of hypoplastic segments and the concept of missing segments, represent reduced or incomplete collateral ability in the CoW; compared to the complete CoW variant and its present or plastic segments.

A possible counterargument is that the diameter of different CoW segments is not constant or fixed. In fact, hypoplastic segments are plastic enough to for instance increase in diameter when correcting arteriovenous malformations with shunting (Chuang et al., 2010). However, this possibility of latent collateral ability would likely only be an issue that is actionable for longitudinal studies or studies with repeated scans, and in our cross-sectional studies with a singular TOF scan per individual this is at worst just another limitation to note.

Despite this worst-case limitation, and assuming at least two repeated TOF scans, our binary classification of segments would still be able to describe diameter changes over time if the measurements crossed the 1.0 mm threshold between scans.

2.5.4 Why not represent segments via ternary ordinal factors?

Considering that the dichotomous classification of segments are a few decades old (Krabbe-Hartkamp et al., 1998), why have we not used ternary classification if the imaging technology has advanced since then? One argument to prefer the ternary segment representation is that it would remove the semantic and statistical issue of choosing either missing or missing and hypoplastic to define one missing segment category. Another reason to begin using the ternary representation is that it would retain more detailed information than the binary one.

The primary reason for not using the ternary representation is that the number of possible CoW variants increases at worst exponentially compared to the binary segment representation. For example, suppose “n” segments were classified for representing CoW variants in either dichotomous or ternary segment representation. Then, in the dichotomous case we have a theoretical number of CoW variants equal to 2 to the power of “n”, while in the ternary case we have 3 to the power of “n”. Even for a relatively small number of “n”, e.g. equal 12 there is more than a theoretical hundredfold increase in the number of unique CoW variants that could be left almost empty when using ternary instead of binary representation.

This would not have been an issue using qualitative methods, but for quantitative methods a ternary representation would have been too difficult to work with assuming that "only" 1864 participants were available for study.

Another reason for not using ternary segment representation is that it would require two thresholds per segment which would bring further uncertainty into the classification of segments. This additional threshold separating missing segments from hypoplastic segments would also be incredibly difficult to enforce consistently in TOF images; e.g. where would the limit between physically non-existing segments, thin segments not showing and thin segments showing be in TOF images? As such, there were fairly detrimental reasons why using ternary segment representation for the CoW variants was unfeasible in our works.

2.5.5 Why not use continuous diameter estimates of segments instead of categories?

At last I should address why we avoided measuring continuous diameter estimates for all segments. The first reason, already mentioned, was that we did not have available an algorithm that could automatically segment the CoW anatomy with radial discs along vertices. As such, it would be necessary to manually measure multiple diameters, at least three times for consistency, for each of the 12 included segments for 1864 participants and also manually log these in a spreadsheet or code equivalent software. Unsurprisingly, this would be very time consuming. The second reason is therefore that it would introduce too much uncertainty compared to how much work is required. Third and last, when compared to using binary indicator variables for CoW variants, an ensemble of 12 separate diameter estimates would not translate well to statistically examining the effect of each whole CoW variant. The only tangible benefit, or exception, in our case could be to use the diameter estimates to examine the effects of resulting whole CoW variants for varying thresholds and

not only one threshold; e.g. brute-force finding critical thresholds of variants which could be more associated with some cerebrovascular health condition than others.

2.6 Circle of Willis representations and corresponding statistical methods in papers

Having presented the relevant CoW representations, argued their rationale and multiple other considerations, we will in this section discuss the representations in the three papers alongside the statistical methods used. Different representations were used in the papers, and corresponding statistical analyses were done in R.

2.6.1 Paper I – Prevalence study

To establish a foundation for studying the CoW we had to classify the CoW anatomy for each participant and estimate prevalences. This was done in **Paper I**. Although it was only strictly necessary to use only one holistic CoW variant representation, I thought the study would age better and be more informative if multiple representations were used instead. As such, we used four different representations of the CoW anatomy and at least one more could have been used.

First, we used the holistic variant representation for the whole CoW and the 12 artery segments of interest. Second, we used the segment-wise representation for each individual artery segment, from which we then derived and used the third segment-by-segment conditional representation. Together, these three representations described the CoW at a unitary level, partial dependent level and at an individual segment level, and they provided much information by themselves and in conjunction with each other. Although not describing larger parts of the CoW anatomy, the second representation and its derivative are logical representation to use since they can be regarded as a recontextualization (i.e. adaption) of the

level of detail used to describe the mean artery diameter of individual segments in the CoW as some studies do (El-Barhoun et al., 2009; Krabbe-Hartkamp et al., 1998).

We also simplified the holistic CoW variant representation into a fourth representation such that our prevalence estimates could be compared with another CoW prevalence study (Qiu et al., 2015). This fourth representation did not include lateral information about missing or hypoplastic segments.

Regarding hypothesis testing, frequency tests such as the Chi-squared test is naturally used in prevalence studies such as **Paper I**. Considering that all our CoW representations are discrete, we used two Cochran-Mantel-Haenszel (CMH) tests and one Chi-squared test, totalling three statistical tests. With the first CMH test, we tested whether CoW variants were conditionally independent of sex while controlling for age (i.e. below or above sample mean age). With the second CMH test, we tested whether CoW variants were conditionally independent of being below or above sample mean age while controlling for sex (i.e. male or female). The one Chi-squared test was done to improve the interpretation of a stacked bar plot of CoW variant prevalences per decade, and tested whether sex was hetero- or homogeneously distributed between an age-as-decades grouping.

In the end, the holistic variant representation was by itself enough to test our hypotheses regarding the frequency of CoW variants and present the CoW variants. The other two representations were used to present other CoW information and data in figures, while the fourth was used to compare with another study.

2.6.2 Paper II – WMH study

In **Paper II** we primarily tested if incomplete CoW variants were associated with increased WMH volumes compared to the complete CoW variant. We first segmented the WMH using

an open source fully convolutional neural network (UNET architecture) algorithm (Li et al., 2018) and then partitioned the segmented WMH into DWMH and PWMH.

We used linear regression analyses with DWMH volume and PWMH volume as the dependent variable in two separate regression models. Since each type of WMH volume can be considered a continuous response variable and there are over thousand observations, we can include a sizeable number of CoW factors and other risk factor variables into linear regression models without substantial risk of overfitting. As such, we decided to use a more simplified version of the holistic CoW variant representation where left-right side symmetric CoW variants were merged. To exemplify, left and right PCoA were regarded as equals, but we still retained information whether the PCoA was ipsilaterally or contralaterally missing to e.g. a missing PCA or an ACA. The rationale being that symmetrical variants should affect the total WMH volume similarly. This also retained as much information about each variant as possible while still not exaggerating the number of tests. We also avoided representing the unique CoW variants through segment-wise factors which would involve a convoluting amount of segment indicator variables, two-way- and three-way interaction variables to assess the effect of all the unique CoW anatomy compositions; i.e. the dismantling of each unitary or holistic CoW variant into many segment-wise indicator variables.

The reduction in the number of tests is also beneficial since we used multiple post-hoc testing with Dunnett contrasts and Dunnett adjusted p-values. The contrasts were one-sided tests to better answer the primary hypothesis for **Paper II**, that incomplete CoW variants would be associated with increased WMH volume compared to the complete CoW. The standard two-sided tests included in the linear regression models were still included due to unexpected results and for the other WMH risk factors. Dunnett contrasting is a rather liberal adjustment procedure that only compares the 16 indicator variables for incomplete CoW variants (i.e. treatments) in each regression model against the complete CoW variant (i.e. control). This is

mainly why we reduced the loss of statistical power by merging left-right side symmetric CoW representations. Without merging some CoW variants, we would have had over 30 comparisons per model. By doing this we assumed that possible hemispheric associations between CoW variants and WMH should not be affected by the merging. This rationale depended further on the flow rates through the two ICAs and the BA being symmetric within merged symmetric variant pairs. Fortunately, ACA hypoplasia and aplasia are associated with ipsilateral (i.e. effectively symmetrical) proportional change in ICA diameters (Carels et al., 2018; Wu et al., 2020) and the flow change accordingly (Hendrikse et al., 2005).

Even though WMH are seen in multiple regions of cerebral white matter, it could be feasible that some CoW variants were associated with more WMH lesions in certain white matter regions, which could have been investigated with spatial statistics, we instead used WMH volume as a dependent variable. There are multiple reasons for this choice. First, it is often done and allows comparison with other studies. Second, results from univariate regression models have results that are easier for most to understand its possible direct numerical implications. Third, full spatial modelling of WMH have inherent power issues in terms of multiple p-maps, which will be multiplied by the many different CoW variants we tested with respect to DWMH and PWMH. Furthermore, and last, using spatial statistics could reduce the validity of merging symmetric CoW variants without additional post processing of images. In our case, with two dependent variables, we have doubled the amount of hypothesis tests and increasing the number of tests in the current setting would be statistically questionable.

2.6.3 Paper III – Intracranial aneurysm study

In **Paper III** we examined how incomplete CoW variants were associated with increased prevalence of saccular IA compared to the complete CoW variant. We used logistic regression models to calculate odds ratios (OR) for IA for two different factor groupings of the

incomplete CoW variants. Of the 120 cases with IA, there were only a small number of cases that had multiple IAs, and participants with IA was defined as participants with at least one IA. IAs were defined by two expert radiologists as saccular IAs with a maximal diameter or length larger than or equal to 2 mm.

We considered multiple representations of the CoW variants. However, due to low prevalence of IA we believed that we would lose more by not satisfying the statistical assumptions of the logistic regression, than what we would lose in terms of detail by pooling and merging CoW variants. Therefore, similar to **Paper II** we used the same left-right merging of CoW variants while retaining information about the ipsilateral and contralateral relationship between segments. However, with only up to 120 participants with IA, there is an upper limit to how many CoW variants, or variables in general, one should include in the logistic model to maximise the probability of true positives and true negatives (Vittinghoff and McCulloch, 2007). Vittinghoff's and McCulloch's study suggests that the events-per-variable (EPV) ratio should be higher than 5 when binary predictors are primarily used (Vittinghoff and McCulloch, 2007). This limit approaches even more quickly when regression models must adjust for important risk factors for IA, such as smoking, hypertension and sex (Cras et al., 2020), and age as well. Depending on the grouping of incomplete CoW variant factors, this left little room in the logistic regression models for factors representing the CoW variants.

Fortunately, this could be overcome by only including the merged CoW variants that were the most prevalent. We chose to include those having a prevalence larger than 2% than in the reference sample (N = 1858) with both IA and CoW status available. These prevalent variants corresponded to eight incomplete CoW variants, and resulted in a reduction in sample size down to 1667 participants with 110 participants with IA. The reduction in participants with IA, or events, was therefore still acceptable compared with the 12 variables we included in the full logistic regression model and had an EPV ratio well above 5. In addition, we also used

the simplest way of representing the CoW anatomy (i.e. incomplete versus complete) to examine the odds of at least one IA for all incomplete CoW variants collectively via another simple logistic regression model also adjusting for the same variables as the full logistic regression model. This also served to double check our findings from the full model with relatively low EPV.

2.7 Standard Protocol Approvals, Registrations, and Consents

The studies in this thesis were approved by the Regional Committee of Medical and Health Research Ethics Northern Norway (2014/1665/REK-Nord) and carried out in accordance with relevant guidelines and regulations at UiT The Arctic University of Norway. All participants gave written informed consent before participating in the studies.

3 Results

3.1 Paper I – Prevalence study

In a population-based sample of 1864 participants, we estimated prevalences of different CoW variants. We found 47 unique CoW variants when including the right and left lateralization of segments. The five most common variants were the 2Pc (27.8%) missing both PCoAs, the Pcl (12.2%) missing the left PCoA, the complete O variant (11.9%), the Ac2Pc (9.3%) missing the ACoA and both PCoAs, and the Pcr (7.3%) missing the right PCoA. These five variants made up 68.5% of the sample (**Figure 11**), while the 25 rarest variants constituted only 3.2% of the sample (See Appendix B for **Table 5**).

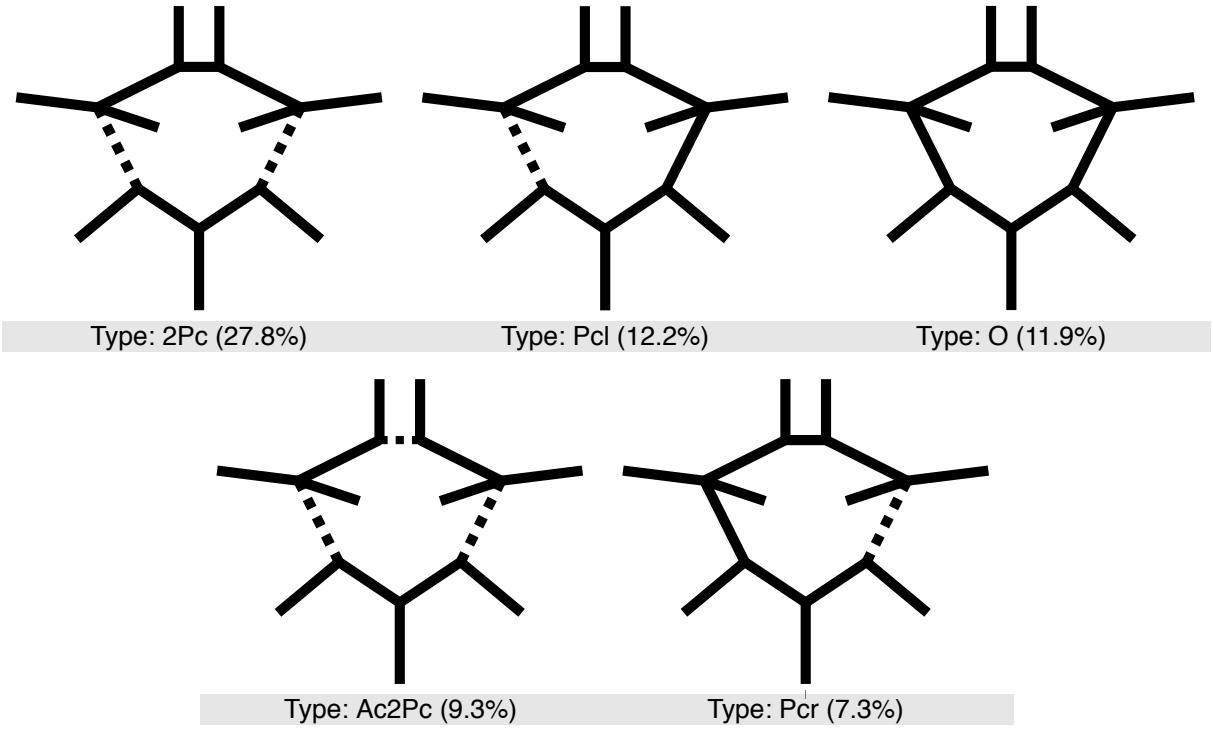

Figure 11. *Illustration of the five most common Circle of Willis variants.*

Comparison of most CoW variant prevalences from our Norwegian population sample, i.e. 99.2% of 1864 observations, with all observations from a male Chinese population (N = 2246) showed excellent agreement (**Table 2**). The complete variant had only a 0.3 percent

point difference in prevalence. Overall, mean and median percent point difference was at 1.6 and 0.8 respectively, with ranges from 0.1 to 10.6 percent points.

Table 2. *Comparison between Qiu et al. and Hindenes et al. (**Paper I**), where Circle of Willis variants' lateralisation and very rare variants are excluded to enable comparison of prevalence estimates.*

Nr.	Variant	Qiu (%)	Hindenes (%)	Difference
1	O	12.2	11.9	0.3
2	A2Pc	1.9	1.6	0.3
3	APc	1.3	1.1	0.2
4	APcP	0.2	1.6	1.4
5	AP	0.2	0.6	0.4
6	A2P	0.1	0.2	0.1
7	Ac2Pc	7.1	9.3	2.2
8	AcPc	4.9	5.8	0.9
9	AcPcP	0.4	2.1	1.7
10	AcP	1.0	1.9	0.9
11	Ac2P	0.5	0.8	0.3
12	A	0.5	0.6	0.1
13	Ac	3.3	2.6	0.7
14	2Pc	38.4	27.8	10.6
15	Pc	22.0	19.5	2.5
16	PcP	2.2	6.2	4.0
17	P	3.3	4.5	1.2
18	2P	0.5	1.1	0.6

Variant abbreviations: O = complete variant, A = missing anterior cerebral artery, Ac = missing anterior communicating artery, Pc = missing posterior communicating artery, P = missing posterior cerebral artery, "2" = prefix indicating both prefixed segments are missing.

By using both the segment-wise and the segment-by-segment dependent conditional CoW representations, we also discovered independent and dependent patterns of associations for segments and across segments. Independent patterns included the right ACA being more often missing than the left ACA, the right PCoA being less often missing than the left PCoA, and both PCAs being approximately equally often missing. Dependent patterns included ACA and PCA being more often simultaneously ipsilaterally missing, and ACA and PCoA being more often simultaneously contralaterally missing, and PCA and PCoA being only contralaterally

missing. The PCoA and PCA artery pair was prone to being missing simultaneously. ACoA tended to be equally likely missing no matter which artery in the posterior of the CoW that was missing, and ACoA was almost never missing if the ACA was already missing.

Furthermore, we found significant conditional dependence in prevalence distribution of CoW variants between older and younger participants using a mean split of the data (i.e. comparing participants younger than 65.4 years old to participants older than 65.4 years old). A stacked bar plot of the CoW variant prevalences per decade suggests that the age-related difference between young and old participants was due to increased number of missing segments in the CoW with increasing age. The decade age distribution was independent of sex, so the observed trend of increasing number of missing segments with older age can be considered valid for both men and women. We found no significant conditional dependence in prevalence distribution of CoW variants between males and females. This lack of prevalence differences between males and females is consistent with the close agreement between our population sample and the male Chinese population sample.

3.2 Paper II – WMH study

Among the 1864 participants examined in **Paper I**, 1751 of those were used in the analyses of the relationship between incomplete CoW variants and DWMH or PWMH (**Figure 12**). The rest were excluded due to circumstances affecting the reliability of the WMH segmentation and subsequent analyses. Briefly, the 113 excluded were excluded due to brain atrophy that might lead to incorrect WMH volume estimates (N = 70), image artefacts (N = 6), failure of the WMH segmentation (N = 11) and infrequent CoW variants (N = 26).

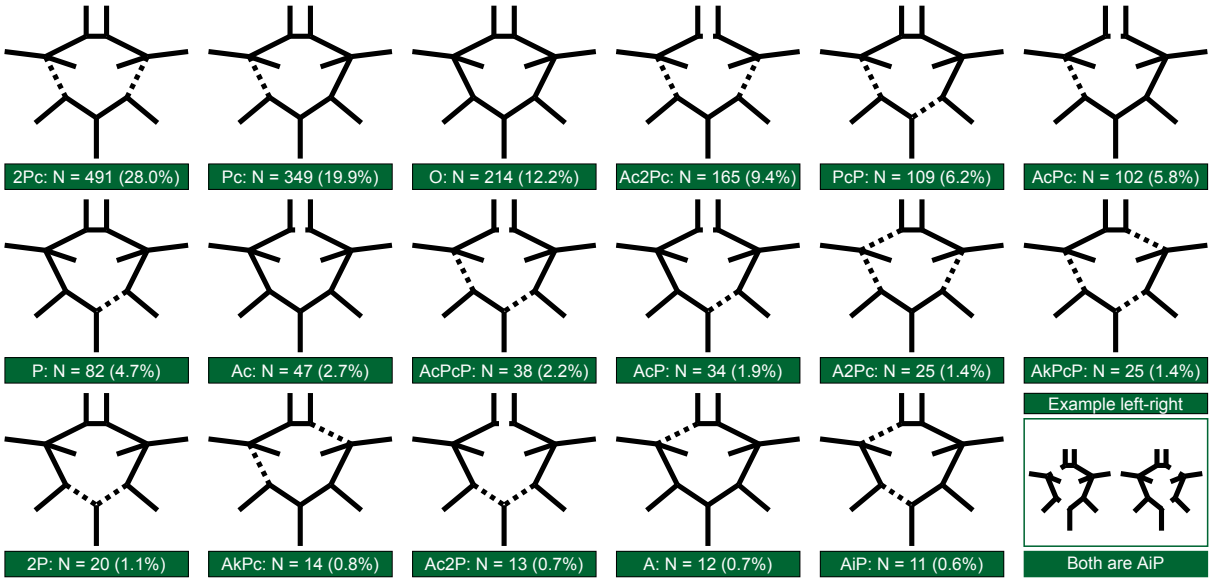

Figure 12. *Illustration of the merged Circle of Willis variants included and analysed in* ***Paper II****. Abbreviations: "i" = ipsilateral and "k" = contralateral relationship between two subsequent segments. Prefix "2" denotes that both left and right segments are missing. Furthermore, "A" = proximal anterior cerebral artery, "Ac" = anterior communicating artery, "Pc" = posterior communicating artery, "P" = proximal posterior cerebral artery. Figure is reused from* ***Paper II****.*

No incomplete CoW variant had significantly higher DWMH volume compared to the complete CoW variant. However, the PcP variant, missing one PCoA and the contralateral PCA, was the sole variant that had an adjusted p-value less than 50% at p = 0.093 for the one-sided test. Besides the Dunnett adjusted p-value, the two-sided test for the PcP variant was significant at the 5% level. See **Table 3** for effect sizes. Optimistically, this indicates a trend of higher DWMH volume for the incomplete CoW variant missing a PCoA and a PCA. Realistically however, unless a specific mechanism can be determined to support the trend for that variant, it appears that no incomplete CoW variant is associated with increased DWMH volume compared to the complete variant. The R^2 for the DWMH model was 0.167, indicating that the model explained only a modest amount of the variance in the data.

Table 3. *Overview of the effect sizes in the two WMH regression models that were significant at the two-sided tests.*

Effect \ WMH type	Deep WMH	Periventricular WMH
A2Pc (1/0)	Not significant	-0.5055
P (1/0)	Not significant	-0.3931
PcP (1/0)	0.2714	Not significant
Age (Continuous)	0.0301	0.0789
Pack year (Continuous)	0.0048	0.0057
Systolic blood pressure (Continuous)	0.0041	0.0041
Diabetes (1/0)	Not significant	0.4280

Abbreviations: WMH = white matter hyperintensities, A2Pc = variant missing proximal anterior cerebral artery and both posterior communicating arteries, P = variant missing proximal posterior cerebral artery, PcP = variant missing a posterior communicating artery contralateral to a missing posterior cerebral artery. Coefficients are not standardised.

Similarly, no incomplete CoW variant was associated with significantly higher PWMH volume compared to the complete CoW variant. In this case, all Dunnett adjusted p-values with the one-sided tests were in the range from 0.85 to 1. Closer inspection of the model showed that two incomplete CoW variants had significant p-values for the two-sided test, but their corresponding coefficient was negative explaining why the one-sided tests had p-values closer to 1 than 0. For the two-sided tests however, the P variant (missing one proximal PCA) and A2Pc variant (missing one proximal ACA and both PCoA) was significant at 1% and 5% level, respectively. This indicated, contrarily to our original hypothesis, that some incomplete CoW variants could be associated with decreased PWMH volume compared to the complete CoW variant. However, with regards to our original hypothesis and risk of false positives, the results still indicate that an incomplete CoW variant was not associated with higher PWMH volume compared to the complete CoW variant. The R^2 for the PWMH model was 0.458, indicating that the model explained a fair amount of variance.

In both models, pack year smoking, systolic blood pressure and age were risk factors for increased DWMH and PWMH as previous studies indicated for WMH. Having diabetes was only a risk factor for increased PWMH volume, not DWMH, which may explain some of the difference in variance explained by the models.

3.3 Paper III – Intracranial aneurysm study

Among the 1864 participants in **Paper I**, 1858 had sufficient image quality on the TOF images to be screened for IAs, and after exclusion of rare CoW variants 1667 participants were included for study. Among the 1667 participants, there were 110 participants with at least one IA and a large number of these IAs were around 5 mm or smaller (**Figure 13**). Only 3.1% of participants with a complete CoW variant had IA compared to 7.1% of participants with an incomplete CoW had at least one IA.

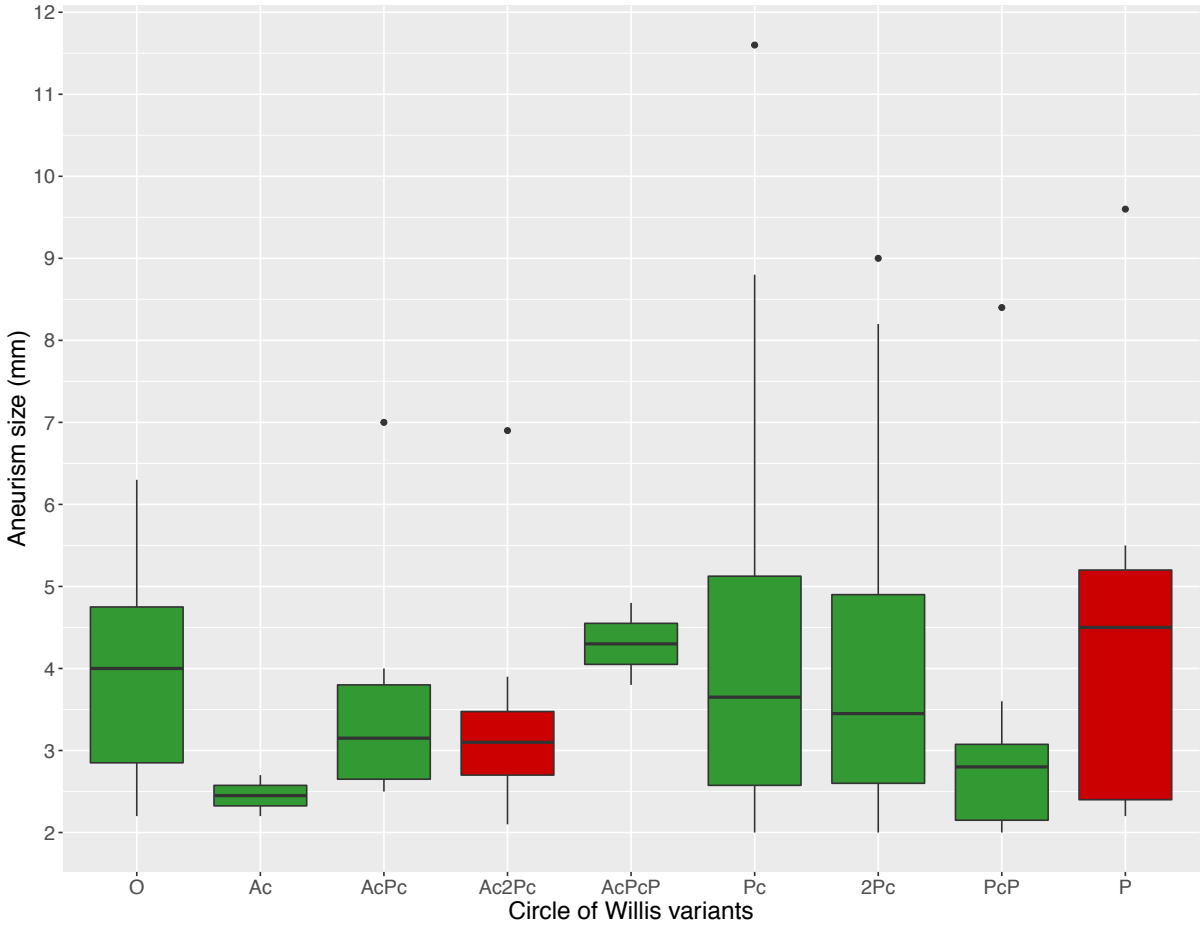

Figure 13. *Box plots of intracranial aneurysm (IA) sizes of the 110 participants (one IA per participant) sorted per Circle of Willis variant. Figure is reused from* ***Paper III*** *supplementary.*

Of the eight incomplete CoW variants included in the logistic regression model, two were associated with increased odds of IA compared to the complete variant (**Figure 14**). The first was the Ac2Pc variant (missing all communicating arteries) with a 4.2 OR (95% CI 1.7 – 10.3), and the second was the P variants (missing either the left or right proximal PCA) with a 3.6 OR (95% CI 1.2 – 10.1). These two variants had quite high OR estimates compared to the other six incomplete CoW variants, which only ranged from 1.2 to 2.3 OR with minimum lower limit and maximum upper limit 95% CI at 0.25 and 8.09, respectively. The relatively high OR estimates of these other six incomplete CoW variants in the full model are reflected in how collectively all the incomplete CoW variants were significantly associated with increased odds of IA at 2.3 OR (95% CI 1.05 – 5.04) in the simple logistic regression model.

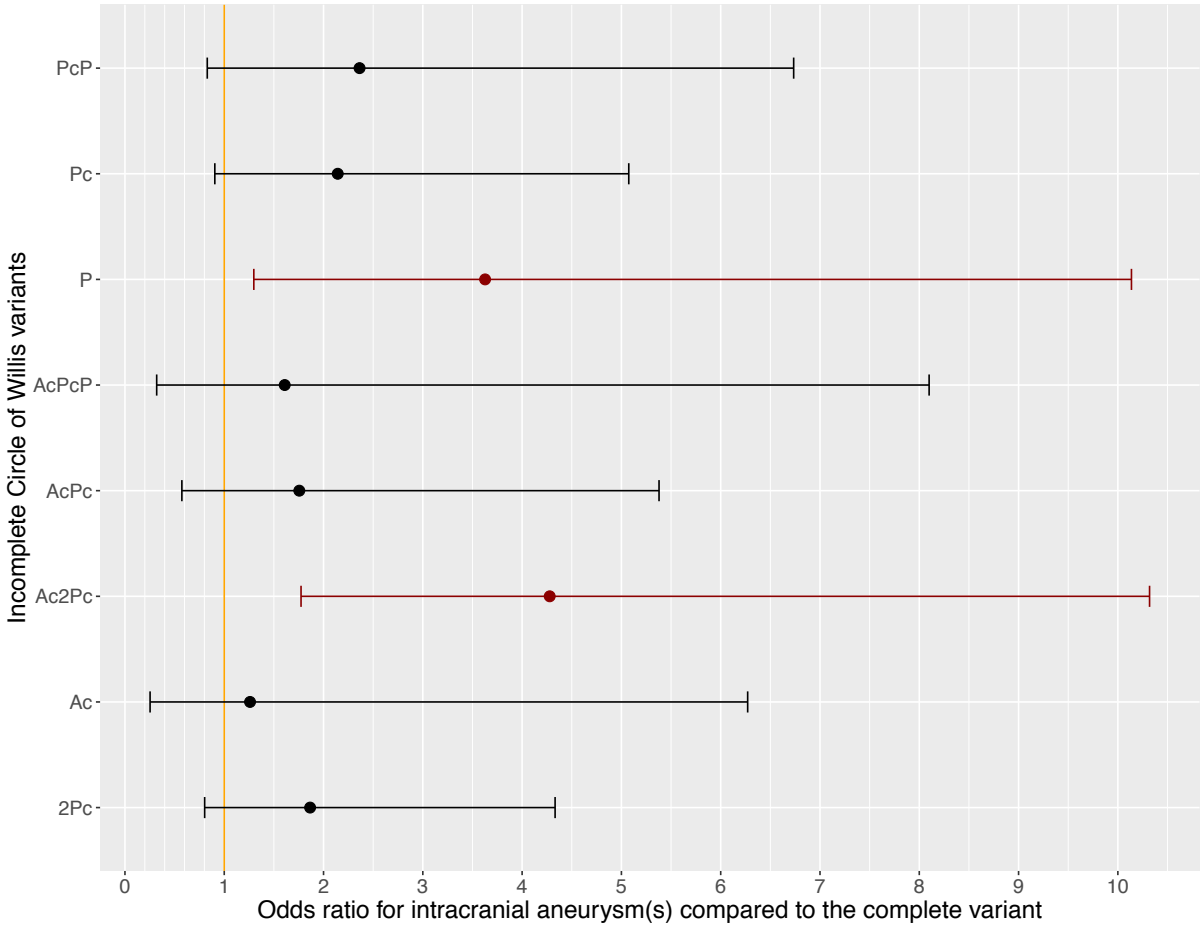

Figure 14. *Confidence intervals from the full logistic model with the eight individual Circle of Willis variants. Abbreviation of missing segments in Circle of Willis: Pc = posterior communicating artery, P = posterior cerebral artery, Ac = anterior communicating artery. Prefix "2" denotes that both left and right segments are missing.*

3.3.1 Location of IA versus Circle of Willis variants

Only seven of the 120 participants (among the 1858) with at least one IA had a complete CoW, and six of seven participants with more than one IA were among the most common CoW variants. For the significant Ac2Pc variant most IAs were in the MCA, while for the significant P variants nearly half of the IAs were in the ICA. **Table 4** show the five CoW variants and corresponding IA sites in the ten participants that were excluded in **Paper III**.

Table 4. *Site of intracranial aneurysms in participants (N = 10) for Circle of Willis (CoW) variants not included in* ***Paper III****.*

IA site(s)	Circle of Willis variants					
	Sum:	**AiP**	**A2Pc**	**AkPcP**	**2P**	**Ac2P**
Sum:	**10**	**1**	**3**	**4**	**1**	**1**
ACoA	**2**	0	2	0	0	0
PCoA	**1**	0	0	1	0	0
ICA	**3**	1	0	1	0	1
MCA	**3**	0	1	2	0	0
ICA + MCA	**1**	0	0	0	1	0

Abbreviations: "i" = ipsilateral and "k" = contralateral relationship between two subsequent segments. Prefix "2" denotes that both left and right segments are missing. "A" = proximal anterior cerebral artery, "ACoA" and "Ac" = anterior communicating artery, "PCoA" and "Pc" = posterior communicating artery, "P" = proximal posterior cerebral artery, "ICA" = internal carotid artery, and "MCA" = middle cerebral artery.

Regarding the 120 participants with IA, most IAs were also in either the ICA or MCA. However, there were a few interesting observations that should be mentioned despite uncertainty from few observations. First, similar to the P variants, the other variants missing a PCA and simultaneously not missing a PCoA, had three of four IAs in the ICA. Second, participants with IA in the BA had mostly incomplete posterior CoW anatomy; i.e. missing or hypoplastic PCoA or PCA. Third, the single IA observed in the proximal PCA and the distal PCA was only associated with missing both PCoA. Fourth, two of seven IAs associated with

a CoW variant missing an ACA were in the ACoA. Fifth and last, all IAs in the terminus were associated with incomplete communicating arteries; i.e. ACoA and PCoA.

Interestingly, from **Table 4** it appears that the distribution of IAs among the common and rare IA sites appear to be independent of the rarity of CoW variants. It should also be noted that two rare incomplete CoW variants, both with at least a hypoplastic or missing ACA, had more participants with at least one IA than two more common incomplete CoW variants.

4 Discussion

The main objectives of this thesis were to examine the prevalence of different CoW variants in an adult population and how these CoW variants were associated with WMH and saccular IA. Main findings were: (**I**) that the complete CoW was uncommon with a prevalence of 12%, (**II**) that incomplete CoW variants were not associated with increased WMH, and (**III**) that incomplete CoW variants were associated with increased odds of saccular IA.

I will discuss key findings and other findings in our work in a broader context and also the clinical relevance of our findings. I refer to the three papers for a detailed discussion of the specific works.

4.1 Anatomical variations: How often is the Circle of Willis anatomy complete?

Studies on the CoW report wildly varying prevalence estimates of the complete CoW variant, and it is therefore considerable uncertainty regarding the "true" prevalence. MRA studies have reported prevalences of the complete CoW variant from 12.2% (Qiu et al., 2015) to 45% (Forgo et al., 2018). Both studies used MRA TOF in healthy adults of similar average age, suggesting that the differences between the two studies are unrelated to the measuring technique. However, the two studies have vastly different sample sizes; i.e. the study that reports the 12.2% prevalence had a sample size 18 times larger than the study reporting a 45% prevalence. This suggests that the sample size may be a major source of the disagreement in prevalence estimates.

In **Paper I**, our sample size was more comparable to the largest study (i.e. N = 1864 versus N = 2246), and we estimated that the CoW was complete in 11.9% of 1864 participants, which was nearly identical to the 12.2% estimate by Qiu et al. (Qiu et al., 2015). This discrepancy in

sample sizes and prevalence estimates suggests via the law of large numbers, that a large number of participants are essential for obtaining more consistent and likely representative estimates of the CoW variants' prevalence. Furthermore, based on the overall close agreement between the two largest in-vivo studies of the incomplete CoW variants (**Table 2**), it is reasonable to say with some confidence that the CoW is not very often complete in participants older than 40 years as we concluded in **Paper I**.

4.1.1 Do the Circle of Willis change with age?

Another key finding in **Paper I** was that the complete CoW variant was less common in older individuals, the same was the case for CoW variants with only one missing or hypoplastic segment. Other MRA studies (El-Barhoun et al., 2009; Krabbe-Hartkamp et al., 1998) CT angiography studies (De Caro et al., 2021; Zaninovich et al., 2017) and a digital subtraction study (Eaton et al., 2020) also report that the complete CoW variant becomes less prevalent with increasing age. The numerous studies reporting the same age trend suggest that the complete CoW variant becomes less prevalent with increasing age.

On that note, one may wonder why our comparison with Qiu et al. (Qiu et al., 2015) showed such close agreement when they have a younger population of only men aged 31 – 60 years (mean age 49.55 years), compared to our study with mean age 65.4 and an age range from 40 – 86 years. One possible reason is that we used a different way of classifying the CoW compared to Qiu et al. (Qiu et al., 2015), which is a separate issue.

Despite this inherent unclarity, some dissection studies with both smaller and larger sample sizes support the findings that the complete CoW variant is rarer in older individuals. First, a recent dissection study with 73 aged specimens (> 90% with atherosclerosis) showed that only 7% of the CoWs were complete (Wijesinghe et al., 2020). Second, an older dissection study from 1963 with 994 adult specimens of unknown age with "clinical neural

dysfunction", found that the CoW is only complete in 21% cases (Riggs and Rupp, 1963); i.e. with no hypoplastic segments. Third and last, this age trend is also inversely reflected in another relatively large dissection study with 1000 younger specimens (i.e. over 50% were younger than 40 years old) reporting a 45.2% prevalence of the complete CoW variant (Kapoor et al., 2008). Although the percent point differences of prevalence estimate for the complete CoW in the two first dissection studies range from 4 to 10 percent points compared to **Paper I**, these three studies arguably support our finding that the incomplete CoW is not very common in adults older than 40 years, and also support the recurring finding that the CoW tend to be more incomplete with older age.

The exact nature of this commonly observed age trend is not fully understood, as no longitudinal study on the prevalence of CoW variants have been performed. However, there are known arterial changes associated with age, which may cause arterial segments to become hypoplastic: increased arterial tortuosity, i.e. curling, turning and twisting of the arteries (Bullitt et al., 2010; Wright et al., 2013), arterial stiffening (Mitchell et al., 2011), and atherosclerosis, which is prevalent in CoW specimen from elderly (Wijesinghe et al., 2020). Furthermore, total cerebral blood flow (Buijs et al., 1998) and pulsatile dampening (Zarrinkoob et al., 2016) decrease with age, which could also play a role in shaping the cerebrovascular anatomy. Despite no causative evidence, it appears unlikely that the age trend associated with the prevalence of the complete CoW variants is random due to the large number of different cross-sectional studies reporting and supporting the age trend.

4.1.2 The way forward for understanding anatomical variations in the Circle of Willis

As all studies on the CoW have been cross sectional, we cannot ascertain which factors affect the CoW anatomy; e.g. genetics, age, health, environmental or generational differences.

Studies on genetic influence on the CoW anatomy suggest that genes play a minor role in the anatomical variation. A twin study found no genetic effect (Forgo et al., 2018), while another family study suggest that variations in the PCoA could be heritable (Van Kammen et al., 2018). As mentioned, cerebrovascular changes such as atherosclerosis and arterial stiffening may affect the COW anatomy, but there is little knowledge on the exact effect on the CoW anatomy. With regards to The Tromsø Study specifically, examples of generational exposure are changes in physical activity (Morseth and Hopstock, 2020), changes in blood pressure and subsequent use of antihypertensives (Sharashova et al., 2020), or cessation of smoking followed by increase in obesity (Løvsletten et al., 2021).

Well-powered longitudinal studies are clearly the way forward in understanding which factors affect the CoW anatomy. However, the timescale for cerebrovascular changes may be long, as the 9-year timespan used in Takeuchi et al. indicates (Takeuchi et al., 2019), which may render such studies difficult. There is also a lack of studies on the CoW anatomy with participants or specimen spanning a large age range, i.e. from youth to elderly. Such studies could also offer insight into which actors shape the CoW anatomy. Finally, there is need for detailed studies on how various CoW variants affect cerebral blood flow, perfusion and pulsatility to understand how the different CoW variants tend to affect the blood supply to the brain.

Future studies should address some common issues hampering research into the CoW anatomy. First, the highly heterogenous classifications of the CoW anatomy among studies can be handled by reporting increasingly more detailed classification and representation of CoW variants to allow for comparisons with both older and future studies. Such repeated practice will eventually converge into the one or more ideal standardised methods for reporting the CoW anatomy, which are needed. Second, studies should maximise their sample sizes; e.g. 150 observations are obviously not enough to reliably estimate prevalences for all

47 CoW variants or a sizeable subset of those variants observed in **Paper I**, and neither were 1800 observations to some extent. Third, studies should have awareness of the discussed age trend and report CoW prevalence estimates' dependence on age; e.g. similar to the stacked bar plot in **Paper I**. This is especially important for studies that manage to study participants or specimen with a wide age range. Without properly accounting for these issues and taking on such challenges, review studies on the prevalence of CoW variants will be difficult.

At last, future CoW review studies should try applying bootstrapping to retroactively compare estimates of CoW variants' prevalence between studies, where the smallest sample size among the studies compared simultaneously is used as sample size for the bootstrap samples. This way, equal uncertainty is applied to all studies compared against each other, and it should be possible to see whether studies with more likely volatile CoW variant prevalence estimates from smaller sample sizes significantly disagree with larger studies that is less likely to have volatile prevalence estimates or vice versa.

4.2 The Circle of Willis anatomy and similar variants may affect the brain health in different ways

Our works together with others suggest a more complex association between CoW anatomy and brain health than initially anticipated. A number of previous studies have shown an association between incomplete CoW variants and increased WMH in patients primarily with atherosclerosis, presumably due to reduced collateral ability of an incomplete CoW. We failed to find a similar association in our population sample in **Paper II**, but we curiously found evidence for a protective effect against WMH in some incomplete CoW variants. In **Paper III** we showed that the CoW anatomy not only affects the brain directly, but also the cerebral arteries, as we found that incomplete CoW variants were associated with increased odds for presence of IA.

4.2.1 WMH and Circle of Willis anatomy: Explaining outcomes

In **Paper II**, we initially only tested whether incomplete CoW variants were associated with increased WMH volume; i.e. using one-sided tests. However, we were surprised by the lack of significant results from these one-sided tests, and after closer examination of the models we observed that the two-sided tests indicated that incomplete CoW variants could be associated with decreased WMH volume; i.e. the effect sizes of two incomplete CoW variants (A2Pc and P variants) corresponding to being 5-6 years younger in the PWMH model (**Table 3**). The possibility of such a protective effect is supported by a study concluding that a fetal posterior type CoW (i.e. essentially a P variant) could be protective factor against DWMH (van der Grond et al., 2004). Despite recurrence of the P variants, because we observed this for PWMH and not DWMH, further experimental evidence and also a causative rationale is needed to validate the possible protective effects. In this section I will attempt the latter.

Originally, we assumed that better collateral ability would equal overall better cerebrovascular health; i.e. less WMH when the CoW is complete, since hypoxia is shown to be a contributing factor to WMH (Fernando et al., 2006). Except for the PcP variants that trended to have increased DWMH volume, the remaining results in **Paper II** contradicted this WMH study hypothesis and suggest that impaired collateral ability is associated with less WMH or not associated with WMH at all; at least in a generally healthy population sample. However, it is difficult to explain the possible protective effect seen in **Paper II** with the notion of reduced collateral function alone, which suggests that other CoW functions should also be considered relevant for explaining the possible outcomes for the CoW anatomy.

Fortunately, in addition to the traditional collateral ability function, possible alternative CoW functions or consequences of the CoW anatomy have already been postulated or considered by other studies (Fenrich et al., 2021; Pascalau et al., 2018; Vrselja et al., 2014; Warnert et al.,

2016). Among these, two of them similarly argue the likelihood of other CoW functions than the traditional collateral ability one as probable, since atherosclerosis is primarily a human lifestyle disease in older age and therefore not a likely source of evolutionary pressure in developing a collateral function (Fenrich et al., 2021; Vrselja et al., 2014). However, only one of the two present a succinctly formulated CoW function that also appears as a valid alternative in the context of this thesis.

Vrselja et al. concludes in their study that the CoW protects cerebral artery and blood-brain-barrier (i.e. microvasculature) from haemodynamic stress (Vrselja et al., 2014). Although Vrselja et al. points to the collaterals in dampening the haemodynamic forces, the dampening effect is not well understood and the hypothesis is also critiqued (Fenrich et al., 2021). As such and by extension, I suspect that there might be some incomplete CoW variants also offering advantageous dampening as some of our results in **Paper II** suggest. Furthermore, the possibility that blood-brain barrier dysfunction plays a role in WMH (Wardlaw et al., 2015) combined with the idea that certain incomplete CoW variants would also protect the blood-brain barrier from haemodynamic stress, may suggest that certain CoW variants negate haemodynamic stress thereby protecting against WMH. Although hypothetical, this would better explain why in **Paper II** that incomplete CoW variants were not associated with increased WMH volumes and instead appeared to be associated with decreased PWMH volume for the P variants and A2Pc variants compared to the complete CoW, or simply not associated with WMH at all.

From another perspective, it is also not completely illogical to suggest that incomplete CoW variants may promote some health benefit and not only poor health outcomes. In retrospect, this notion appears plausible considering how frequently incomplete CoW variants appeared in adult participants compared to the complete CoW variant as seen in **Paper I**. Furthermore, the idea that something considered incomplete could also be beneficial is perhaps overlooked,

e.g. due to expectation bias (Jeng, 2006) from associating something labelled incomplete or unfinished with being worse off than something that is complete or finished. A simulation study on the CoW and carotid stenosis also discuss the possibility that the complete CoW may not always be the anatomy yielding better clinical outcomes (Kang et al., 2021). Still, considering all the evidence in section 1.3 indicating that incomplete CoW variants are associated with adverse outcomes, it may be more nuanced to postulate that incomplete CoW anatomy may be beneficial up until some critical point where the negatives then outweigh the positives. One may think of incomplete CoW variants as having some eventual double-edged consequences.

4.2.2 The Circle of Willis anatomy and intracranial aneurysm: Explaining outcomes

The association between incomplete CoW variants and increased odds for IA prevalence may to a certain degree be understood by changes in the flow pattern in the CoW as we argued in **Paper III**. However, some of the associations, in particular with respect to aneurysms downstream to the CoW may be better explained by the dampening hypothesis by Vrselja et al. (Vrselja et al., 2014), which suggests that the CoW protects cerebral arteries from haemodynamic stress. If development of IAs are strictly dependent on weakening of the vessel wall and subsequent wall expansion, then it makes more sense that incomplete CoW variants with reduced ability to dampen asynchronous pressure pulses, as Vrselja et al. proposes (Vrselja et al., 2015, 2014), to have higher prevalence or odds of IA compared to the complete variant.

In **Paper III** specifically, this appears to apply to the Ac2Pc variant associated with IAs in the MCA, where all three communicating arteries are hypoplastic or missing. The rationale is that no or reduced cross flow or dampening between the three in-flow arteries (i.e. ICAs and BA)

providing possible asynchronous flow pulses induces increased haemodynamic stress and subsequent IA in the MCA. Once again, as with the outcomes in **Paper II**, we were unable to explain the outcomes observed in **Paper III** by restricting ourselves to only one possible function or consequence of the CoW anatomy.

4.2.3 Potential double-edged outcomes of incomplete posterior variants

Interestingly, one comprehensive study has proposed that incomplete posterior circulation in the CoW combined with a hypoplastic vertebral artery (located upstream of the BA segment) can be a partial trigger for increased blood pressure to maintain sufficient blood flow to the brain (Warnert et al., 2016); i.e. a so called selfish brain hypothesis. Also, in **Paper III** we documented in the supplementary (See Appendix C for **Table 6**) that participants with incomplete CoW variants had substantially higher rates of hypertension compared to those with a complete CoW; i.e. specifically individuals with CoW anatomy missing both the PCA and the contralateral PCoA simultaneously had the highest rates of hypertension. Another study also report this association between incomplete CoW variants and hypertension (Eaton et al., 2020).

Furthermore, hypertension is also a known risk factor for WMH (Dufouil et al., 2001), presence of IA (Cras et al., 2020), IA rupture (Isaksen et al., 2002) and ischemic stroke (O'Donnell et al., 2016). Supposing then that incomplete CoW posterior anatomy has a key role in triggering the postulated self-preservation tactic of the brain by inducing hypertension, as suggested (Warnert et al., 2016). One should then, due to the considerable risk attributed to hypertension, assume that a CoW with an incomplete posterior anatomy inducing hypertension for prolonged amounts of time to be associated with some of these unfavourable health conditions; e.g. as we see in **Paper III** for the P and Ac2Pc variants (i.e. both have incomplete posterior by definition) and as we see in **Paper II** for the PcP variants (missing a

PCA and PCoA) that trended to have more DWMH. Without regard to the long-term consequences, the brain's apparent short-sighted self-preservation tactic may still be beneficial short term. See **Figure 15** for an illustration of this concept. This argued short-sightedness of this hypothetical self-preservation tactic of the brain could partly explain the high prevalence of incomplete posterior CoW anatomy that is not, yet, significantly associated with higher prevalence of WMH or IA in **Paper II** and **Paper III** although the incomplete CoW variants have higher rates of hypertension in **Paper III**.

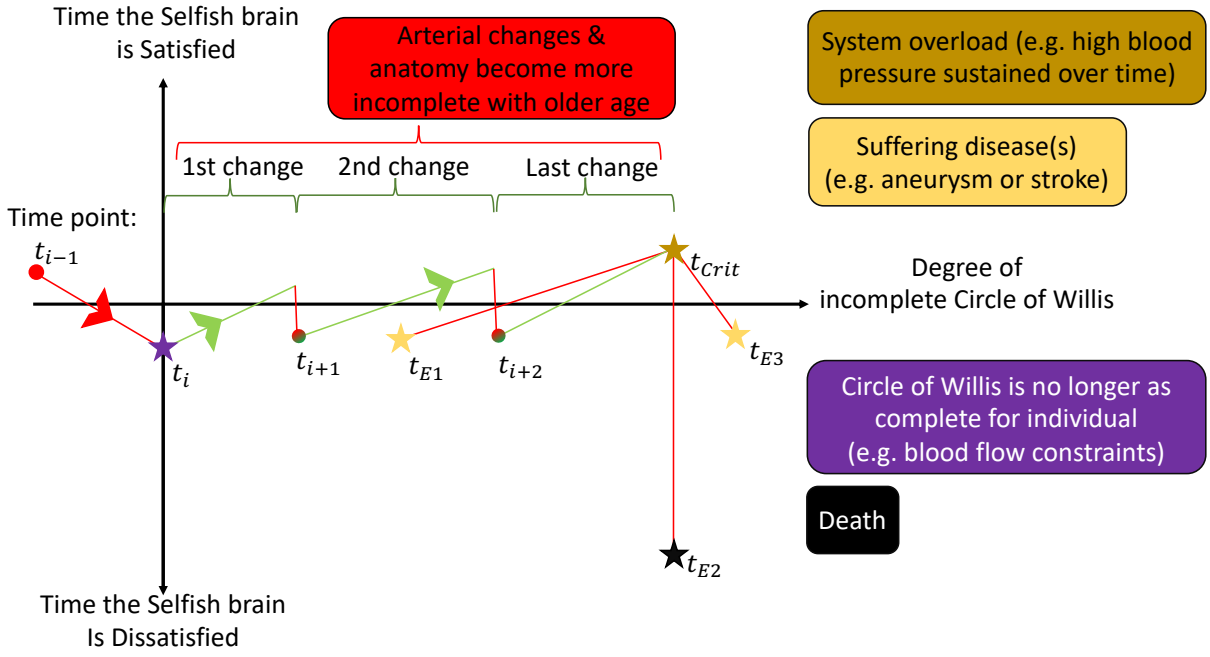

Figure 15. *Illustration of how an incomplete Circle of Willis could be beneficial (e.g. counteracting low blood flow) and also detrimental to the overall brain health due to increased or sustained high blood pressure over time. Number of anatomical changes can be less, but are limited to three to align with the Circle of Willis representations presented in this thesis. Furthermore, time of critical events (stars) and anatomical changes would likely be different for each individual. Anatomical changes in the Circle of Willis is synchronised with improved satisfaction of the selfish brain to match with the known cross-sectional association between higher rates of hypertension and incomplete Circle of Willis anatomy.*

Furthermore, regarding **Paper II** and **Paper III**, the P variants are also interesting in terms of double-edged effects. The P variants were associated with increased prevalence of IA while

also trended to be associated with decreased PWMH volume. This seemingly indicates that the same CoW variant or anatomy can be associated with both beneficial and adverse outcomes.

4.2.4 Potential sensitivity of similar Circle of Willis posterior anatomy and corresponding outcomes

Similar to how one incomplete CoW variant could be associated with both positive and negative outcomes, some incomplete CoW variants had different outcomes despite having similar incomplete posterior anatomy. The PcP variants trended to have more DWMH volume in **Paper II**, and had the third highest OR for presence of IAs and the highest rates of hypertension as presented in **Paper III**. Comparing it to the P variants, that trended to have less PWMH volume in **Paper II** and were significantly associated with odds of IA in **Paper III**, the difference between the two becomes readily apparent. In addition, the second most common Pc variants had no results of significance in **Paper II** and only the fourth highest OR for IA in **Paper III**. However, this consideration of the next similar CoW variant could continue for a while. Still, from these limited examples of posterior CoW anatomy, it appears that the possible positive, negative or neutral outcomes of CoW anatomy can be sensitive to single artery differences even though the three variants are superficially "similar". Similar in the regard that they are sometimes merged into one homogeneous incomplete posterior CoW category (van der Grond et al., 2004; van Seeters et al., 2015). As such, merging of "similar" CoW anatomy for statistical analysis could potentially convolute contradicting outcomes or effects, and other ways of representing CoW variants, perhaps at more tailored functional or anatomical levels, could be better.

Also, regarding the pressure dissipation function of the CoW. This evident sensitivity in outcomes could support the derived notion presented earlier that the specific incomplete CoW

variants may also be important for improving the resulting outcome, and not only whether a CoW is complete or not.

4.2.5 Other potential drawbacks of the incomplete posterior variants

In **Paper III** we also observed that all IAs in the BA location were associated with incomplete posterior CoW anatomy. Unfortunately, as the posterior variations in the CoW is more prevalent than other variations in the CoW, these observations may as well be natural coincidences. However, one longitudinal study reports enlarged BA diameter over time also in association with fetal-type CoW (Takeuchi et al., 2019). Where a fetal-type CoW is any CoW with smaller diameter of the PCA compared to the ipsilateral PCoA (Krabbe-Hartkamp et al., 1998; Takeuchi et al., 2019; van der Grond et al., 2004), which essentially is a CoW with incomplete posterior as defined in our studies. This is the case if the PCA diameter is less than 1 mm in our representation; i.e. the P variants in which 1 of 10 IAs were located in the BA in **Paper III**. Arguably, such partial isolation of the BA from the ICA via the fetal-type CoW also associated with simultaneous increase of BA diameter (Takeuchi et al., 2019), in which the same incomplete posterior anatomy also could induce increased blood pressure (Warnert et al., 2016) could have local consequences. Together with some findings in **Paper III**, this suggests that the few IAs located in the BA associated with incomplete posterior CoW anatomy may be due to induced hypertension in combination with elongation or widening of the BA and not necessarily just due to randomness. It is also possible that changes in pulsatile dampening with older age in the BA could be related (Zarrinkoob et al., 2016).

4.2.6 The way forward concerning alternative Circle of Willis functions, consequences and outcomes

Similar to how CoW prevalence studies need longitudinal studies, it is evident that longitudinal studies are required for improving assessment of the causes and effects related to the different CoW variants. As other studies have considered alternative CoW functions or consequences (Eglit et al., 2020; Fenrich et al., 2021; Li et al., 2021; Pascalau et al., 2018; Vrselja et al., 2014; Warnert et al., 2016), the future importance of longitudinal studies that include the CoW anatomy and at least one cerebrovascular condition that also span a substantial amount of time, e.g. similar to the nine years in Takeuchi et al. (Takeuchi et al., 2019), cannot be overstated at this moment.

Cross-sectional studies that examines changes in flow, perfusion and pulsatility relative to single-artery changes in CoW anatomy would also be required to improve the understanding of how the CoW anatomy affects the parameters. The study by Mukherjee et al. (Mukherjee et al., 2018) is an example of such a study simulating the effect of missing one segment after another in five originally complete CoW. The use of imaging techniques that can in-vivo capture average magnitude and direction of blood flow through the CoW per time unit for at least one in-flow artery and associating certain flow patterns with certain CoW variants or certain lengths, curvature and tortuosity of CoW segments would be optimal.

4.3 Clinical relevance

Our findings did not have any direct clinical implications, as we have studied associations in a cross-sectional population sample, however several of our findings may be helpful for clinicians. In particular, the low prevalence of the complete “textbook-type” CoW and the association between CoW anatomy and presence of IA.

4.3.1 Segments in incomplete Circle of Willis variants observed in living individuals tend to be missing/hypoplastic in certain patterns

In **Paper I**, the prevalence study, we calculated the probability that a segment in the CoW was missing while assuming another segment was already missing. From these estimates we saw that certain artery segments were more likely to be missing at the same time compared to other arteries. Also, from the figure or tables of all unique CoW variants, most CoW variants never had more than three segments that were missing or hypoplastic at the same time; i.e. an upper bound "rule of three" regarding hypoplastic/missing arteries, or a lower bound "rule of four" regarding plastic arteries in the CoW.

Such interdependences of arteries' diameters close to or in the CoW is not new. In fact, multiple studies report that the proximal ACA-pair diameter asymmetry is associated with ipsilateral ICA-pair diameter asymmetry (Carels et al., 2018; Kane et al., 1996; Wu et al., 2020). Those knowledgeable about the CoW anatomy may also look at the complete CoW and determine correctly that the PCoA and proximal PCA are never missing at the same time. However, the same guess is not equally valid for the ACoA and proximal ACA, as there may be only one predominant distal ACA segment (Dimmick and Faulder, 2009).

Although such simple guesses can be made, the results of **Paper I** indicate that interdependence between segments in such a small structure as the CoW becomes fairly nuanced quickly. For example, would one have guessed that a hypoplastic or missing proximal ACA occurred more often simultaneously with a hypoplastic or missing ipsilateral proximal PCA and not contralaterally? See **Figure 16** for a summary illustration of the most common ways segments in the CoW tend to relate to each other in terms of diameter, or in terms of being hypoplastic or missing.

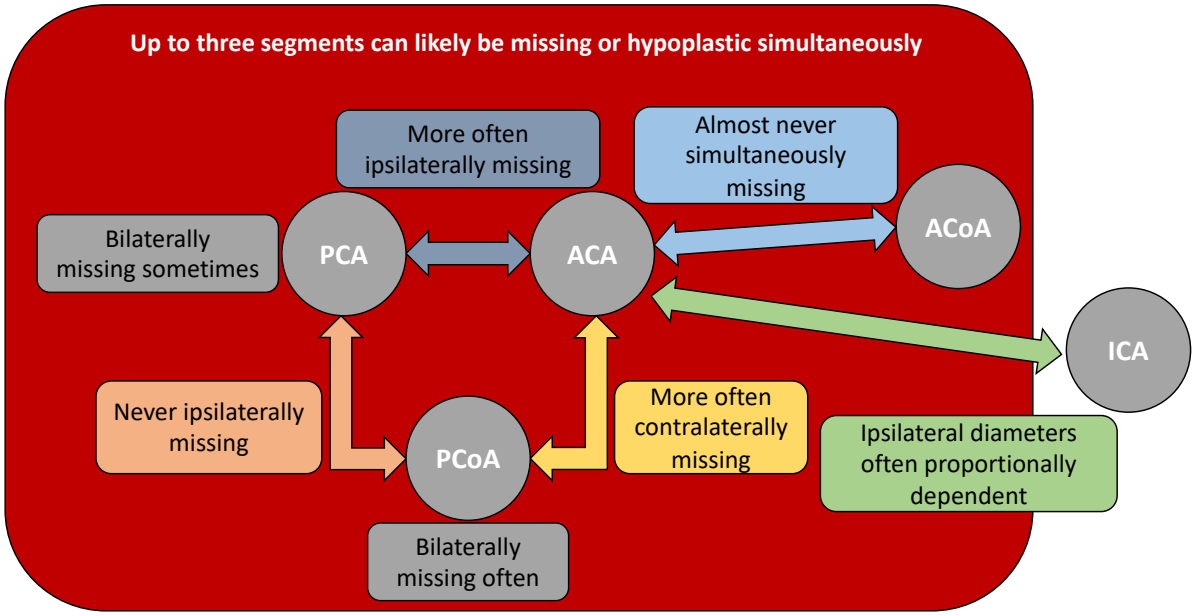

Figure 16. *Illustration of the interdependence of how segments in the Circle of Willis tend to be related in terms of being missing or hypoplastic, or in terms of diameter. ACA = anterior cerebral artery, ACoA = anterior communicating artery, ICA = internal carotid artery, PCA = posterior cerebral artery, PCoA = posterior communicating artery. This figure mainly reflects the findings in* ***Paper I*** *(red box).*

Assuming that the CoW anatomy may change over time. The knowledge of which segments in the CoW that are more likely to be missing or hypoplastic simultaneously could help in creating medical risk profiles or anatomical trajectories (i.e. changes over times) of CoW variants and their risk of one or more cerebrovascular conditions. For instance, suppose there is a 40-year-old patient with the Pcl variant missing the left PCoA, which artery is most likely to become hypoplastic or missing next? According to **Figure 16** and the exact numbers presented in **Paper I**, I would personally guess the other PCoA to become the second hypoplastic or missing artery for this individual, since the 2Pc variant is very common. Despite the effective clinical usefulness of such risk profiles being dependent on undiscovered practical longitudinal properties of the CoW anatomy, a single scan at any point in time could and should be sufficient for creating such basic risk profiles in the future. Such risk profiles should be able to assist in predicting the risk associated with present and possible future CoW anatomy.

4.3.2 Overlooked hypoplastic or missing ACA, and ACA variations in conjunction with ICA diameters?

As this thesis have not examined patients, and due to the evident association between the proximal ACA diameter and ipsilateral ICA diameter in CoW variations (**Figure 16**) (Carels et al., 2018; Kane et al., 1996; Wu et al., 2020), one should worry that CoW variants with rather infrequently observed hypoplastic or missing proximal ACA were severely understudied in this thesis. Consider for instance first **Paper III** and the ten participants with IA that were excluded from the paper, but revisited in this thesis. Here three of the five rare CoW variants excluded were associated with at least one IA and had at least a hypoplastic or missing ACA among other variations. Furthermore, two of those three CoW variants had more participants with at least one IA than two more common incomplete CoW variants included in **Paper III**.

All three CoW variants in question (**Table 4**), with incomplete anterior and also incomplete posterior anatomy, have arguably fairly logical locations of IAs; i.e. two in the ICA, three in the MCA, and two in the ACoA. The two variants missing at least both the ACA and PCA have IAs in the ICA similar to the P variants in **Paper III**, and the two variants with IA in the MCA have at least one or two hypoplastic or missing PCoA also similar to the Ac2Pc variant in **Paper III**. The two IAs in the ACoA associated with a hypoplastic or missing ACA, was similar to one previous dissection study (Kayembe et al., 1984).

In terms of ischemic stroke or infarction, which we did not study in this thesis, ACA variations combined with posterior variations have been associated with future anterior stroke (van Seeters et al., 2015). Furthermore, as the ACA variations are also associated with ipsilateral proportional ICA diameter asymmetry (Carels et al., 2018; Kane et al., 1996; Wu et al., 2020), it appears, to my knowledge, that a specific combination of ACA anatomy and corresponding ICA diameter is overlooked. It may have been overlooked that equal flow or

diameter of ICAs in tandem with unilateral ACA variations could be unfortunate (e.g. when incomplete posterior anatomy prohibits collateral flow) for the anterior circulation, because the contralateral ICA alone is expected to provide blood for both distal ACA flow territories, its ipsilateral MCA territory, and maybe also its ipsilateral distal PCA territory.

As such, I would argue that the importance of elusive ACA variations should not be disregarded even though we were unable to examine associations related to those CoW variants for both IAs and ischemic infarction. Rather the clinical importance of the ACA being hypoplastic or missing may in the context of this thesis be derived from our main results on related or similar anatomy; e.g. based on the argued function or consequence of the CoW anatomy which could make IAs likely at certain locations. Regarding IAs and **Paper III** this could correspond to being open to the possibility that incomplete CoW variants with proximal ACA variations can be associated with increased odds for IA, as the locations of the IAs could be explained with the arguments in **Paper III** and by a similar observation from another study.

To summarise, clinicians should be particularly aware of the possible association between ACA variations and subsequent increased flow through the ACoA and risk of IAs in the ACoA, and the absence of ICA diameter asymmetry which is reportedly common to observe with ACA variations.

4.3.3 WMH and Circle of Willis anatomy in different study populations

Paper II showed that nearly all incomplete CoW variants were not significantly associated with increased WMH volume in a general population-sample of participants. The only tangible exception was the PcP variants associated with increased DWMH at a 10% significance level for the one-sided test in **Paper II**. The same type of CoW anatomy (missing a PCoA and a PCA) was also shown to have the highest rate of hypertension in **Paper III**. In

hindsight this may attribute some importance to the PcP variants in **Paper II**, since systolic blood pressure (SBP) was adjusted for and also significant in the same DWMH model.

Among the three studies showing similar results for the remaining incomplete CoW variants, one was in a general population (Del Brutto and Lama, 2015) and two was in patients with carotid artery stenosis (Li et al., 2015; van der Grond et al., 2004). However, there were five studies in patients primarily with atherosclerosis showing that incomplete CoW anatomy is associated with increases in WMH (Chuang et al., 2011; Ryan et al., 2015; Saba et al., 2017, 2015; Ye et al., 2019). Considering these contradicting studies, it is difficult to ascertain to which extent incomplete CoW anatomy should explain increased prevalence of WMH in patients. Assuming however that there is a difference in effect of incomplete CoW anatomy for patients with atherosclerosis compared to other individuals, one still needs to define some atherosclerotic threshold to distinguish the two cases.

Fortunately, a simulation study on the CoW anatomy and degree of carotid artery stenosis show that the prevalence of the complete CoW peaked at 50% degree of carotid stenosis, and that the collateral capability of the ACoA and PCoAs significantly activated at a 75% degree of carotid stenosis and upward (Kang et al., 2021). This may give some idea at which atherosclerotic degree or state the complete CoW anatomy and collateral capacity becomes important for protecting against WMH, and could in a clinical setting encourage follow-up imaging of either both carotid arteries or the CoW depending on which was coincidentally examined first to assess possible risk of WMH.

In terms of the CoW anatomy and hypertension, Warnert et al. could have a possible outset regarding the hypertension that is potentially "wrongfully" treated with negative outcomes due to certain cerebrovascular anatomy inducing necessary hypertension (Warnert et al., 2016). Similarly, the evident contrast and sensitivity in outcomes in **Paper II** for the P and Pc

variants compared to the PcP variants may also be a relevant outset. Nonetheless, the distinction between individuals with or without atherosclerosis is probably the most important for clinicians to be aware of until more specific information about the link between CoW variants and WMH is uncovered.

4.3.4 Presence of intracranial aneurysms associated with certain incomplete Circle of Willis variants

In **Paper III** we found that two of the eight incomplete CoW variants were significantly associated with increased odds for presence of IAs compared to the complete CoW. The first variant (i.e. Ac2Pc) had missing all communicating arteries in the CoW (i.e. PCoAs and ACoA), such that all three in-flow arteries (i.e. ICAs and BA) seemingly have to feed their own cerebrovascular flow territories in isolation. This incomplete variant also seemingly had no or reduced ability to dampen possible asynchronous blood pulses between the three in-flow arteries, which we suspect could have caused the high prevalence of IAs. The second variant (i.e. P) had one missing or hypoplastic PCA. In **Paper III** we argued that the high prevalence of IAs in the ICA associated with the P variants may be due to the ipsilateral ICA being forced to feed more of the ipsilateral distal PCA's flow territory that is usually also fed by the BA. It is also possible that the one hypoplastic or missing PCA could cause a counter-clock-wise or clock-wise shift of blood flow throughout the CoW when the left or right PCA is missing, respectively (Mukherjee et al., 2018), in the process also activating all communicating arteries. This activation would induce additional haemodynamic stress throughout the communicating arteries in the CoW.

Clinicians should therefore be especially aware of these two CoW variants, i.e. Ac2Pc and P variants. However, the argued and presented rationale for why these CoW variants should be associated with IAs are yet to be corroborated by additional studies. The point is, until further

studies are conducted, clinicians should consider exercising patient specific judgement as normal and not completely accept the argued rationales of the results at face value. Furthermore, it may also be especially worthwhile to pay extra attention to individuals with other predispositions for prevalence of IA, e.g. genetically. Awareness of other incomplete CoW variants may also be worthwhile, but since our findings in **Paper III** were inconclusive for the other specific incomplete CoW variants, their exact clinical importance remains unclear for now.

If Warnert et al. are correct in assuming that incomplete posterior CoW anatomy induces hypertension (Warnert et al., 2016), which is a risk factor for IA rupture (Isaksen et al., 2002; Lindekleiv et al., 2012). Then, further clinical importance should be attributed to the P variants, and maybe also the Ac2Pc variant, mainly because these CoW variants are commonly defined as having the incomplete posterior CoW anatomy which could hypothetically induce hypertension. Lastly, although most of the IAs associated with incomplete CoW variants were relatively small (< 10 mm) (**Figure 13**), this does not diminish any expressed clinical importance of the incomplete CoW variants since three patients studies indicate that such smaller IAs can rupture (Duan et al., 2018; Figueredo et al., 2019; Zheng et al., 2019), if not eventually after the IAs grow larger.

4.4 Strengths, weaknesses and limitations of the project

The primary strength of this project has been the large number of participants that was invited from The Seventh Tromsø Study to undergo 3T MR examinations. This large number of participants have allowed us to examine many different CoW variants and their associations to health conditions, which can be generalised for a broader Norwegian population.

Other strengths included the use of semi-automatic software for classifying CoW variants, also yielding negligible intra- and inter rater errors, the use of fully automated software for WMH segmentation, and detection of IA by two expert neuroradiologists.

A limitation related to examining many detailed CoW variants was that many CoW variants are seldom observed, which imply that we were unable to obtain reliable estimates on these variants. This was specifically the case for CoW variants with at least a hypoplastic or missing ACA, and those with ICA not showing close to the CoW. Similarly, the reliability or validity of prevalence estimates and regression model coefficients of CoW variants vary across our studies due to the skewed prevalence estimates of CoW variants. The same weakness is also a problem in the context of relatively rare cerebrovascular conditions; e.g. saccular IAs in this thesis. Furthermore, the CoW representations, although allowing for examination of many different CoW variants, could also in retrospect have been more tailored toward each specific outcome we studied to improve viability. I could also have considered not simplifying CoW representations to fit as many variants within a single framework based on the collateral capacity of the CoW, but instead have excluded CoW with anatomy not conforming exactly to the representations used.

Another central weakness across this project was that we classified CoW variants from TOF images, which can falsely show segments as missing or hypoplastic arteries when the net flow through arteries are zero. Although, non-invasive alternatives to the TOF technique do not exist to our knowledge, but it is still important to be aware of its limitations.

4.5 Future works

Longitudinal studies that examine possible causes and effects related to CoW anatomy are without doubt the most needed type of future works for studying the CoW, in addition to

more detailed studies on how anatomical variations in the CoW affect cerebral flow, blood pulsatility and cerebral perfusion.

Future studies should also put a lot of thought and work into creating more detailed representations that can be compared across studies, and also creating more tailored CoW representations that best fit the pathogenesis of the disease one is studying. A universal classification scheme for the CoW is also highlighted by another independent review study as important for allowing better estimation of CoW variants' prevalence (Jones et al., 2020), and a simulation study also state that the classifications of CoW variants have to be contemplated further for improving statistical analyses regarding the CoW (Kang et al., 2021). Researchers should also strive to be aware of the age dependency of CoW anatomy and present prevalence estimates of CoW variants for narrower age groups if a sufficient number of observations are available for study.

Fortunately, due to the relatively modern imaging technology, one is no longer bound by dissection studies where it is impossible to measure changes over time. Larger population studies that already have done at least one cross-sectional study of the CoW anatomy should be in an advantageous position to begin shape the longitudinal understanding of the CoW anatomy within a decade. At least when considering a similar nine year time period as used in the longitudinal study by Takeuchi et al. (Takeuchi et al., 2019).

To help with the assumed work load from measuring, thresholding, or classifying the CoW anatomy, future works should also consider developing and make available fully automatic segmentation, measurement and classification software. Achieving this may in the long-term help clinicians in effortlessly being alerted of participants with certain CoW variants associated with known cerebrovascular risks. However, in the short term it can also alleviate

much of the burden associated with manually classifying the CoW variants, and also enable larger studies to classify the CoW of many participants without inter- and intra rater biases.

Regarding the cerebrovascular conditions studied in this thesis. Future works should look into the possibility that certain incomplete CoW variants may be associated with decreases in WMH volume or corroborate the atherosclerosis threshold for when incomplete CoW anatomy becomes unfavourable. It may also be informative to look at the statistical interaction between CoW anatomy and carotid stenosis in WMH studies. Regarding IAs, future works may benefit from collecting larger number of participants and try replicating and narrowing the confidence intervals of all incomplete CoW variants, not just the two variants we found significant in our study. The rationale is that individuals with these other incomplete CoW variants are presumably also at odds for higher prevalence of IA, albeit maybe not as often as the two we found. Another approach could be to collect flow data to see which segments in the CoW experience elevated flow for each CoW variant. At last, elevated blood pressure and hypertension in the context of PCoA and proximal PCA in the CoW (i.e. PcP variants and WMH), and maybe also the proximal ACA (i.e. then related to ischemic stroke or IA), should be an intriguing study with possibility for novel findings.

5 Conclusion

In conclusion, the complete CoW variant is likely not very common in adults older than 40 years old. Incomplete CoW variants appeared to not be associated with increased WMH volumes, at least in a general population. Incomplete CoW variants appeared to be possible risk factors for developing IA, as two CoW variants were significantly associated with increased odds of IA presence.

Despite being a structure that has been studied for centuries, the knowledge about CoW variants and anatomy are still lacking, in particular whether and how the anatomy changes through one's lifetime or not. The relatively modern invention of in vivo imaging should change this by enabling testing of the multiple ways the CoW may or may not, directly or indirectly, affect the brain's health. The way the CoW variants observed in living individuals tend to be incomplete in more or less likely patterns should help simplify this work, since different incomplete CoW variants can share certain functional properties between themselves. With this in mind, it remains to see whether incomplete CoW variants are either both beneficial and harmful, or just harmful for our cerebrovascular health as original suspected.

References

Alnaes, M.S., Isaksen, J., Mardal, K.-A., Romner, B., Morgan, M.K., Ingebrigtsen, T., 2007. Computation of hemodynamics in the circle of Willis. Stroke 38, 2500–2505. https://doi.org/10.1161/STROKEAHA.107.482471

Armstrong, N.J., Mather, K.A., Sargurupremraj, M., Knol, M.J., Malik, R., Satizabal, C.L., Yanek, L.R., Wen, W., Gudnason, V.G., Dueker, N.D., Elliott, L.T., Hofer, E., Bis, J., Jahanshad, N., Li, S., Logue, M.A., Luciano, M., Scholz, M., Smith, A. V., Trompet, S., Vojinovic, D., Xia, R., Alfaro-Almagro, F., Ames, D., Amin, N., Amouyel, P., Beiser, A.S., Brodaty, H., Deary, I.J., Fennema-Notestine, C., Gampawar, P.G., Gottesman, R., Griffanti, L., Jack, C.R., Jenkinson, M., Jiang, J., Kral, B.G., Kwok, J.B., Lampe, L., C.M. Liewald, D., Maillard, P., Marchini, J., Bastin, M.E., Mazoyer, B., Pirpamer, L., Rafael Romero, J., Roshchupkin, G. V., Schofield, P.R., Schroeter, M.L., Stott, D.J., Thalamuthu, A., Trollor, J., Tzourio, C., van der Grond, J., Vernooij, M.W., Witte, V.A., Wright, M.J., Yang, Q., Morris, Z., Siggurdsson, S., Psaty, B., Villringer, A., Schmidt, H., Haberg, A.K., van Duijn, C.M., Jukema, J.W., Dichgans, M., Sacco, R.L., Wright, C.B., Kremen, W.S., Becker, L.C., Thompson, P.M., Mosley, T.H., Wardlaw, J.M., Ikram, M.A., Adams, H.H.H., Seshadri, S., Sachdev, P.S., Smith, S.M., Launer, L., Longstreth, W., DeCarli, C., Schmidt, R., Fornage, M., Debette, S., Nyquist, P.A., 2020. Common Genetic Variation Indicates Separate Causes for Periventricular and Deep White Matter Hyperintensities. Stroke 51, 2111–2121. https://doi.org/10.1161/STROKEAHA.119.027544

Barber, R., Scheltens, P., Gholkar, A., Ballard, C., McKeith, I., Ince, P., Perry, R., O'Brien, J., 1999. White matter lesions on magnetic resonance imaging in dementia with Lewy bodies, Alzheimer's disease, vascular dementia, and normal aging. J. Neurol. Neurosurg. Psychiatry 67, 66–72. https://doi.org/10.1136/jnnp.67.1.66

Brisman, J.L., Song, J.K., Newell, D.W., 2006. Cerebral Aneurysms. N. Engl. J. Med. 355, 928–939. https://doi.org/10.1056/NEJMra052760

Buijs, P.C., Krabbe-Hartkamp, M.J., Bakker, C.J., de Lange, E.E., Ramos, L.M., Breteler, M.M., Mali, W.P., 1998. Effect of age on cerebral blood flow: measurement with ungated two-dimensional

phase-contrast MR angiography in 250 adults. Radiology 209, 667–674. https://doi.org/10.1148/radiology.209.3.9844657

Bullitt, E., Zeng, D., Mortamet, B., Ghosh, A., Aylward, S.R., Lin, W., Marks, B.L., Smith, K., 2010. The effects of healthy aging on intracerebral blood vessels visualized by magnetic resonance angiography. Neurobiol. Aging 31, 290–300. https://doi.org/10.1016/j.neurobiolaging.2008.03.022

Carels, K., Cornelissen, S.A., Robben, D., Coudyzer, W., Demaerel, P., Wilms, G., 2018. Smaller caliber of the internal carotid artery in patients with ipsilateral aplasia of the A1 segment of the anterior cerebral artery: a study with CTA. Acta Neurol. Belg. 118, 297–302. https://doi.org/10.1007/s13760-018-0935-7

Chuang, Y.-M., Guo, W., Lin, C.-P., 2010. Appraising the Plasticity of the Circle of Willis: A Model of Hemodynamic Modulation in Cerebral Arteriovenous Malformations. Eur. Neurol. 63, 295–301. https://doi.org/10.1159/000292431

Chuang, Y.-M., Huang, K.-L., Chang, Y.-J., Chang, C.-H., Chang, T.-Y., Wu, T.-C., Lin, C.-P., Wong, H.-F., Liu, S.-J., Lee, T.-H., 2011. Associations between Circle of Willis Morphology and White Matter Lesion Load in Subjects with Carotid Artery Stenosis. Eur. Neurol. 66, 136–144. https://doi.org/10.1159/000329274

Coulier, B., 2021. Morphologic variants of the Cerebral Arterial Circle on computed tomographic angiography (CTA): a large retrospective study. Surg. Radiol. Anat. 43, 417–426. https://doi.org/10.1007/s00276-020-02661-x

Cras, T.Y., Bos, D., Ikram, M.A., Vergouwen, M.D.I., Dippel, D.W.J., Voortman, T., Adams, H.H.H., Vernooij, M.W., Roozenbeek, B., 2020. Determinants of the Presence and Size of Intracranial Aneurysms in the General Population. Stroke 51, 2103–2110. https://doi.org/10.1161/STROKEAHA.120.029296

De Caro, J., Ciacciarelli, A., Tessitore, A., Buonomo, O., Calzoni, A., Francalanza, I., Dell'Aera, C., Cosenza, D., Currò, C.T., Granata, F., Vinci, S.L., Trimarchi, G., Toscano, A., Musolino, R.F., La Spina, P., 2021. Variants of the circle of Willis in ischemic stroke patients. J. Neurol. https://doi.org/10.1007/s00415-021-10454-4

de Leeuw, F.-E., de Groot, J.C., Achten, E., Oudkerk, M., Ramos, L.M.P., Heijboer, R., Hofman, A., Jolles, J., van Gijn, J., Breteler, M.M.B., 2001. Prevalence of cerebral white matter lesions in elderly people: a population based magnetic resonance imaging study. The Rotterdam Scan Study. J. Neurol. Neurosurg. Psychiatry 70, 9–14. https://doi.org/10.1136/jnnp.70.1.9

Del Brutto, O.H., Lama, J., 2015. Variants in the Circle of Willis and White Matter Disease in Ecuadorian Mestizos. J. Neuroimaging 25, 124–126. https://doi.org/10.1111/jon.12077

Dimmick, S.J., Faulder, K.C., 2009. Normal Variants of the Cerebral Circulation at Multidetector CT Angiography. RadioGraphics 29, 1027–1043. https://doi.org/10.1148/rg.294085730

Duan, Z., Li, Y., Guan, S., Ma, C., Han, Y., Ren, X., Wei, L., Li, W., Lou, J., Yang, Z., 2018. Morphological parameters and anatomical locations associated with rupture status of small intracranial aneurysms. Sci. Rep. 8, 6440. https://doi.org/10.1038/s41598-018-24732-1

Dufouil, C., de Kersaint-Gilly, A., Besancon, V., Levy, C., Auffray, E., Brunnereau, L., Alperovitch, A., Tzourio, C., 2001. Longitudinal study of blood pressure and white matter hyperintensities: The EVA MRI Cohort. Neurology 56, 921–926. https://doi.org/10.1212/WNL.56.7.921

Dunås, T., Wåhlin, A., Ambarki, K., Zarrinkoob, L., Malm, J., Eklund, A., 2017. A Stereotactic Probabilistic Atlas for the Major Cerebral Arteries. Neuroinformatics 15, 101–110. https://doi.org/10.1007/s12021-016-9320-y

Eaton, R., Shah, V., Dornbos III, D., Zaninovich, O., Wenger, N., Dumont, T., Powers, C., 2020. Demographic age-related variation in Circle of Willis completeness assessed by digital subtraction angiography. Brain Circ. 6, 31. https://doi.org/10.4103/bc.bc_43_19

Eftekhar, B., Dadmehr, M., Ansari, S., Ghodsi, M., Nazparvar, B., Ketabchi, E., 2006. Are the distributions of variations of circle of Willis different in different populations? – Results of an anatomical study and review of literature. BMC Neurol. 6, 22. https://doi.org/10.1186/1471-2377-6-22

Eglit, G.M.L., Weigand, A.J., Nation, D.A., Bondi, M.W., Bangen, K.J., 2020. Hypertension and Alzheimer's disease: indirect effects through circle of Willis atherosclerosis. Brain Commun. 2. https://doi.org/10.1093/braincomms/fcaa114

El-Barhoun, E., Gledhill, S., Pitman, A., 2009. Circle of Willis artery diameters on MR angiography:

An Australian reference database. J. Med. Imaging Radiat. Oncol. 53, 248–260. https://doi.org/10.1111/j.1754-9485.2009.02056.x

Fenrich, M., Habjanovic, K., Kajan, J., Heffer, M., 2021. The circle of Willis revisited: Forebrain dehydration sensing facilitated by the anterior communicating artery. BioEssays 43, 2000115. https://doi.org/10.1002/bies.202000115

Fernando, M.S., Simpson, J.E., Matthews, F., Brayne, C., Lewis, C.E., Barber, R., Kalaria, R.N., Forster, G., Esteves, F., Wharton, S.B., Shaw, P.J., O'Brien, J.T., Ince, P.G., 2006. White Matter Lesions in an Unselected Cohort of the Elderly. Stroke 37, 1391–1398. https://doi.org/10.1161/01.STR.0000221308.94473.14

Figueredo, L.F., Camila Pedraza-Ciro, M., Sebastian Lopez-McCormick, J., Javier Rueda-Esteban, R., Armando Mejía-Cordovez, J., 2019. Aneurysmal Subarachnoid Hemorrhage Associated with Small Aneurysms in Smokers and Women: A Retrospective Analysis. World Neurosurg. X 4, 100038. https://doi.org/10.1016/j.wnsx.2019.100038

Forgo, B., Tarnoki, A.D., Tarnoki, D.L., Kovacs, D.T., Szalontai, L., Persely, A., Hernyes, A., Szily, M., Littvay, L., Medda, E., Szabo, A., Kozak, L.R., Rudas, G., Sas, A., Sepsi, M., Kostyal, L., Olah, C., 2018. Are the Variants of the Circle of Willis Determined by Genetic or Environmental Factors? Results of a Twin Study and Review of the Literature. Twin Res. Hum. Genet. 21, 384–393. https://doi.org/10.1017/thg.2018.50

Griffanti, L., Jenkinson, M., Suri, S., Zsoldos, E., Mahmood, A., Filippini, N., Sexton, C.E., Topiwala, A., Allan, C., Kivimäki, M., Singh-Manoux, A., Ebmeier, K.P., Mackay, C.E., Zamboni, G., 2018. Classification and characterization of periventricular and deep white matter hyperintensities on MRI: A study in older adults. Neuroimage 170, 174–181. https://doi.org/10.1016/j.neuroimage.2017.03.024

Hakim, A., Gralla, J., Rozeik, C., Mordasini, P., Leidolt, L., Piechowiak, E., Ozdoba, C., El-Koussy, M., 2018. Anomalies and Normal Variants of the Cerebral Arterial Supply: A Comprehensive Pictorial Review with a Proposed Workflow for Classification and Significance. J. Neuroimaging 28, 14–35. https://doi.org/10.1111/jon.12475

Hendrikse, J., van Raamt, A.F., van der Graaf, Y., Mali, W.P.T.M., van der Grond, J., 2005.

Distribution of Cerebral Blood Flow in the Circle of Willis. Radiology 235, 184–189. https://doi.org/10.1148/radiol.2351031799

Horikoshi, T., Akiyama, I., Yamagata, Z., Sugita, M., Nukui, H., 2002. Magnetic resonance angiographic evidence of sex-linked variations in the circle of Willis and the occurrence of cerebral aneurysms. J. Neurosurg. 96, 697–703. https://doi.org/10.3171/jns.2002.96.4.0697

Ingebrigtsen, T., Morgan, M.K., Faulder, K., Ingebrigtsen, L., Sparr, T., Schirmer, H., 2004. Bifurcation geometry and the presence of cerebral artery aneurysms. J. Neurosurg. 101, 108–113. https://doi.org/10.3171/jns.2004.101.1.0108

Iqbal, S., 2013. A comprehensive study of the anatomical variations of the circle of Willis in adult human brains. J. Clin. Diagnostic Res. 7, 2423–2427. https://doi.org/10.7860/JCDR/2013/6580.3563

Isaksen, J., Egge, A., Waterloo, K., Romner, B., Ingebrigtsen, T., 2002. Risk factors for aneurysmal subarachnoid haemorrhage: the Tromso study. J. Neurol. Neurosurg. Psychiatry 73, 185–187. https://doi.org/10.1136/jnnp.73.2.185

Jacobsen, B.K., Eggen, A.E., Mathiesen, E.B., Wilsgaard, T., Njolstad, I., 2012. Cohort profile: The Tromso Study. Int. J. Epidemiol. 41, 961–967. https://doi.org/10.1093/ije/dyr049

Jeng, M., 2006. A selected history of expectation bias in physics. Am. J. Phys. 74, 578–583. https://doi.org/10.1119/1.2186333

Jones, J.D., Castanho, P., Bazira, P., Sanders, K., 2020. Anatomical variations of the circle of Willis and their prevalence, with a focus on the posterior communicating artery: A literature review and meta-analysis. Clin. Anat. ca.23662. https://doi.org/10.1002/ca.23662

Kane, A.G., Dillon, W.P., Barkovich, A.J., Norman, D., Dowd, C.F., Kane, T.T., 1996. Reduced caliber of the internal carotid artery: a normal finding with ipsilateral absence or hypoplasia of the A1 segment. AJNR. Am. J. Neuroradiol. 17, 1295–301.

Kang, T., Mukherjee, D., Kim, J.-M., Park, K.-Y., Ryu, J., 2021. Effects of progressive carotid stenosis on cerebral haemodynamics: aortic-cerebral 3D patient-specific simulation. Eng. Appl. Comput. Fluid Mech. 15, 830–847. https://doi.org/10.1080/19942060.2021.1916601

Kapoor, K., Kak, V.K., Singh, B., 2003. Morphology and Comparative Anatomy of Circulus

Arteriosus Cerebri in Mammals. Anat. Histol. Embryol. J. Vet. Med. Ser. C 32, 347–355. https://doi.org/10.1111/j.1439-0264.2003.00492.x

Kapoor, K., Singh, B., Dewan, L.I.J., 2008. Variations in the configuration of the circle of Willis. Anat. Sci. Int. 83, 96–106. https://doi.org/10.1111/j.1447-073X.2007.00216.x

Kayembe, K.N., Sasahara, M., Hazama, F., 1984. Cerebral aneurysms and variations in the circle of Willis. Stroke 15, 846–850. https://doi.org/10.1161/01.STR.15.5.846

Klimek-Piotrowska, W., Kopeć, M., Kochana, M., Krzyżewski, R.M., Tomaszewski, K.A., Brzegowy, P., Walocha, J., 2013. Configurations of the circle of Willis: a computed tomography angiography based study on a Polish population. Folia Morphol. (Warsz). 72, 293–299. https://doi.org/10.5603/FM.2013.0049

Klimek-Piotrowska, W., Rybicka, M., Wojnarska, A., Wójtowicz, A., Koziej, M., Hołda, M.K., 2016. A multitude of variations in the configuration of the circle of Willis: an autopsy study. Anat. Sci. Int. 91, 325–333. https://doi.org/10.1007/s12565-015-0301-2

Krabbe-Hartkamp, M.J., van der Grond, J., de Leeuw, F.E., de Groot, J.C., Algra, A., Hillen, B., Breteler, M.M., Mali, W.P., 1998. Circle of Willis: morphologic variation on three-dimensional time-of-flight MR angiograms. Radiology 207, 103–111. https://doi.org/10.1148/radiology.207.1.9530305

Kuijf, H.J., Casamitjana, A., Collins, D.L., Dadar, M., Georgiou, A., Ghafoorian, M., Jin, D., Khademi, A., Knight, J., Li, H., Llado, X., Biesbroek, J.M., Luna, M., Mahmood, Q., McKinley, R., Mehrtash, A., Ourselin, S., Park, B.-Y., Park, H., Park, S.H., Pezold, S., Puybareau, E., De Bresser, J., Rittner, L., Sudre, C.H., Valverde, S., Vilaplana, V., Wiest, R., Xu, Y., Xu, Z., Zeng, G., Zhang, J., Zheng, G., Heinen, R., Chen, C., van der Flier, W., Barkhof, F., Viergever, M.A., Biessels, G.J., Andermatt, S., Bento, M., Berseth, M., Belyaev, M., Cardoso, M.J., 2019. Standardized Assessment of Automatic Segmentation of White Matter Hyperintensities and Results of the WMH Segmentation Challenge. IEEE Trans. Med. Imaging 38, 2556–2568. https://doi.org/10.1109/TMI.2019.2905770

Lazzaro, M.A., Ouyang, B., Chen, M., 2012. The role of circle of Willis anomalies in cerebral aneurysm rupture. J. Neurointerv. Surg. 4, 22–26. https://doi.org/10.1136/jnis.2010.004358

Li, H., Jiang, G., Zhang, J., Wang, R., Wang, Z., Zheng, W.-S., Menze, B., 2018. Fully convolutional network ensembles for white matter hyperintensities segmentation in MR images. Neuroimage 183, 650–665. https://doi.org/10.1016/j.neuroimage.2018.07.005

Li, H., Xiong, Y., Xu, G., Zhang, R., Zhu, W., Yin, Q., Ma, M., Fan, X., Yang, F., Liu, W., Duan, Z., Liu, X., 2015. The Circle of Willis and White Matter Lesions in Patients with Carotid Atherosclerosis. J. Stroke Cerebrovasc. Dis. 24, 1749–1754. https://doi.org/10.1016/j.jstrokecerebrovasdis.2015.03.048

Li, J., Zheng, L., Yang, W.-J., Sze-To, C.-Y., Leung, T.W.-H., Chen, X.-Y., 2021. Plaque Wall Distribution Pattern of the Atherosclerotic Middle Cerebral Artery Associates With the Circle of Willis Completeness. Front. Neurol. 11. https://doi.org/10.3389/fneur.2020.599459

Li, M.-H., Chen, S.-W., Li, Y.-D., Chen, Y.-C., Cheng, Y.-S., Hu, D.-J., Tan, H.-Q., Wu, Q., Wang, W., Sun, Z.-K., Wei, X.-E., Zhang, J.-Y., Qiao, R.-H., Zong, W.-H., Zhang, Y., Lou, W., Chen, Z.-Y., Zhu, Y., Peng, D.-R., Ding, S.-X., Xu, X.-F., Hou, X.-H., Jia, W.-P., 2013. Prevalence of Unruptured Cerebral Aneurysms in Chinese Adults Aged 35 to 75 Years. Ann. Intern. Med. 159, 514. https://doi.org/10.7326/0003-4819-159-8-201310150-00004

Li, Q., Li, J., Lv, F., Li, K., Luo, T., Xie, P., 2011. A multidetector CT angiography study of variations in the circle of Willis in a Chinese population. J. Clin. Neurosci. 18, 379–383. https://doi.org/10.1016/j.jocn.2010.07.137

Lindekleiv, H., Sandvei, M.S., Romundstad, P.R., Wilsgaard, T., Njølstad, I., Ingebrigtsen, T., Vik, A., Mathiesen, E.B., 2012. Joint effect of modifiable risk factors on the risk of aneurysmal subarachnoid hemorrhage: A cohort study. Stroke 43, 1885–1889. https://doi.org/10.1161/STROKEAHA.112.651315

Løvsletten, O., Njølstad, I., Wilsgaard, T., Hopstock, L.A., Jacobsen, B.K., Bønaa, K.H., Eggen, A.E., Løchen, M.-L., 2021. Is the ongoing obesity epidemic partly explained by concurrent decline in cigarette smoking? Insights from a longitudinal population study. The Tromsø Study 1994–2016. Prev. Med. (Baltim). 147, 106533. https://doi.org/10.1016/j.ypmed.2021.106533

Mitchell, G.F., van Buchem, M.A., Sigurdsson, S., Gotal, J.D., Jonsdottir, M.K., Kjartansson, Ó., Garcia, M., Aspelund, T., Harris, T.B., Gudnason, V., Launer, L.J., 2011. Arterial stiffness,

pressure and flow pulsatility and brain structure and function: the Age, Gene/Environment Susceptibility – Reykjavik Study. Brain 134, 3398–3407. https://doi.org/10.1093/brain/awr253

Molnár, Z., 2021. On the 400th anniversary of the birth of Thomas Willis. Brain 144, 1033–1037. https://doi.org/10.1093/brain/awab016

Morseth, B., Hopstock, L.A., 2020. Time trends in physical activity in the Tromsø study: An update. PLoS One 15, e0231581. https://doi.org/10.1371/journal.pone.0231581

Mukherjee, D., Jani, N.D., Narvid, J., Shadden, S.C., 2018. The Role of Circle of Willis Anatomy Variations in Cardio-embolic Stroke: A Patient-Specific Simulation Based Study. Ann. Biomed. Eng. 46, 1128–1145. https://doi.org/10.1007/s10439-018-2027-5

Müller, T.B., Sandvei, M.S., Kvistad, K.A., Rydland, J., Håberg, A., Vik, A., Gårseth, M., Stovner, L.J., 2013. Unruptured Intracranial Aneurysms in the Norwegian Nord-Trøndelag Health Study (HUNT). Neurosurgery 73, 256–261. https://doi.org/10.1227/01.neu.0000430295.23799.16

Murray, M.E., Senjem, M.L., Petersen, R.C., Hollman, J.H., Preboske, G.M., Weigand, S.D., Knopman, D.S., Ferman, T.J., Dickson, D.W., Jack, C.R., 2010. Functional Impact of White Matter Hyperintensities in Cognitively Normal Elderly Subjects. Arch. Neurol. 67. https://doi.org/10.1001/archneurol.2010.280

Nieuwkamp, D.J., Setz, L.E., Algra, A., Linn, F.H., de Rooij, N.K., Rinkel, G.J., 2009. Changes in case fatality of aneurysmal subarachnoid haemorrhage over time, according to age, sex, and region: a meta-analysis. Lancet Neurol. 8, 635–642. https://doi.org/10.1016/S1474-4422(09)70126-7

Nixon, A.M., Gunel, M., Sumpio, B.E., 2010. The critical role of hemodynamics in the development of cerebral vascular disease. J. Neurosurg. 112, 1240–1253. https://doi.org/10.3171/2009.10.JNS09759

Njølstad, I., Mathiesen, E.B., Schirmer, H., Thelle, D.S., 2016. The Tromsø study 1974–2016: 40 years of cardiovascular research. Scand. Cardiovasc. J. 50, 276–281. https://doi.org/10.1080/14017431.2016.1239837

Nyquist, P.A., Bilgel, M., Gottesman, R., Yanek, L.R., Moy, T.F., Becker, L.C., Cuzzocreo, J.L., Prince, J., Wasserman, B.A., Yousem, D.M., Becker, D.M., Kral, B.G., Vaidya, D., 2015. Age

differences in periventricular and deep white matter lesions. Neurobiol. Aging 36, 1653–1658. https://doi.org/10.1016/j.neurobiolaging.2015.01.005

O'Donnell, M.J., Chin, S.L., Rangarajan, S., Xavier, D., Liu, L., Zhang, H., Rao-Melacini, P., Zhang, X., Pais, P., Agapay, S., Lopez-Jaramillo, P., Damasceno, A., Langhorne, P., McQueen, M.J., Rosengren, A., Dehghan, M., Hankey, G.J., Dans, A.L., Elsayed, A., Avezum, A., Mondo, C., Diener, H.-C., Ryglewicz, D., Czlonkowska, A., Pogosova, N., Weimar, C., Iqbal, R., Diaz, R., Yusoff, K., Yusufali, A., Oguz, A., Wang, X., Penaherrera, E., Lanas, F., Ogah, O.S., Ogunniyi, A., Iversen, H.K., Malaga, G., Rumboldt, Z., Oveisgharan, S., Al Hussain, F., Magazi, D., Nilanont, Y., Ferguson, J., Pare, G., Yusuf, S., 2016. Global and regional effects of potentially modifiable risk factors associated with acute stroke in 32 countries (INTERSTROKE): a case-control study. Lancet 388, 761–775. https://doi.org/10.1016/S0140-6736(16)30506-2

Ozaki, T., Handa, H., Tomimoto, K., Hazama, F., 1977. Anatomical Variations of the Arterial System of the Base of the Brain. Arch. für japanische Chir. 46, 3–17.

Pascalau, R., Padurean, V.A., Bartoș, D., Bartoș, A., Szabo, B.A., 2018. The geometry of the circle of willis anatomical variants as a potential cerebrovascular risk factor. Turk. Neurosurg. https://doi.org/10.5137/1019-5149.JTN.21835-17.3

Provenzano, F.A., Muraskin, J., Tosto, G., Narkhede, A., Wasserman, B.T., Griffith, E.Y., Guzman, V.A., Meier, I.B., Zimmerman, M.E., Brickman, A.M., Alzheimer's Disease Neuroimaging Initiative, for the, 2013. White Matter Hyperintensities and Cerebral Amyloidosis. JAMA Neurol. 70, 455. https://doi.org/10.1001/jamaneurol.2013.1321

Qiu, C., Zhang, Y., Xue, C., Jiang, S., Zhang, W., 2015. MRA study on variation of the circle of Willis in healthy Chinese male adults. Biomed Res. Int. 2015, 8. https://doi.org/10.1155/2015/976340

Riggs, H.E., Rupp, C., 1963. Variation in Form of Circle of Willis. Arch. Neurol. 8, 8–14. https://doi.org/10.1001/archneur.1963.00460010024002

Robben, D., Sunaert, S., Thijs, V., Wilms, G., Maes, F., Suetens, P., 2013. Anatomical Labeling of the Circle of Willis Using Maximum A Posteriori Graph Matching, in: Miccai. pp. 566–573. https://doi.org/10.1007/978-3-642-40811-3_71

Robben, D., Türetken, E., Sunaert, S., Thijs, V., Wilms, G., Fua, P., Maes, F., Suetens, P., 2016. Simultaneous segmentation and anatomical labeling of the cerebral vasculature. Med. Image Anal. 32, 201–215. https://doi.org/10.1016/j.media.2016.03.006

Román, G.C., Erkinjuntti, T., Wallin, A., Pantoni, L., Chui, H.C., 2002. Subcortical ischaemic vascular dementia. Lancet Neurol. 1, 426–436. https://doi.org/10.1016/S1474-4422(02)00190-4

Ryan, D.J., Byrne, S., Dunne, R., Harmon, M., Harbison, J., 2015. White Matter Disease and an Incomplete Circle of Willis. Int. J. Stroke 10, 547–552. https://doi.org/10.1111/ijs.12042

Saba, L., Raz, E., Fatterpekar, G., Montisci, R., di Martino, M., Bassareo, P.P., Piga, M., 2015. Correlation between Leukoaraiosis Volume and Circle of Willis Variants. J. Neuroimaging 25, 226–231. https://doi.org/10.1111/jon.12103

Saba, L., Sanfilippo, R., Porcu, M., Lucatelli, P., Montisci, R., Zaccagna, F., Suri, J.S., Anzidei, M., Wintermark, M., 2017. Relationship between white matter hyperintensities volume and the circle of Willis configurations in patients with carotid artery pathology. Eur. J. Radiol. 89, 111–116. https://doi.org/10.1016/j.ejrad.2017.01.031

Sharashova, E., Wilsgaard, T., Ball, J., Morseth, B., Gerdts, E., Hopstock, L.A., Mathiesen, E.B., Schirmer, H., Løchen, M.-L., 2020. Long-term blood pressure trajectories and incident atrial fibrillation in women and men: the Tromsø Study. Eur. Heart J. 41, 1554–1562. https://doi.org/10.1093/eurheartj/ehz234

Silbert, L.C., Nelson, C., Howieson, D.B., Moore, M.M., Kaye, J.A., 2008. Impact of white matter hyperintensity volume progression on rate of cognitive and motor decline. Neurology 71, 108–113. https://doi.org/10.1212/01.wnl.0000316799.86917.37

Skodvin, T.Ø., Evju, Ø., Sorteberg, A., Isaksen, J.G., 2019. Prerupture Intracranial Aneurysm Morphology in Predicting Risk of Rupture: A Matched Case-Control Study. Neurosurgery 84, 132–140. https://doi.org/10.1093/neuros/nyy010

Songsaeng, D., Geibprasert, S., Willinsky, R., Tymianski, M., Terbrugge, K.G., Krings, T., 2010. Impact of anatomical variations of the circle of Willis on the incidence of aneurysms and their recurrence rate following endovascular treatment. Clin. Radiol. 65, 895–901. https://doi.org/10.1016/j.crad.2010.06.010

Stojanović, N.N., Kostić, A., Mitić, R., Berilažić, L., Radisavljević, M., 2019. Association between Circle of Willis Configuration and Rupture of Cerebral Aneurysms. Medicina (B. Aires). 55, 338. https://doi.org/10.3390/medicina55070338

Takeuchi, M., Miwa, K., Tanaka, M., Zhou, Y., Todo, K., Sasaki, T., Sakaguchi, M., Kitagawa, K., Mochizuki, H., 2019. A 9-Year Longitudinal Study of Basilar Artery Diameter. J. Am. Heart Assoc. 8. https://doi.org/10.1161/JAHA.118.011154

ten Dam, V.H., van den Heuvel, D.M.J., de Craen, A.J.M., Bollen, E.L.E.M., Murray, H.M., Westendorp, R.G.J., Blauw, G.J., van Buchem, M.A., 2007. Decline in Total Cerebral Blood Flow Is Linked with Increase in Periventricular but Not Deep White Matter Hyperintensities. Radiology 243, 198–203. https://doi.org/10.1148/radiol.2431052111

Uston, C., 2005. NEUROwords Dr. Thomas Willis' Famous Eponym: The Circle of Willis. J. Hist. Neurosci. 14, 16–21. https://doi.org/10.1080/096470490512553

van der Grond, J., van Raamt, A.F., van der Graaf, Y., Mali, W.P.T.M., Bisschops, R.H.C., 2004. A fetal circle of Willis is associated with a decreased deep white matter lesion load. Neurology 63, 1452–1456. https://doi.org/10.1212/01.WNL.0000142041.42491.F4

van der Kouwe, A.J.W., Benner, T., Fischl, B., Schmitt, F., Salat, D.H., Harder, M., Sorensen, A.G., Dale, A.M., 2005. On-line automatic slice positioning for brain MR imaging. Neuroimage 27, 222–230. https://doi.org/10.1016/j.neuroimage.2005.03.035

van Dijk, E.J., Prins, N.D., Vrooman, H.A., Hofman, A., Koudstaal, P.J., Breteler, M.M.B., 2008. Progression of Cerebral Small Vessel Disease in Relation to Risk Factors and Cognitive Consequences. Stroke 39, 2712–2719. https://doi.org/10.1161/STROKEAHA.107.513176

Van Kammen, M.S., Moomaw, C.J., Van Der Schaaf, I.C., Brown, R.D., Woo, D., Broderick, J.P., Mackey, J.S., Rinkel, G.J.E., Huston, J., Ruigrok, Y.M., 2018. Heritability of circle of Willis variations in families with intracranial aneurysms. PLoS One 13, 1–9. https://doi.org/10.1371/journal.pone.0191974

van Laar, P.J., Hendrikse, J., Golay, X., Lu, H., Van Osch, M.J.P., Van Der Grond, J., 2006. In vivo flow territory mapping of major brain feeding arteries. Neuroimage 29, 136–144. https://doi.org/10.1016/j.neuroimage.2005.07.011

van Seeters, T., Hendrikse, J., Biessels, G.J., Velthuis, B.K., Mali, W.P., Kappelle, L.J., van der Graaf, Y., 2015. Completeness of the circle of Willis and risk of ischemic stroke in patients without cerebrovascular disease. Neuroradiology 57, 1247–1251. https://doi.org/10.1007/s00234-015-1589-2

Vangberg, T.R., Eikenes, L., Håberg, A.K., 2019. The effect of white matter hyperintensities on regional brain volumes and white matter microstructure, a population-based study in HUNT. Neuroimage 203, 116158. https://doi.org/10.1016/j.neuroimage.2019.116158

Vernooij, M.W., Ikram, M.A., Tanghe, H.L., Vincent, A.J.P.E., Hofman, A., Krestin, G.P., Niessen, W.J., Breteler, M.M.B., van der Lugt, A., 2007. Incidental Findings on Brain MRI in the General Population. N. Engl. J. Med. 357, 1821–1828. https://doi.org/10.1056/NEJMoa070972

Vittinghoff, E., McCulloch, C.E., 2007. Relaxing the Rule of Ten Events per Variable in Logistic and Cox Regression. Am. J. Epidemiol. 165, 710–718. https://doi.org/10.1093/aje/kwk052

Vlak, M.H.M., Algra, A., Brandenburg, R., Rinkel, G.J.E., 2011. Prevalence of unruptured intracranial aneurysms, with emphasis on sex, age, comorbidity, country, and time period: a systematic review and meta-analysis. Lancet Neurol. 10, 626–636. https://doi.org/10.1016/S1474-4422(11)70109-0

Vrselja, Z., Brkic, H., Curic, G., 2015. Arterial tree asymmetry reduces cerebral pulsatility. Med. Hypotheses 85, 622–627. https://doi.org/10.1016/j.mehy.2015.07.030

Vrselja, Z., Brkic, H., Mrdenovic, S., Radic, R., Curic, G., 2014. Function of Circle of Willis. J. Cereb. Blood Flow Metab. 34, 578–584. https://doi.org/10.1038/jcbfm.2014.7

Wardlaw, J.M., Allerhand, M., Doubal, F.N., Morris, Z., Gow, A.J., Bastin, M.E., Starr, J.M., Dennis, M.S., 2014. Vascular risk factors , large-artery atheroma , and brain white matter hyperintensities. Neurology 82, 1331–1338. https://doi.org/10.1212/WNL.0000000000000312

Wardlaw, J.M., Valdés Hernández, M.C., Muñoz-Maniega, S., 2015. What are White Matter Hyperintensities Made of? Relevance to Vascular Cognitive Impairment. J. Am. Heart Assoc. 4, e001140. https://doi.org/10.1161/JAHA.114.001140

Warnert, E.A.H., Rodrigues, J.C.L., Burchell, A.E., Neumann, S., Ratcliffe, L.E.K., Manghat, N.E., Harris, A.D., Adams, Z., Nightingale, A.K., Wise, R.G., Paton, J.F.R., Hart, E.C., 2016. Is High

Blood Pressure Self-Protection for the Brain? Circ. Res. 119, e140–e151. https://doi.org/10.1161/CIRCRESAHA.116.309493

Wijesinghe, P., Steinbusch, H.W.M., Shankar, S.K., Yasha, T.C., De Silva, K.R.D., 2020. Circle of Willis abnormalities and their clinical importance in ageing brains: A cadaveric anatomical and pathological study. J. Chem. Neuroanat. 106, 101772. https://doi.org/10.1016/j.jchemneu.2020.101772

Wright, S.N., Kochunov, P., Mut, F., Bergamino, M., Brown, K.M., Mazziotta, J.C., Toga, A.W., Cebral, J.R., Ascoli, G. a, 2013. Digital reconstruction and morphometric analysis of human brain arterial vasculature from magnetic resonance angiography. Neuroimage 82, 170–181. https://doi.org/10.1016/j.neuroimage.2013.05.089

Wu, T.-C., Chen, T.-Y., Ko, C.-C., Chen, J.-H., Lin, C.-P., 2020. Correlation of internal carotid artery diameter and carotid flow with asymmetry of the circle of Willis. BMC Neurol. 20, 251. https://doi.org/10.1186/s12883-020-01831-z

Ye, H., Wu, X., Yan, J., Wang, J., Qiu, J., Wang, Y., 2019. Completeness of circle of Willis and white matter hyperintensities in patients with severe internal carotid artery stenosis. Neurol. Sci. 40, 509–514. https://doi.org/10.1007/s10072-018-3683-9

Zaninovich, O.A., Ramey, W.L., Walter, C.M., Dumont, T.M., 2017. Completion of the Circle of Willis Varies by Gender, Age, and Indication for Computed Tomography Angiography. World Neurosurg. 106, 953–963. https://doi.org/10.1016/j.wneu.2017.07.084

Zarrinkoob, L., Ambarki, K., Wåhlin, A., Birgander, R., Carlberg, B., Eklund, A., Malm, J., 2016. Aging alters the dampening of pulsatile blood flow in cerebral arteries. J. Cereb. Blood Flow Metab. 36, 1519–1527. https://doi.org/10.1177/0271678X16629486

Zheng, Y., Zhou, B., Wang, X., Chen, H., Fang, X., Jiang, P., Yang, H., He, C., Yang, G., Song, Y., An, Q., Leng, B., 2019. Size, Aspect Ratio and Anatomic Location of Ruptured Intracranial Aneurysms: Consecutive Series of 415 Patients from a Prospective, Multicenter, Observational Study. Cell Transplant. 28, 739–746. https://doi.org/10.1177/0963689718817227

Paper I

PLOS ONE

RESEARCH ARTICLE

Variations in the Circle of Willis in a large population sample using 3D TOF angiography: The Tromsø Study

Lars B. Hindenes[1,2]*, **Asta K. Håberg**[3,4], **Liv Hege Johnsen**[1], **Ellisiv B. Mathiesen**[1,5], **David Robben**[6,7], **Torgil R. Vangberg**[1,2]

1 Department of Clinical Medicine, Faculty of Health Sciences, UiT The Arctic University of Norway, Tromsø, Norway, **2** PET Centre, University Hospital of North Norway, Tromsø, Norway, **3** Department of Radiology and Nuclear Medicine, St. Olav University Hospital, Trondheim, Norway, **4** Department of Neuromedicine and Movement Science, Norwegian University of Science and Technology (NTNU), Trondheim, Norway, **5** Department of Neurology, University Hospital of North Norway, Tromsø, Norway, **6** ESAT-PSI, Department of Electrical Engineering, KU Leuven, Leuven, Belgium, **7** Icometrix, Leuven, Belgium

* lars.b.hindenes@uit.no

Citation: Hindenes LB, Håberg AK, Johnsen LH, Mathiesen EB, Robben D, Vangberg TR (2020) Variations in the Circle of Willis in a large population sample using 3D TOF angiography: The Tromsø Study. PLoS ONE 15(11): e0241373. https://doi.org/10.1371/journal.pone.0241373

Editor: Pascal A. T. Baltzer, Medical University of Vienna, AUSTRIA

Received: July 3, 2020

Accepted: October 14, 2020

Published: November 3, 2020

Data Availability Statement: Ethical and legal restrictions prohibit the authors from making the dataset available outside The Tromsø Study database, which is available by contacting The Tromsø Study. Please see https://en.uit.no/forskning/forskningsgrupper/sub?p_document_id=453582&sub_id=669706 for detail on how to obtain access to all relevant data.

Funding: This work was supported by a Helse Nord project grant (HNF1369-17) to LBH and (SFP1271-16) for collecting the MR data. Icometrix provided

Abstract

The main arteries that supply blood to the brain originate from the Circle of Willis (CoW). The CoW exhibits considerable anatomical variations which may have clinical importance, but the variability is insufficiently characterised in the general population. We assessed the anatomical variability of CoW variants in a community-dwelling sample (N = 1,864, 874 men, mean age = 65.4, range 40–87 years), and independent and conditional frequencies of the CoW's artery segments. CoW segments were classified as present or missing/hypoplastic (w/1mm diameter threshold) on 3T time-of-flight magnetic resonance angiography images. We also examined whether age and sex were associated with CoW variants. We identified 47 unique CoW variants, of which five variants constituted 68.5% of the sample. The complete variant was found in 11.9% of the subjects, and the most common variant (27.8%) was missing both posterior communicating arteries. Conditional frequencies showed patterns of interdependence across most missing segments in the CoW. CoW variants were associated with mean-split age (P = .0147), and there was a trend showing more missing segments with increasing age. We found no association with sex (P = .0526). Our population study demonstrated age as associated with CoW variants, suggesting reduced collateral capacity with older age.

Introduction

The primary blood supply to the brain originates from the left and right internal carotid arteries and the basilar artery. These arteries anastomose to form the Circle of Willis (CoW) at the base of the brain (S1 Fig in S1 File). The circular arrangement of the arteries enables the redistribution of blood flow when arteries in or upstream of the CoW experience reduced flow. This collateral ability of the CoW provides redundancy in the blood supply to the brain.

salary for DR. Helse Nord and Icometrix had no role in study design, data collection and analysis, decision to publish, or preparation of the manuscript. The specific roles of these authors are articulated in the 'author contributions' section.

Competing interests: The authors declare no conflict of interests. DR received salary from Icometrix during this study, but this does not alter our adherence to PLOS ONE policies on sharing data and materials.

Segments in the CoW are commonly missing or hypoplastic rendering the CoW incomplete, thereby reducing the collateral capacity of the CoW and increasing the brain's vulnerability to changes in the blood flow [1–3].

The CoW anatomy is clinically relevant as incomplete CoW variants are associated with an increased risk of cerebrovascular disease. Studies on patient samples find that incomplete CoW variants are associated with stroke [4, 5], aneurisms [6, 7] and white matter hyperintensities [8–11]. The CoW variants are also important in certain surgical procedures [12, 13]. It is not clear if incomplete variants pose a similar risk in the general population.

Greatly varying prevalence estimates limit our understanding of the anatomical variability in the CoW. For example, the estimated prevalence of the complete variant range from 12.2% [3] to 45.0% [14]. Differences in sample characteristic [1, 12, 15, 16], sample size [17], and measuring techniques [1, 15] are sources of variability. Additionally, many CoW classification schemes cannot be compared fully, complicating the comparison between studies [1, 11, 18–20]. Common classification schemes include using one or more diameter thresholds for arteries [5, 12, 18, 19, 21, 22], comparing diameters of arteries relative to other arteries' diameter [3, 6, 23], or a mix of both [1, 8, 15, 24]. Other schemes split the CoW classification into anterior and posterior circulation [1, 5], or omit distinguishing between left and right sided variants [2, 3, 20]. One study did not report its classification scheme [2].

The primary goal of this study was to report population-based estimates of the prevalence of CoW variants based on 3T MR angiography images using a classification scheme adapted for more detailed quantitative analyses. We also examined if CoW variants were associated with age and sex, and we reported the frequency of individual missing arteries in the CoW and similarly their conditional frequencies, independently of CoW variants.

Materials and methods

The Tromsø Study

The Tromsø Study is a population-based cohort study recruiting from the Tromsø municipality in Norway. This study has been performed every six to seven years since 1974 and the seventh survey (Tromsø 7) was performed in 2015–2016. Tromsø 7 consisted of two visits. All inhabitants above age 40 were invited to the 1st visit, and 20,183 subjects participated (65% participation rate). A subset of participants in the first part of the Tromsø 7 Study were invited to a 2nd visit, where 8,346 subjects participated. Of these, 2,973 were invited to partake in a cross-sectional magnetic resonance (MR) study. Of the invited, 525 declined, 396 did not respond, 169 had conditions prohibiting MR examinations, and five had moved or were dead. Furthermore, for 14 cases we were unable to find at least one of three baseline MRI series, consequently yielding 1,864 subjects with time-of-flight (TOF) angiography series, T1-weighted series, and T2-weighted fluid-attenuated inversion recovery (FLAIR) series (Fig 1). The study was approved by the Regional Committee of Medical and Health Research Ethics Northern Norway (2014/1665/REK-Nord) and carried out in accordance with relevant guidelines and regulations at UiT The Arctic University of Norway. All participants gave written informed consent before participating in the study.

MRI protocol

Participants were scanned at the University Hospital North Norway in a 3T Siemens Skyra MR scanner (Siemens Healthcare, Erlangen, Germany). A 64-channel head coil was used in most examinations, but in 39 examinations, a slightly larger 20-channel head coil had to be used. The MRI protocol consisted of a 3D T1-weighted series, a 3D T2-weighted FLAIR series, a susceptibility weighted series and a TOF angiography series, with a total scan time of 22

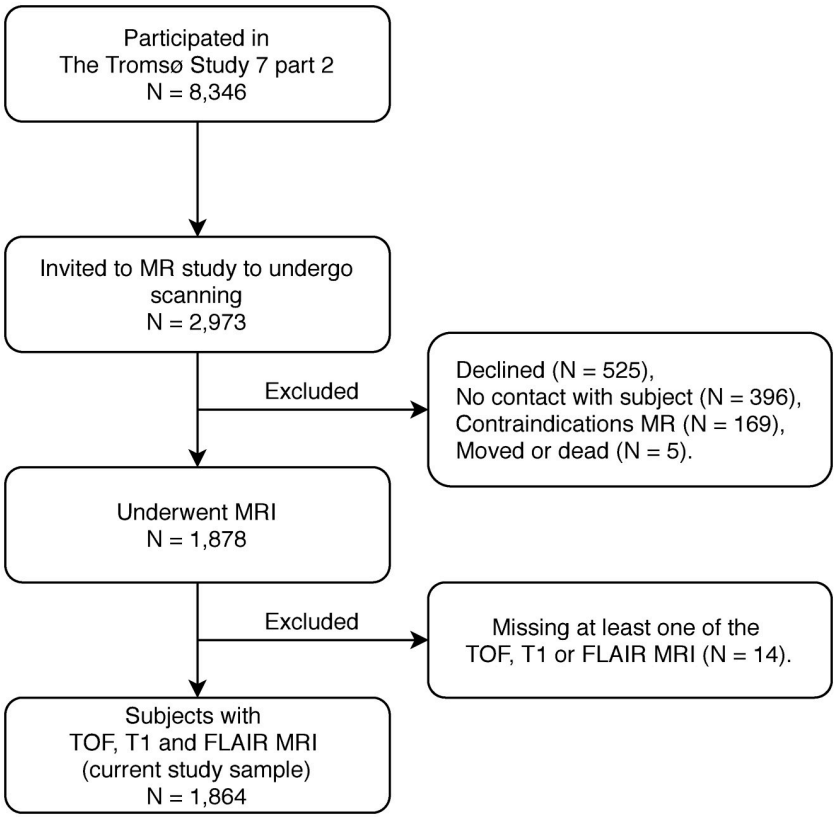

Fig 1. Flow chart of the selection of subjects from the seventh Tromsø Study to the current study. MR = Magnetic resonance, MRI = Magnetic resonance imaging, TOF = Time-of-flight angiography series, T1 = T1-weighted series, FLAIR = T2-weighted fluid-attenuated inversion recovery series.

https://doi.org/10.1371/journal.pone.0241373.g001

minutes. Only the TOF images were used in this study. These were acquired with a 3D transversal fast low angle shot sequence with flow compensation (TR/TE = 21/3.43 ms, parallel imaging acceleration factor 3, FOV 200 × 181 mm, slice thickness 0.5 mm, 7 slabs with 40 slices each). Reconstructed image resolution was 0.3 × 0.3 × 0.5 mm. The slice prescription was automatically aligned to a standardized brain atlas ensuring consistency across examinations [25].

Classification of CoW variants

TOF images were evaluated by LBH, using a program created in MeVisLab (v3.0.1). The program displays the TOF images both as a 3D rendering or a maximum intensity projection (MIP), and in 2D with a lumen diameter measurement tool. For rating an artery as present, the following criteria were used: (1) visible along its entire segment on the 3D rendering, (2) have a diameter larger than 1 mm, (3) connected to other arteries as in the complete textbook CoW. It is difficult to reliably identify smaller than 1 mm on TOF MRI due to the image resolution and possibly low flow rates in small arteries. Due to these limitations, we followed the convention as in most studies of the CoW [1, 5, 12, 18, 19, 21, 22] and did not differentiate between missing and hypoplastic segments. We emphasize, however, that when we refer to missing segments of the CoW we mean "missing or hypoplastic". The classification criteria are illustrated in Fig 2 with different degrees of hypoplastic/missing arteries. Compare it to S1 Fig in S1 File for a complete "textbook-type" CoW.

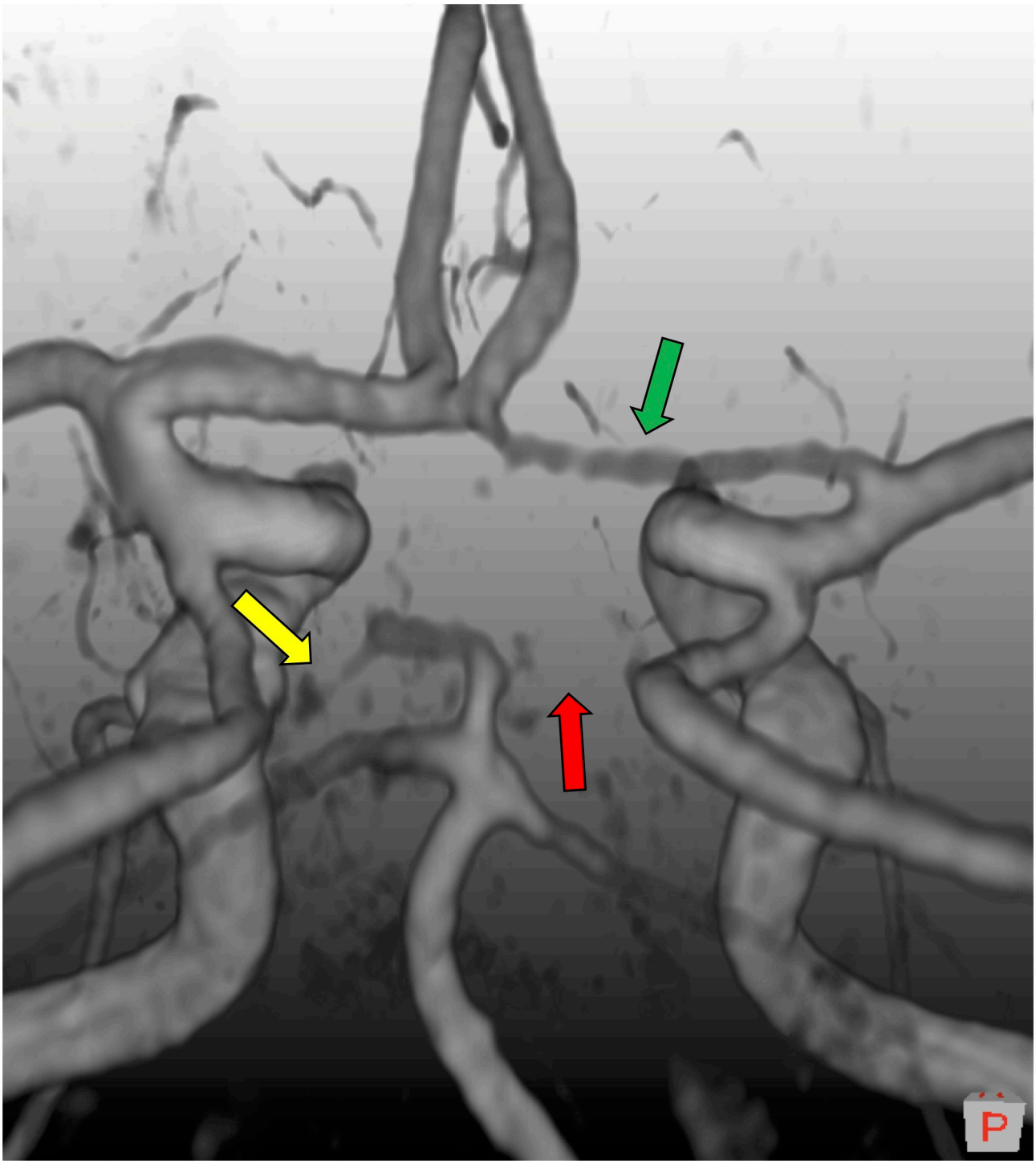

Fig 2. 3D volume rendering of a time-of-flight image depicting three classification cases within our classification scheme. Green arrow: The right anterior cerebral artery is present. Yellow arrow: The left posterior cerebral artery is hypoplastic or missing, and just below 1mm in diameter. Red arrow: The right posterior cerebral artery is clearly missing. The configuration itself is of bilateral missing posterior cerebral artery (2P) type. Image follows neurological convention, where left is left and right is right. An orientation cube in the lower right corner show orientation, and its P denotes posterior.

https://doi.org/10.1371/journal.pone.0241373.g002

The CoW consists of seven arteries, all of which were considered in our variants. First, the left and right proximal anterior cerebral artery (ACA), the anterior communicating artery (ACoA), the left and right posterior communicating artery (PCoA), and the left and right proximal posterior cerebral artery (PCA). We also considered the three largest in-flow arteries, both the left and right internal carotid artery (ICA) and the basilar artery (BA), and the left and right middle cerebral artery (MCA) in relation to the variants, because they, although rarely, can be missing and are important for interpreting the collateral flow in a CoW. The distal ACA and distal PCA segments were not considered since they are almost always present and can receive collateral flow through ACoA, and PCoA or PCA, respectively. A textbook CoW is visualised in S1 Fig in S1 File. There were some rare variants that did not fit into the regular classification of the CoW, such as the persistent primitive trigeminal artery, described in Dimmick et al. [26], which was ignored. Arterial segments that did not connect to their expected locations were classified according to the third criterion. For instance, variations in the ACoA, of which there are many of [3], were all regarded as a single ACoA. Furthermore, a posterior CoW variant named unilateral dual PCA (S2 Fig in S1 File) was categorized as missing a PCoA using the third criterion, because of the missing connection between the PCoA and its ipsilateral PCA. This simplification via the third criterion does not compromise the descriptions of the collateral flow ability within each CoW variant.

We labelled the CoW variants using a nomenclature similar to previous studies [1, 6], where each variant's name signified the missing segments. For brevity, ACA were denoted by "A", ACoA by "Ac", PCA by "P", PCoA by "Pc", ICA by "I", MCA by "M", and BA by "B". Alternatively, when no artery segment was missing a complete CoW was denoted by "O". To specify whether a missing segment was in the left or right hemisphere, an "l" or "r" suffix is used. If the same segment was missing on both sides the number "2" was instead used as a prefix, e.g. "2Pc" for the variant where both PCoA are missing. This scheme ensured unique names for all CoW variants. See Fig 3 for illustrations of variants with their corresponding label.

A random sample (N = 100) was blinded and reclassified by the same rater (LBH), and also another rater (TRV) blinded to the original classification, in order to measure intra- and inter rater accuracy.

Comparison with other studies

To contextualise our CoW variant frequencies, we wanted to compare with other studies. Unfortunately, to our knowledge, there is only one other CoW TOF MR study with a similar sample size compared to ours. The study is in 2246 healthy Chinese men [3], and we were able to perform comparisons with their study with only minor adaptations of the classification of the CoW variants. Main changes included removing left and right lateralization in our CoW variants, and translating their CoW variants to our nomenclature. Further information about the comparison is found in the S1 and S2 Files.

Statistical analysis

We split the CoW data at mean age of participants, grouping subjects into a "younger" and "older" group (Table 1). We also grouped the subjects into age per decade (5 categories, 40 years to 90 years). Formulas used to calculate all frequencies for every CoW segment and variant are described in the S1 File. CoW variants observed less than ten times were grouped into a single composite category of rare variants (S1 Table in S1 File). This composite category was created to include all subjects when testing without having too few observations in the array elements (see S1 File for details). The Cochran-Mantel-Haenszel test was used to test whether

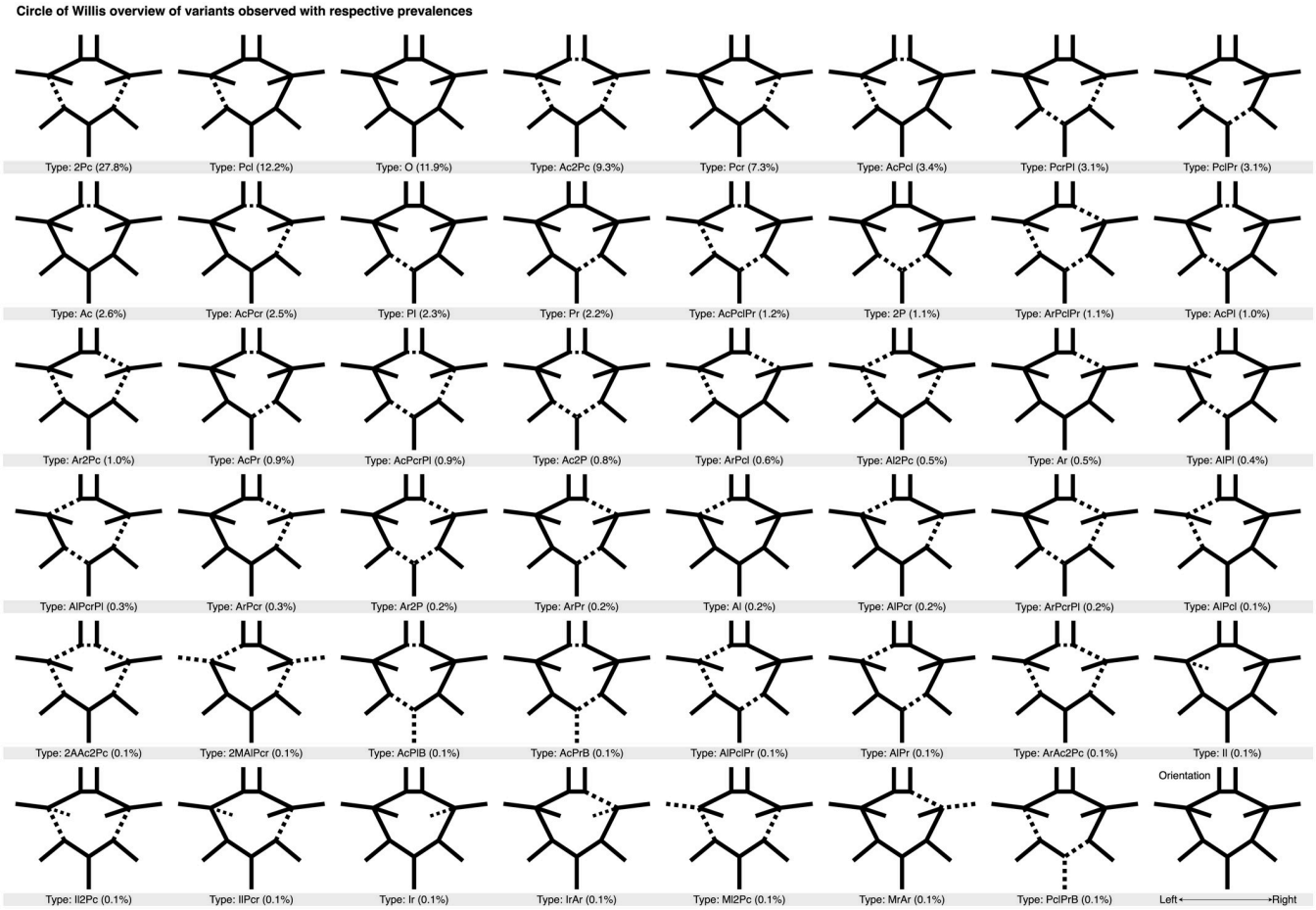

Fig 3. Complete graphical overview of all Circle of Willis variants observed in the current study. All variants are sorted first by (descending) frequency and then, in case of equal frequencies, by alphanumerical ordering. Each variant's name is put together by the missing segments with the following notation: O = Complete variant (no missing arteries), Ac = Anterior communicating artery, A = Anterior cerebral artery, Pc = Posterior communicating artery, P = Posterior cerebral artery, I = Internal carotid artery, M = Middle cerebral artery, B = Basilar artery, while the suffixes "r" and "l" denote right and left lateralization of arteries. The prefix "2" denotes bilateral missing arteries.

https://doi.org/10.1371/journal.pone.0241373.g003

Table 1. Age distributions per sex of subjects.

	Men n = 874:	Women n = 990:
Mean split age		
Above mean age*	503 (57.6)	513 (51.8)
Below mean age*	371 (42.4)	477 (48.2)
Age by decade		
40–49	84 (9.6)	123 (12.4)
50–59	135 (15.4)	177 (17.9)
60–69	313 (35.8)	353 (35.6)
70–79	273 (31.2)	264 (26.7)
80–89	69 (7.8)	73 (7.4)

(*) = Average age is 65.4 years.

https://doi.org/10.1371/journal.pone.0241373.t001

CoW variant frequencies were associated with sex, and age. This test allows for testing conditional independence between two factors while controlling for a third factor. As such, we used the Cochran-Mantel-Haenszel test to test for conditional independence between CoW variants and sex while controlling for the dichotomic age variable, and to test for conditional independence between CoW variants and dichotomic age while controlling for sex. Both of these tests had array dimensions $23 \times 2 \times 2$. The effect of age was further examined by plotting the distribution of CoW variants for each decade. To assess whether sex might affect this plot, a 5×2 Chi-squared test between age per decade and sex was performed to assess independence (Table 1). We considered a Bonferroni corrected $P < 0.05$ as significant (nominal $P < 0.0167$). At last, the accuracy metric was used to assess the intra- and inter rater validation. All computations were performed in R (v3.4.4) and three figures were created using the ggplot2 package [27].

Results

Study participants

The mean age for all participants was 65.4 years (SD = 10.6). There were 874 men (47%), mean age 66.1 years (SD = 10.4, range = 40–86 years), and 990 women (53%), mean age 64.7 years (SD = 10.7, range = 41–87 years). Distributions of both mean-split age and decade age groupings with respect to sex are shown in Table 1, and distribution of age for men and women are shown in S3 Fig in S1 File.

Frequencies of CoW variants

We found 47 unique variants of the CoW (Fig 3). Of these, 22 made up 96.8% of the sample (Table 2), while the remaining 25 variants had less than ten observations each and constituted in total only 3.2% of the sample (S1 Table in S1 File). The most common variants were, 2Pc (27.8%), with both PCoA segments missing, Pcl (12.2%), with the left PCoA segment missing, the complete O variant (11.9%), Ac2Pc (9.3%), with the ACoA and both PCoA missing, and Pcr (7.3%) with the right PCoA missing. These five most common CoW variants constituted 68.5% of the total sample. These findings suggest that only about 12% of the adult population have a complete CoW, while the remaining 88% have one or more missing segments, thus reducing their collateral capacity.

Comparison of adapted CoW estimates with a previous study

After adapting the CoW estimates, we were able to compare 18 of our resulting prevalence estimates to the well-powered Chinese study [3] (S1 and S2 Files). This comparison showed excellent agreement; with mean and median percent point differences of 1.6 and 0.8 respectively (range 0.1–10.6 percent points). The difference between the complete variant estimates was only 0.3 percent points. Most of the total 28.4 percent point difference could be attributed to variants missing PCoA or PCA. In the end, we compared 99.2% of our sample with 100% of the other study, resulting in only an additional 0.8 percent point bias. In sum, the comparison showed near-perfect agreement for nearly all CoW variants.

Frequencies of missing segments independent of CoW variant

The frequencies of missing CoW segments in the whole sample are shown in Fig 4. The left and right PCoA were most frequently missing (60.6% and 53.6%), followed by the ACoA (22.7%). There was a notable right-left asymmetry in the frequencies of missing ACA and

Table 2. Frequencies of common Circle of Willis variants for the whole sample, and their frequencies for men and women, and for being below and above mean age [number of cases (percentage of column total)].

Variant:	Total n = 1,864:	Men n = 874:	Women n = 990:	Below mean age n = 848:	Above mean age n = 1,016:
2Pc	518 (27.8)	266 (30.4)	252 (25.5)	222 (26.2)	296 (29.1)
Pcl	227 (12.2)	95 (10.9)	132 (13.3)	116 (13.7)	111 (10.9)
O	221 (11.9)	88 (10.1)	133 (13.4)	123 (14.5)	98 (9.6)
Ac2Pc	173 (9.3)	72 (8.2)	101 (10.2)	73 (8.6)	100 (9.8)
Pcr	137 (7.3)	69 (7.9)	68 (6.9)	71 (8.4)	66 (6.5)
AcPcl	63 (3.4)	33 (3.8)	30 (3.0)	31 (3.7)	32 (3.1)
PcrPl	58 (3.1)	26 (3.0)	32 (3.2)	29 (3.4)	29 (2.9)
PclPr	57 (3.1)	35 (4.0)	22 (2.2)	25 (2.9)	32 (3.1)
Ac	49 (2.6)	19 (2.2)	30 (3.0)	26 (3.1)	23 (2.3)
AcPcr	46 (2.5)	18 (2.1)	28 (2.8)	20 (2.4)	26 (2.6)
Pl	43 (2.3)	16 (1.8)	27 (2.7)	13 (1.5)	30 (3.0)
Pr	41 (2.2)	22 (2.5)	19 (1.9)	17 (2.0)	24 (2.4)
AcPclPr	23 (1.2)	11 (1.3)	12 (1.2)	9 (1.1)	14 (1.4)
2P	21 (1.1)	11 (1.3)	10 (1.0)	9 (1.1)	12 (1.2)
ArPclPr	21 (1.1)	9 (1.0)	12 (1.2)	7 (0.8)	14 (1.4)
AcPl	19 (1.0)	10 (1.1)	9 (0.9)	8 (0.9)	11 (1.1)
Ar2Pc	19 (1.0)	10 (1.1)	9 (0.9)	9 (1.1)	10 (1.0)
AcPr	17 (0.9)	6 (0.7)	11 (1.1)	9 (1.1)	8 (0.8)
AcPcrPl	16 (0.9)	8 (0.9)	8 (0.8)	3 (0.4)	13 (1.3)
Ac2P	14 (0.8)	7 (0.8)	7 (0.7)	3 (0.4)	11 (1.1)
ArPcl	11 (0.6)	2 (0.2)	9 (0.9)	4 (0.5)	7 (0.7)
Al2Pc	10 (0.5)	4 (0.5)	6 (0.6)	3 (0.4)	7 (0.7)
Rare/Other	60 (3.2)	37 (4.2)	23 (2.3)	18 (2.1)	42 (4.1)

Each variant is put together by the missing segments with the following notation: 2P: Missing bilateral posterior cerebral artery. 2Pc: Missing bilateral posterior communicating artery. Ac: Missing anterior communicating artery. Pc: Missing posterior communicating artery. P: Missing proximal posterior cerebral artery. A: Missing proximal anterior cerebral artery. Left and right lateralization are denoted by using "l" or "r" respectively as a suffix for eligible segments. Special cases exempt from the preceding are: O: Complete variant, i.e. no missing segments. Rare/Other: Composite category of other rare variants with missing segment(s).

https://doi.org/10.1371/journal.pone.0241373.t002

PCoA, but not for PCA. The right-to-left ratio for ACAs (4.3%/1.8%) was large, considering how infrequent the ACAs were missing.

Pairwise conditional frequencies of missing segments

The heatmap of conditional frequencies (Fig 5) shows the conditional probabilities between CoW segments that were commonly missing, i.e. PCoA, PCA, ACA and ACoA (Fig 4). Although the conditional frequencies ultimately reflect the observed variant frequencies, the heatmap representation reveals several interesting patterns. First, ACoA was seldom missing if the left or right ACA was missing. Second, each ACA, PCoA and PCA segment pairs had approximately equal probability of being missing if the ACoA was missing. Third, if ACA was missing on one side, it was much more likely that the PCA was missing on the same side than on the opposite side, suggesting an ipsilateral pattern. Fourth, a contralateral pattern existed between ACA and PCoA, i.e., if the ACA was missing on one side, it was more likely that the PCoA was missing on the other side. Lastly, similar contralateral patterns were also seen between PCA and PCoA, within the PCoA pair, and within the PCA pair.

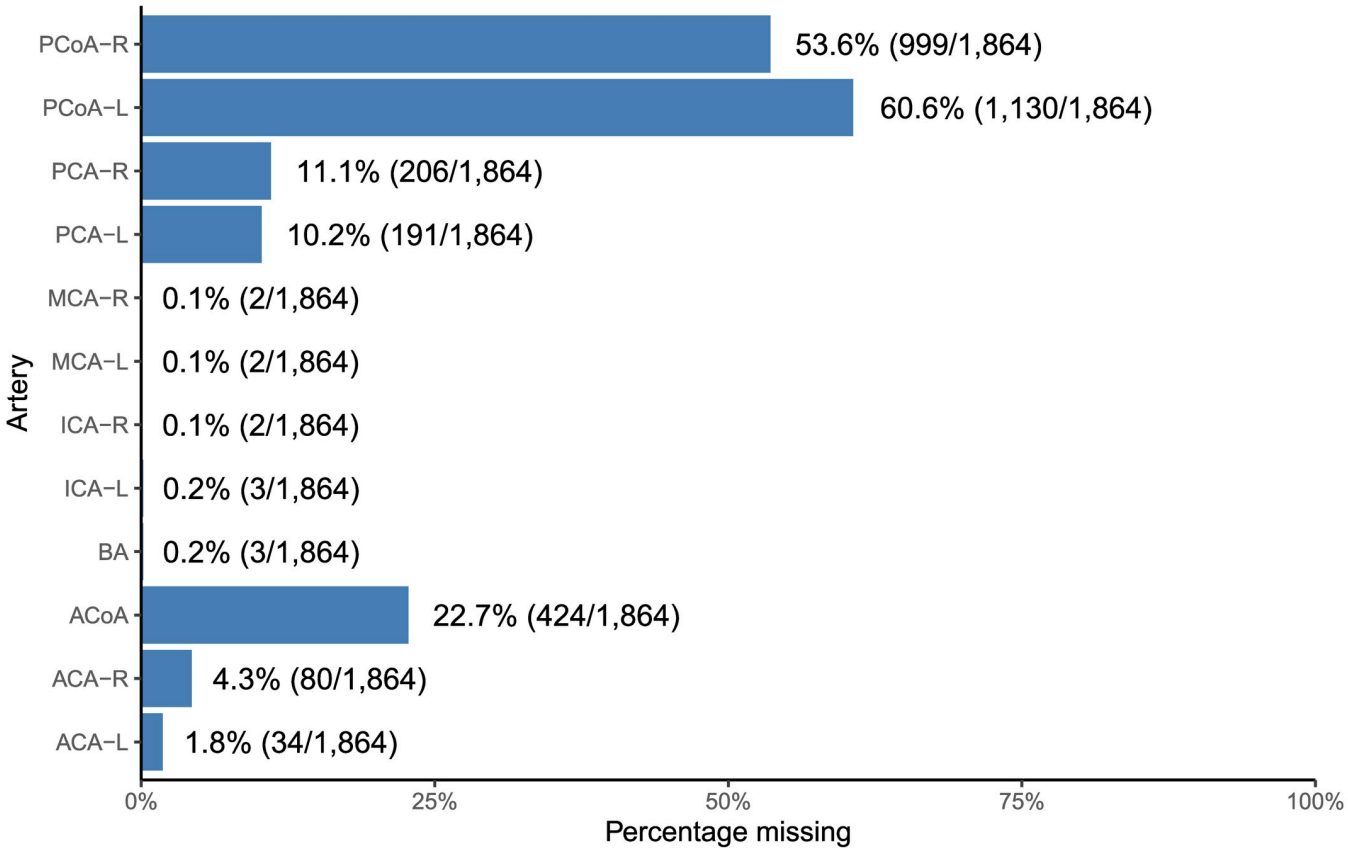

Fig 4. Frequency that each artery is missing independently of Circle of Willis variants and other arteries. Nominators and denominators are in corresponding parentheses, and represent respectively the number of times an artery is missing and the total number of subjects. ACA: Anterior cerebral artery. ACoA: Anterior communicating artery. PCoA: Posterior communicating artery. PCA: Posterior cerebral artery. ICA: Internal carotid artery. MCA: Middle cerebral Artery. BA: Basilar artery. Hemispheric left and right lateralization are denoted by "L" and "R" respectively.

https://doi.org/10.1371/journal.pone.0241373.g004

Tests of conditional independence between CoW variant frequencies and sex, and age, while controlling for the other

The Cochran-Mantel-Haenszel test of conditional independence between sex and CoW variant frequencies while controlling for age (Table 2), resulted in $M^2(22, N = 1,864) = 33.702$ with unadjusted P = .0526. This result imply that sex is not significantly associated with the frequency of CoW variants when corrected for mean split age.

The second Cochran-Mantel-Haenszel test (Table 2) tested whether CoW variant frequencies were conditionally independent of being above or below sample mean age while controlling for sex. This test returned $M^2(22, N = 1,864) = 38.849$ with unadjusted P = .0147, demonstrating that the mean-split age group was associated with the distribution of CoW variants, when corrected for sex.

CoW variant frequencies per decade

Fig 6 shows CoW variant frequencies per decade. From this figure, we observed that for each increasing decade the CoW variants that were missing a single artery (Ac, Pcl and Pcr) and the complete variant became less common. We also observed that the composite category of rare CoW variants became more common in later decades. These observations suggest that it is more common in older age to have more missing segments in the CoW.

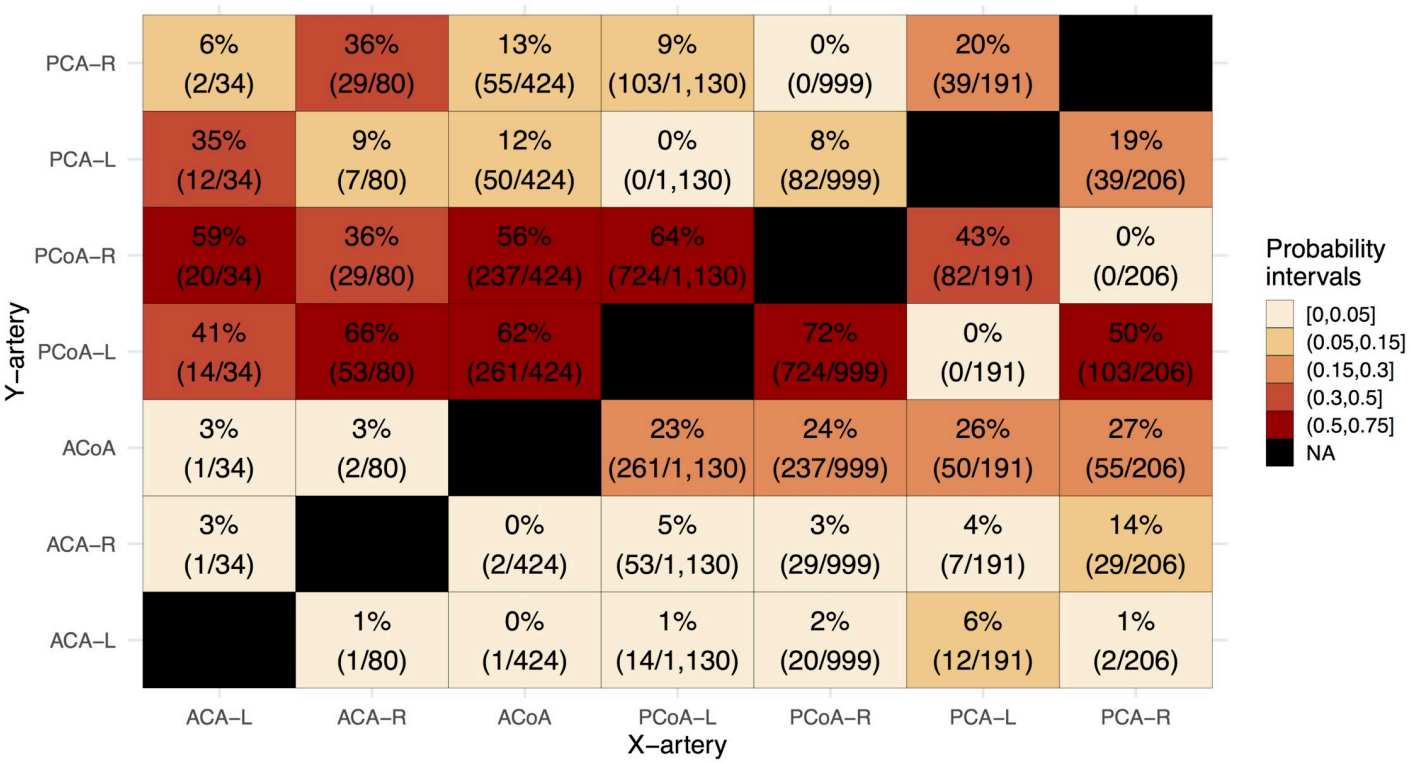

Fig 5. Heatmap of conditional probabilities that Y-artery is missing given that X-artery was missing. Numerators and denominators of conditional probability estimates are provided in the brackets, and represent respectively the number of times two segments are missing at the same time (joint probability) and per column the number of times the artery X is missing (independent probability). The common denominator of the joint probabilities and independent probabilities have cancelled. ACA: Anterior cerebral artery. ACoA: Anterior communicating artery. PCoA: Posterior communicating artery. PCA: Posterior cerebral artery. Left and right lateralization are denoted by "L" and "R" respectively. Each successive heatmap interval increases in size with 0.05.

https://doi.org/10.1371/journal.pone.0241373.g005

Test of independence between sex and decade age groups

The 5 × 2 Chi-squared test was carried out (Table 1) to test for independence between the sex and age as decades group in Fig 6. This test yielded $X^2(4, N = 1,864) = 8.482$ with unadjusted P = .075, implying homogeneous distribution of men and women across the five decades. Thus, due to the homogeneity result, Fig 6 is statistically appropriate to interpret equally for both sexes.

Intra- and inter rater validation

The intra rater validation yielded an accuracy score of 79% (conflicting classification in 21 of 100 cases). Closer inspection showed that only a single artery was mismatched for all 21 variant mismatches (S4 Fig in S1 File). The ACoA was prone to ambiguity with a total of 12 mismatches. ACA and PCA were misclassified as present instead of missing in four and three cases, respectively.

The inter rater validation yielded an accuracy score of 82% (conflicting classification in 18 of 100 cases). Compared to the intra rater validation, the inter rater validation had higher accuracy score, but had on the contrary more severe misclassifications. In other words, the mismatches were not only single artery mismatches. See S5 Fig in S1 File for details on the inter rater validation.

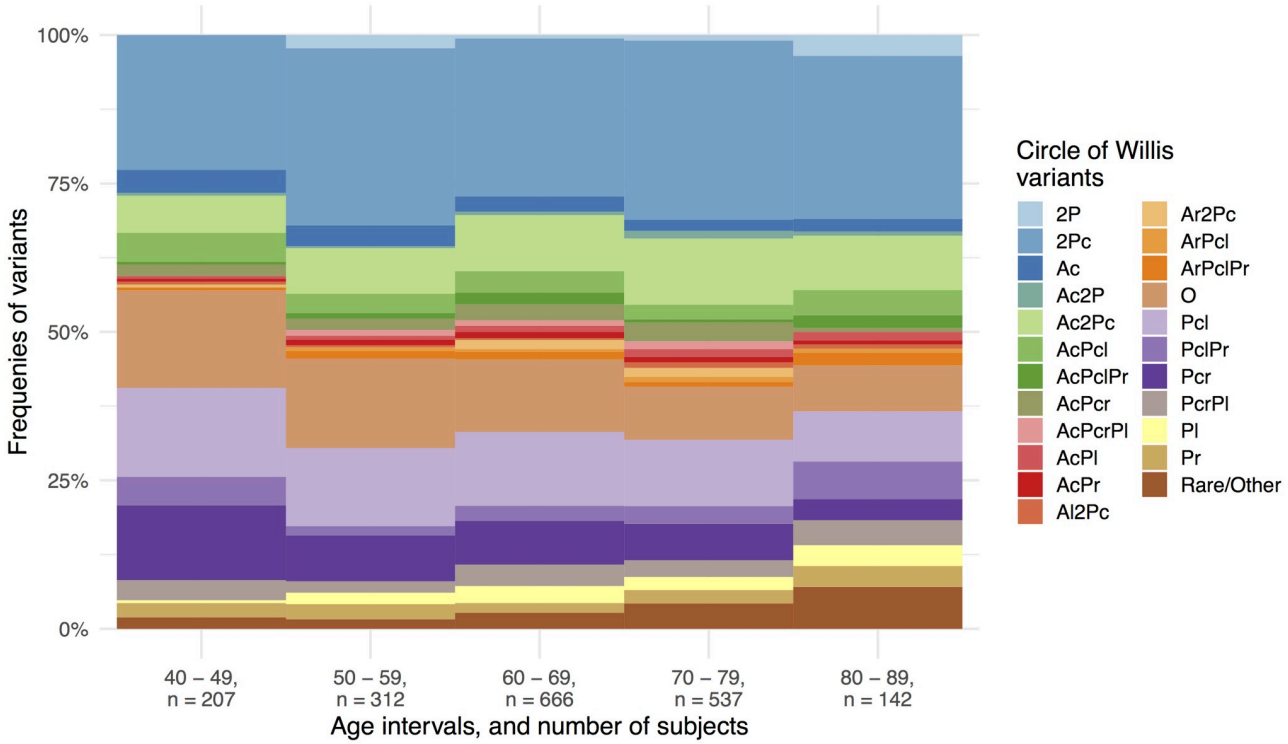

Fig 6. Stacked bar plot of the frequencies of the most common Circle of Willis variants divided into age intervals as decades. Each variant is put together by the missing segments with the following notation: 2P: Missing bilateral posterior cerebral artery. 2Pc: Missing bilateral posterior communicating artery. Ac: Missing anterior communicating artery. Pc: Missing posterior communicating artery. P: Missing proximal posterior cerebral artery. A: Missing proximal anterior cerebral artery. Left and right lateralization are denoted by using "l" or "r" respectively as a suffix for eligible segments. Special cases exempt from the preceding are: O: Complete variant, i.e. no missing segments. Rare/Other: Composite category of other rare variants with one or more missing segments.

https://doi.org/10.1371/journal.pone.0241373.g006

Discussion

This is, to our knowledge, the largest population-based study on the anatomical variation of the CoW, that included both men and women. The large sample size and recruitment of participants from the general population provide prevalence estimates of the anatomical variation in the CoW according to our classification scheme for people between 40 to 90 years of age. Main findings were that only 11.9% had a complete textbook CoW variant, while the remaining 88.1% had one or more missing segments in the CoW. In total, we found 47 variants of the CoW, but only five of these variants were very common (i.e. present in $> 5\%$). Further notable findings were that CoW frequencies were associated with age, but not with sex, and that there were patterns of interdependent missing segment patterns across CoW variants.

The agreement in prevalence estimates between our study and a comparable well-powered study [3] has several possible implications. First, the similarities between a male Chinese population and a Norwegian population suggest that variations in the CoW are similar across populations. A notion consistent with a study on twins finding no genetic effect on the variability of the CoW [14]. Second, it supports our finding that sex is not associated with the anatomical variability in the CoW, since the study by Qiu et al. [3] only included men, while our study included both women and men in an approximately equal proportion. Third, since most previous studies have relied on sample sizes of up to a few hundred participants, it is likely, considering the agreement between two studies with a sample size of about 2000, that the

disagreement between prevalence estimates in previous studies stems from too small study samples.

We found that CoW frequencies were associated with age, which has been observed in other studies [1, 22, 28]. These studies found, similarly to our study, that the number of missing arteries increased with age. Although the underlying cause of the increase in missing segments with age is not clear, atherosclerosis has been suggested as a possible cause [22], since plaque in an arterial segment might reduce the flow so that the segment is not detected on flow-sensitive TOF MRI. The reduction in cerebral blood flow with age [29] possibly in conjunction to the increase in tortuosity of blood vessels with age [30] could also alter the flow pattern in the CoW such that there is no, or very little flow in some segments, which would also appear as missing segments in the CoW. It is therefore not impossible that the increased rate of missing segments with age is caused by atherosclerosis or other factors affecting the blood flow in the CoW.

We did not find an association between sex and the frequencies of CoW variants. Previous studies have reported conflicting findings regarding the effect of sex; some find that the complete variant is more prevalent in women [1, 28], that specific variations are more common in men or women [6], or that there is no association [22]. Differences in methods, sample sizes and statistics, make it difficult to compare our results to the previous findings. However, the large sample size and correction for a possible age bias in our analysis, suggest that the effect of sex on the anatomy of the CoW is not substantial.

Study limitations were as follows. First, the TOF MR technique is sensitive to blood flow, i.e. it is necessary for blood to flow with a sufficient speed to be visible on the TOF images. As such we are only visualising blood flow, not arteries, and some of the missing CoW vessels might well be present, but not visible on the TOF images. This is supported by the higher frequency of the complete CoW variant in dissection studies [31, 32], but it is worth noting that dissection studies also show that some sections in the CoW can be completely absent as well [31]. Second, we did not differentiate between missing and hypoplastic segments. Although this is done in most CoW studies [1, 5, 12, 18, 19, 21, 22], our prevalences do not reflect all the nuances in the CoW. There is also a functional distinction between missing and hypoplastic segments as hypoplastic segment may provide some collateral flow, which is overlooked with our classification. Third, as seen from the intra- and inter rater validation there were some misclassifications in ambiguous cases of certain arteries. In particular, the ACoA was associated with higher rate of misclassification than other arteries. Some cases of ACA, PCoA and PCA were also mismatched, but not of the same magnitude as ACoA. As such, estimates including ACoA should be considered less accurate. Last, because of the large number of variants found, the precision of frequencies for a given variant should be judged relatively to its number of observations. On the other hand, our study strengths were as follows: (1) a large sample size, (2) a rigorous and reproducible classification scheme, and (3) intra- and inter rater validation indicating similar classification robustness across each rater.

In conclusion, in a large population sample, 47 anatomical variants of the CoW were found, but only 5 variants were commonly encountered. The complete CoW variant was the third most frequent variant present in 11.9% of the sample. Mean-split age was significantly associated with CoW variant frequencies, which could be partially explained by the increased number of hypoplastic or missing arteries with increasing age. We also found interdependent hypoplastic or missing segment patterns between the ACAs, ACoA, PCoAs, and the PCAs, highlighting the importance of also including the whole CoW during assessment to retain information about the CoW variants' collateral ability. Our variant frequencies agreed well with another large-scale MRI study in Chinese men suggesting the possibility of similar CoW variant frequencies across different populations, and that large variability in CoW variant

frequency in the literature possibly stems from using too small samples. The observed increasing number of hypoplastic or missing segments with age suggests that the collateral ability of the CoW may become an increasingly important risk factor for brain health with older age.

Supporting information

S1 File. Main supporting document containing nearly all supplementary information.
(DOCX)

S2 File. Comparison of our Circle of Willis estimates against the Chinese study.
(XLSX)

Acknowledgments

We warmly thank the participants of the Tromsø Study, the administration of the Tromsø Study, the Department of Radiology at the University Hospital North Norway and the MR imaging technologists for their contributions to the study.

Author Contributions

Conceptualization: Asta K. Håberg, Ellisiv B. Mathiesen, Torgil R. Vangberg.

Data curation: Lars B. Hindenes, Liv Hege Johnsen, Ellisiv B. Mathiesen, Torgil R. Vangberg.

Formal analysis: Lars B. Hindenes, Torgil R. Vangberg.

Funding acquisition: Asta K. Håberg, Ellisiv B. Mathiesen, Torgil R. Vangberg.

Investigation: Lars B. Hindenes, Torgil R. Vangberg.

Methodology: Lars B. Hindenes, David Robben, Torgil R. Vangberg.

Project administration: Torgil R. Vangberg.

Resources: Torgil R. Vangberg.

Software: Lars B. Hindenes, David Robben, Torgil R. Vangberg.

Supervision: Torgil R. Vangberg.

Validation: Lars B. Hindenes, Liv Hege Johnsen, Ellisiv B. Mathiesen, Torgil R. Vangberg.

Visualization: Lars B. Hindenes.

Writing – original draft: Lars B. Hindenes, Torgil R. Vangberg.

Writing – review & editing: Lars B. Hindenes, Asta K. Håberg, Liv Hege Johnsen, Ellisiv B. Mathiesen, David Robben, Torgil R. Vangberg.

References

1. Krabbe-Hartkamp MJ, van der Grond J, de Leeuw FE, de Groot JC, Algra A, Hillen B, et al. Circle of Willis: morphologic variation on three-dimensional time-of-flight MR angiograms. Radiology. 1998; 207 (1):103–11. https://doi.org/10.1148/radiology.207.1.9530305 PMID: 9530305
2. Riggs HE, Rupp C. Variation in Form of Circle of Willis. Arch Neurol. 1963; 8(1):8–14. https://doi.org/10.1001/archneur.1963.00460010024002 PMID: 13973856
3. Qiu C, Zhang Y, Xue C, Jiang S, Zhang W. MRA study on variation of the circle of Willis in healthy Chinese male adults. Biomed Res Int. 2015; 2015:8.
4. Hoksbergen AWJ, Legemate DA, Csiba L, Csáti G, Síró P, Fülesdi B. Absent Collateral Function of the Circle of Willis as Risk Factor for Ischemic Stroke. Cerebrovasc Dis. 2003; 16(3):191–8. https://doi.org/10.1159/000071115 PMID: 12865604

5. van Seeters T, Hendrikse J, Biessels GJ, Velthuis BK, Mali WP, Kappelle LJ, et al. Completeness of the circle of Willis and risk of ischemic stroke in patients without cerebrovascular disease. Neuroradiology. 2015 Dec 10; 57(12):1247–51. https://doi.org/10.1007/s00234-015-1589-2 PMID: 26358136

6. Horikoshi T, Akiyama I, Yamagata Z, Sugita M, Nukui H. Magnetic resonance angiographic evidence of sex-linked variations in the circle of willis and the occurrence of cerebral aneurysms. J Neurosurg. 2002; 96(4):697–703. https://doi.org/10.3171/jns.2002.96.4.0697 PMID: 11990810

7. Tarulli E, Sneade M, Clarke A, Molyneux AJ, Fox AJ. Effects of Circle of Willis Anatomic Variations on Angiographic and Clinical Outcomes of Coiled Anterior Communicating Artery Aneurysms. Am J Neuroradiol. 2014 Aug 1; 35(8):1551–5. https://doi.org/10.3174/ajnr.A3991 PMID: 24948501

8. Ryan DJ, Byrne S, Dunne R, Harmon M, Harbison J. White Matter Disease and an Incomplete Circle of Willis. Int J Stroke. 2015 Jun 22; 10(4):547–52. https://doi.org/10.1111/ijs.12042 PMID: 23521864

9. Saba L, Raz E, Fatterpekar G, Montisci R, di Martino M, Bassareo PP, et al. Correlation between Leukoaraiosis Volume and Circle of Willis Variants. J Neuroimaging. 2015; 25(2):226–31. https://doi.org/10.1111/jon.12103 PMID: 24593769

10. Chuang Y-M, Huang K-L, Chang Y-J, Chang C-H, Chang T-Y, Wu T-C, et al. Associations between Circle of Willis Morphology and White Matter Lesion Load in Subjects with Carotid Artery Stenosis. Eur Neurol. 2011; 66(3):136–44. https://doi.org/10.1159/000329274 PMID: 21865763

11. Saba L, Sanfilippo R, Porcu M, Lucatelli P, Montisci R, Zaccagna F, et al. Relationship between white matter hyperintensities volume and the circle of Willis configurations in patients with carotid artery pathology. Eur J Radiol. 2017 Apr; 89:111–6. https://doi.org/10.1016/j.ejrad.2017.01.031 PMID: 28267525

12. Klimek-Piotrowska W, Rybicka M, Wojnarska A, Wójtowicz A, Koziej M, Hołda MK. A multitude of variations in the configuration of the circle of Willis: an autopsy study. Anat Sci Int. 2016; 91(4):325–33. https://doi.org/10.1007/s12565-015-0301-2 PMID: 26439730

13. Papantchev V, Stoinova V, Aleksandrov A, Todorova-Papantcheva D, Hristov S, Petkov D, et al. The role of willis circle variations during unilateral selective cerebral perfusion: A study of 500 circles. Eur J Cardio-thoracic Surg. 2013; 44(4):743–53. https://doi.org/10.1093/ejcts/ezt103 PMID: 23471152

14. Forgo B, Tarnoki AD, Tarnoki DL, Kovacs DT, Szalontai L, Persely A, et al. Are the Variants of the Circle of Willis Determined by Genetic or Environmental Factors? Results of a Twin Study and Review of the Literature. Twin Res Hum Genet. 2018; 21(5):384–93. https://doi.org/10.1017/thg.2018.50 PMID: 30201058

15. Li Q, Li J, Lv F, Li K, Luo T, Xie P. A multidetector CT angiography study of variations in the circle of Willis in a Chinese population. J Clin Neurosci. 2011; 18(3):379–83. https://doi.org/10.1016/j.jocn.2010.07.137 PMID: 21251838

16. Van Kammen MS, Moomaw CJ, Van Der Schaaf IC, Brown RD, Woo D, Broderick JP, et al. Heritability of circle of Willis variations in families with intracranial aneurysms. PLoS One. 2018; 13(1):1–9.

17. Liebeskind DS. Mapping the collaterome for precision cerebrovascular health: Theranostics in the continuum of stroke and dementia. J Cereb Blood Flow Metab. 2018; 38(9):1449–60. https://doi.org/10.1177/0271678X17711625 PMID: 28555527

18. De Silva KR, Silva R, Gunasekera WS, Jayesekera R. Prevalence of typical circle of Willis and the variation in the anterior communicating artery: A study of a Sri Lankan population. Ann Indian Acad Neurol. 2009; 12(3):157–61. https://doi.org/10.4103/0972-2327.56314 PMID: 20174495

19. Hashemi SM, Mahmoodi R, Amirjamshidi A. Variations in the Anatomy of the Willis' circle: A 3-year cross-sectional study from Iran (2006–2009). Are the distributions of variations of circle of Willis different in different populations? Result of an anatomical study and review of literature. Surg Neurol Int. 2013; 4(1):65. https://doi.org/10.4103/2152-7806.112185 PMID: 23772335

20. Eftekhar B, Dadmehr M, Ansari S, Ghodsi M, Nazparvar B, Ketabchi E. Are the distributions of variations of circle of Willis different in different populations?–Results of an anatomical study and review of literature. BMC Neurol. 2006; 6(1):22.

21. Tanaka H, Fujita N, Enoki T, Matsumoto K, Watanabe Y, Murase K, et al. Relationship between variations in the circle of Willis and flow rates in internal carotid and basilar arteries determined by means of magnetic resonance imaging with semiautomated lumen segmentation: reference data from 125 healthy volunteers. AJNR Am J Neuroradiol. 2006; 27(8):1770–5. PMID: 16971634

22. El-Barhoun E, Gledhill S, Pitman A. Circle of Willis artery diameters on MR angiography: An Australian reference database. J Med Imaging Radiat Oncol. 2009; 53(3):248–60. https://doi.org/10.1111/j.1754-9485.2009.02056.x PMID: 19624291

23. Ozaki T, Handa H, Tomimoto K, Hazama F. Anatomical Variations of the Arterial System of the Base of the Brain. Arch für japanische Chir. 1977; 46(1):3–17. PMID: 561574

24. Barkeij Wolf JJ, Foster-Dingley JC, Moonen JE, van Osch MJ, de Craen AJ, de Ruijter W, et al. Unilateral fetal-type circle of Willis anatomy causes right–left asymmetry in cerebral blood flow with pseudo-continuous arterial spin labeling: A limitation of arterial spin labeling-based cerebral blood flow measurements? J Cereb Blood Flow Metab. 2016; 36(9):1570–8. https://doi.org/10.1177/0271678X15626155 PMID: 26755444

25. van der Kouwe AJW, Benner T, Fischl B, Schmitt F, Salat DH, Harder M, et al. On-line automatic slice positioning for brain MR imaging. Neuroimage. 2005 Aug; 27(1):222–30. https://doi.org/10.1016/j.neuroimage.2005.03.035 PMID: 15886023

26. Dimmick SJ, Faulder KC. Normal Variants of the Cerebral Circulation at Multidetector CT Angiography. RadioGraphics. 2009 Jul; 29(4):1027–43. https://doi.org/10.1148/rg.294085730 PMID: 19605654

27. Wickham H. ggplot2: Elegant Graphics for Data Analysis. Springer-Verlag New York; 2016.

28. Zaninovich OA, Ramey WL, Walter CM, Dumont TM. Completion of the Circle of Willis Varies by Gender, Age, and Indication for Computed Tomography Angiography. World Neurosurg. 2017; 106:953–63. https://doi.org/10.1016/j.wneu.2017.07.084 PMID: 28736349

29. Buijs PC, Krabbe-Hartkamp MJ, Bakker CJ, de Lange EE, Ramos LM, Breteler MM, et al. Effect of age on cerebral blood flow: measurement with ungated two-dimensional phase-contrast MR angiography in 250 adults. Radiology. 1998 Dec; 209(3):667–74. https://doi.org/10.1148/radiology.209.3.9844657 PMID: 9844657

30. Wright SN, Kochunov P, Mut F, Bergamino M, Brown KM, Mazziotta JC, et al. Digital reconstruction and morphometric analysis of human brain arterial vasculature from magnetic resonance angiography. Neuroimage. 2013 Nov 15; 82:170–81. https://doi.org/10.1016/j.neuroimage.2013.05.089 PMID: 23727319

31. Kapoor K, Singh B, Dewan LIJ. Variations in the configuration of the circle of Willis. Anat Sci Int. 2008; 83(2):96–106. https://doi.org/10.1111/j.1447-073X.2007.00216.x PMID: 18507619

32. Gunnal SA, Farooqui MS, Wabale RN. Anatomical Variations of the Circulus Arteriosus in Cadaveric Human Brains. Neurol Res Int. 2014; 2014:1–16. https://doi.org/10.1155/2014/687281 PMID: 24891951

Paper II

Journal of the Neurological Sciences 420 (2021) 117268

Contents lists available at ScienceDirect

Journal of the Neurological Sciences

journal homepage: www.elsevier.com/locate/jns

An incomplete Circle of Willis is not a risk factor for white matter hyperintensities: The Tromsø Study

Lars B. Hindenes [a,b,*], Asta K. Håberg [c,d], Ellisiv B. Mathiesen [a,e], Torgil R. Vangberg [a,b]

[a] Department of Clinical Medicine, Faculty of Health Sciences, UiT The Arctic University of Norway, Postboks 6050 Langnes, 9037 Tromsø, Norway
[b] PET Centre, University Hospital of North Norway, 9038 Tromsø, Norway
[c] Department of Radiology and Nuclear Medicine, St. Olav University Hospital, Postboks 3250 Torgarden, 7030 Trondheim, Norway
[d] Department of Neuromedicine and Movement Science, Norwegian University of Science and Technology (NTNU), NTNU 7491 Trondheim, Norway
[e] Department of Neurology, University Hospital of North Norway, 9038 Tromsø, Norway

ARTICLE INFO

Keywords:
Circulation
Leukoaraiosis
Health survey
Epidemiology

ABSTRACT

Objective: The Circle of Willis (CoW) is often underdeveloped or incomplete, leading to suboptimal blood supply to the brain. As hypoperfusion is thought to play a role in the aetiology of white matter hyperintensities (WMH), the objective of this study was to assess whether incomplete CoW variants were associated with increased WMH volumes compared to the complete CoW.

Methods: In a cross-sectional population sample of 1751 people (age 40–84 years, 46.4% men), we used an automated method to segment WMH using T1-weighted and T2-weighted fluid-attenuated inversion recovery image obtained at 3T. CoW variants were classified from time-of-flight scans, also at 3T. WMH risk factors, including age, sex, smoking and blood pressure, were obtained from questionnaires and clinical examinations. We used linear regression to examine whether people with incomplete CoW variants had greater volumes of deep WMH (DWMH) and periventricular WMH (PWMH) compared to people with the complete CoW, correcting for WMH risk factors.

Results: Participants with incomplete CoW variants did not have significantly higher DWMH or PWMH volumes than those with complete CoW when accounting for risk factors. Age, pack-years smoking, and systolic blood pressure were risk factors for increased DWMH and PWMH volume. Diabetes was a unique risk factor for increased PWMH volume.

Conclusion: Incomplete CoW variants do not appear to be risk factors for WMH in the general population.

1. Introduction

White matter hyperintensities (WMH) are seen as a marker of cerebral small vessel disease [51]. They are common in older adults, and their prevalence rapidly increases with age [5]. WMH have been associated with cognitive decline and dementia [6], and impaired motor function [15]. Risk factors of cerebrovascular disease have also been associated with WMH, including hypertension [10,46,47], type 1 and 2 diabetes [20,25], body mass index (BMI) [25], and smoking [16,20,47]. Although the aetiology of WMH is not fully understood [51], hypoperfusion may play a role as histology shows signs of hypoxia in WMH [12] and WMH commonly occur in watershed regions in cerebral white matter.

The Circle of Willis (CoW), located at the base of the brain, is an anastomosis of the carotid arteries and the basilar artery. Its circular structure enables redistribution of the cerebral blood flow in case of reduced upstream flow, subsequently providing redundancy to the brain's blood supply. However, it is very common that at least one of the

Abbreviations: CoW, Circle of Willis; WMH, white matter hyperintensities; DWMH, deep white matter hyperintensities; PWMH, periventricular white matter hyperintensities; MPRAGE, magnetisation prepared rapid acquisition gradient-echo; GRAPPA, Generalized Autocalibrating Partially Parallel Acquisition; FLASH, fast low angle shot; TOF, time-of-flight; FLAIR, fluid-attenuated inversion recovery; T1w, T1-weighted; SVD, small vessel disease; MNI, Montreal Neurological Institute; ANTs, Advanced Normalization Tools.

* Corresponding author at: Department of Clinical Medicine, Faculty of Health Sciences, UiT The Arctic University of Norway, Postboks 6050 Langnes, 9037 Tromsø, Norway.

E-mail addresses: lars.b.hindenes@uit.no (L.B. Hindenes), asta.haberg@ntnu.no (A.K. Håberg), ellisiv.mathiesen@uit.no (E.B. Mathiesen), torgil.vangberg@uit.no (T.R. Vangberg).

https://doi.org/10.1016/j.jns.2020.117268
Received 7 October 2020; Received in revised form 18 November 2020; Accepted 9 December 2020
Available online 13 December 2020

segments in the CoW are hypoplastic or missing. A recent dissection study found that only 7% of adults have a complete CoW [52], suggesting that the CoW does not inherently have a critical influence on human survival. A non-patent CoW may, however, cause suboptimal blood supply to some brain regions due to diminished collateral capacity, particularly in combination with atherosclerosis or other arterial occlusions.

Indeed, previous studies have found an association between incomplete CoW variants and increased WMH burden. In a convenience sample of 163 patients, it was found that patients with incomplete variants had a significantly higher Fazekas score compared to those with a complete CoW [37]. In patients with carotid artery stenosis, incomplete CoW variants were associated with greater WMH volume and number of WMH lesions [38,39], increased WMH rating [4], and increased deep WMH (DWMH) and periventricular WMH (PWMH) ratings [54]. However, the results are not unison, as some studies fail to find a link between more WMH and decreased completeness of the CoW, both in patients with carotid stenosis [29,45] and in the general population [7]. Interestingly, atherosclerosis patients with an incomplete CoW also have more carotid intraplaque haemorrhage than those with a complete CoW [56]. As carotid intraplaque haemorrhage accelerate plaque progression [42] this may pose an additional risk for WMH in people with incomplete CoW, and indeed carotid intraplaque haemorrhage has been associated with increased WMH volume [1]. Despite diverging results from prior studies, there is evidence suggesting that an incomplete CoW may be a risk factor for WMH possibly via impaired autoregulation of cerebral blood flow [19] which has been shown to be associated with WMH [33]. Furthermore, PWMH is more strongly associated with cerebral blood flow [43], blood pressure [17] and vasculature in general [2] than DWMH. Therefore, PWMH may be more sensitive to variations in the CoW than DWMH, and this may in part explain possible diverging findings relating to WMH and anatomical variants of the CoW. Since WMH and also incomplete CoW variants [11,21,55] are more prevalent among older people, it is of interest to examine whether incomplete CoW variants pose a risk of WMH in the general population.

In this study, we therefore assessed whether incomplete CoW variants might be risk factors for increased WMH burden in a large population-based sample of middle-aged and older people. We grouped the incomplete CoW variants according to the segments of the CoW that were missing, similar to Saba et al. [39], as opposed to broad categories (e.g. incomplete/complete CoW), since this would increase the sensitivity of detecting specific CoW variants strongly associated with WMH. We used linear regression models to compare DWMH and PWMH volumes of each incomplete CoW variant to the complete variant while correcting for cerebrovascular risk factors.

2. Methods

The study was approved by the Regional Committee of Medical and Health Research Ethics Northern Norway (2014/1665/REK-Nord) and carried out in accordance with relevant guidelines and regulations at UiT The Arctic University of Norway. All participants gave written informed consent before participating in the study.

2.1. Study population

Eligible for the study were 1864 participants (40–84 years) of the seventh wave of the population-based Tromsø Study [30] who underwent time-of-flight (TOF) MRI scanning of the brain and had complete imaging data [21]. We excluded participants with image artefacts or brain pathology that could lead to unreliable WMH volume estimates, and participants with rare CoW variants (less than ten observations) as parameter estimates would be unreliable.

2.2. MRI protocol

Participants were scanned at the University Hospital North Norway with the same 3T Siemens Skyra MR scanner (Siemens Healthcare, Erlangen, Germany). We used a 64-channel head coil in the majority of examinations, but in 38 examinations a slightly larger 20-channel head coil had to be used to accommodate the participants' head. The MRI protocol consisted of T1-weighted (T1w), T2-weighted fluid-attenuated inversion recovery (FLAIR), TOF angiography and susceptibility-weighted sequences.

T1w images were acquired with a 3D magnetisation prepared rapid acquisition gradient-echo (MPRAGE) sequence (flip angle = 9°, TR/TE/TI = 2300 ms/4.21 ms/996 ms). The T2-weighted FLAIR images were acquired with a 3D turbo spin-echo sequence with variable flip angle (TR/TE/TI = 5000 ms/388 ms/1800 ms, partial Fourier = 7/8). The T1w and FLAIR scans were acquired sagittally with 1 mm isotropic resolution, Generalized Autocalibrating Partially Parallel Acquisition (GRAPPA) parallel imaging acceleration factor 2, FOV = 256 mm, 176 slices, 1 mm slice thickness, and 256 × 256 image matrix. The T1w and FLAIR were used to measure the WMH volume. TOF angiography images were acquired with a 3D transversal fast low angle shot (FLASH) sequence with flow compensation (TR/TE = 21/3.43 ms, GRAPPA parallel imaging acceleration factor 3, FOV 200 × 181 mm, slice thickness 0.5 mm, 7 slabs with 40 slices each). Reconstructed image resolution was 0.3 × 0.3 × 0.5 mm.

2.3. Defining Circle of Willis segments and mirrored variants

The CoW consists of the left and right proximal anterior cerebral artery (A), the anterior communicating artery (Ac), the left and right posterior communicating artery (Pc), and the left and right proximal posterior cerebral artery (P). In figures and tables, we refer to the complete CoW variant as "O", while the incomplete variants are denoted by their missing segments. We also did not differentiate between left-right mirrored CoW variants in order to reduce the number of tested variants. Including the complete variant, we then had in total 17 unique CoW variants to be included in statistical testing (Fig. 1). The classification of anatomical variants in the CoW was done in a previous study, in which segments not visible or with a diameter less than 1 mm were classified as missing/hypoplastic [21]. The previous study identified 47 unique CoW variants [21], but due to exclusion of some participants and merging of left-right symmetrical CoW variants, we ended up with 17 variants. Specifically, we first excluded participants with no WMH measurement such that 45 unique CoW variants remained. Then, due to merging of 30 left-right mirrored CoW variants 30 unique CoW variants remained. At last, due to removing CoW variants having less than ten observations the 17 unique CoW variants remained.

2.4. WMH segmentation

We segmented WMH using a fully convolutional neural network algorithm [28] using the T1w and FLAIR images as input. The algorithm used 2D convolution in a U-NET architecture with different data pathways to evaluate images slice by slice. Despite not using 3D convolution, this algorithm was the best performer in the WMH Segmentation Challenge at MICCAI 2017 [27] and was trained on images from five different scanners. The algorithm should therefore be more robust for use on images from a different scanner, compared to an algorithm that is trained on images from only one scanner.

The T1w and FLAIR images were first co-registered, and then rigid body aligned to the MNI (i.e. Montreal Neurological Institute) template using ANTs (i.e. Advanced Normalization Tools) toolkit (http://stnava.github.io/ANTs/, v.2.3.1). The latter was done to ensure consistent orientation of the images, which were found to improve the reliability of the U-NET algorithm. We ran the U-NET algorithm following Li's and colleagues' recommendations [28] and with default settings, except that

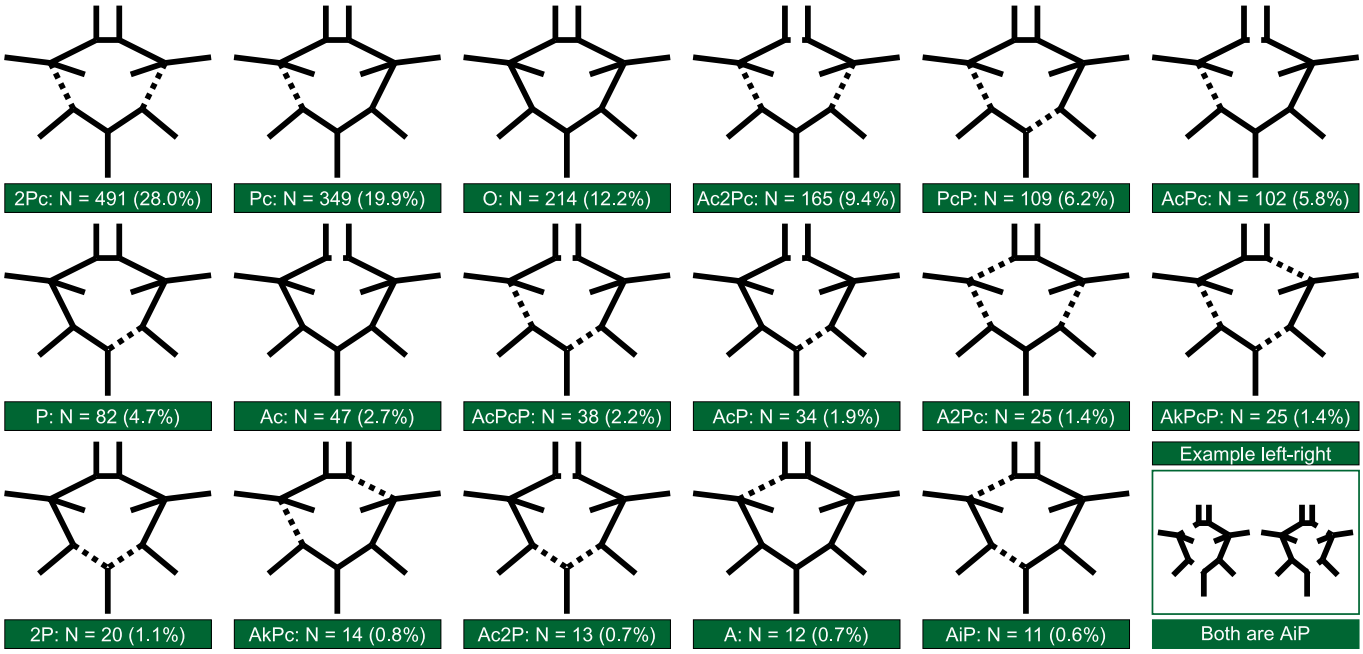

Fig. 1. The 17 Circle of Willis variants used in the analyses. "N" and "%" denotes count and percentage of each variant. If asymmetric, each schematic Circle of Willis and label contain both left and right variants as shown by the example in the lower right corner. "i" = ipsilateral and "k" = contralateral relationship between two subsequent segments. Prefix "2" denotes that both left and right segments are missing. "A" = proximal anterior cerebral artery, "Ac" = anterior communicating artery, "Pc" = posterior communicating artery, "P" = proximal posterior cerebral artery, and "O" = complete Circle of Willis.

we did not use bias-field correction, as an initial validation showed that this degraded the segmentation. After U-NET, the segmentation was corrected for misclassifications in grey matter by applying a white matter mask derived from the FreeSurfer (v6.0) subcortical segmentation of the T1w images [13,14].

We validated the WMH segmentation against 30 manually segmented images with a wide range of WMH volumes, from almost no WMH to severe volumes. A master student in the field of medicine

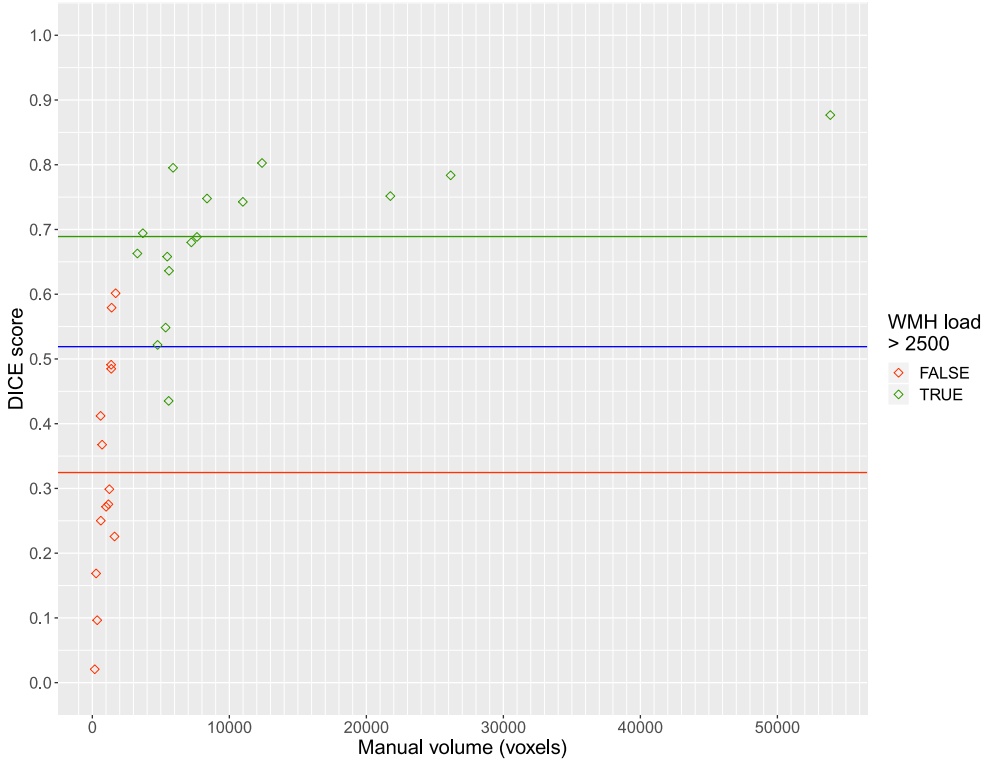

Fig. 2. Validation of the WMH segmentation algorithm: Dice score and relative absolute volume difference between ground truth WMH and segmented WMH. The blue line shows the overall mean Dice score, while the green and red line show the mean Dice score for segmentations with respective ground truth WMH load over and under 2500 voxels. (For interpretation of the references to colour in this figure legend, the reader is referred to the web version of this article.)

manually segmented the WMH with supervision from author TRV. The automatic segmentation showed similar performance in terms of the similarity coefficient Dice (mean Dice = 0.519 [SD = 0.234]) compared to many other available WMH segmentation methods [18,23,24,35,41,44]. Note that the Dice score becomes more sensitive to errors at small volumes, thereby decreasing the mean Dice score for the validation dataset, but for participants with WMH volumes >2.5 ml (2500 voxels) the individual Dice scores were almost always greater than the overall mean Dice score, averaging close to 0.7, see Fig. 2.

2.5. Partitioning WMH into deep and periventricular segments

We partitioned the WMH masks into PWMH and DWMH using a 10 mm distance from the ventricles. We chose 10 mm as a threshold based on a recent study [17] which showed that this threshold gives the most comparable results to previous studies and also the best separation between PWMH and DWMH in terms of the cardiovascular risk factors. Masks separating PWMH and DWMH were created by spherically dilating ventricle masks from the FreeSurfer segmentation by 10 mm.

2.6. Demographic and WMH risk variables

We included ten adjustment variables in our models that have been associated with WMH: age [31,47], sex [31,36], BMI [25], education [20], smoking [16,20,47] as pack-years, diabetes [20,25], blood glucose levels [3], high-sensitive C-reactive protein (CRP) levels [40], systolic blood pressure (SBP) [10,46,47], and total cholesterol to high-density lipoprotein (HDL) ratio [9]. The independent and dependent variables are further characterised in Table 1. Missing values in continuous variables were imputed by mean or median depending on their distribution, and missing values in categorical variables were imputed by rounded median.

2.7. Statistical analysis

All statistical analyses were done with R (v3.5.2). In the linear regression analyses, we used (1) DWMH volume, and (2) PWMH volume as dependent variables. Both volume estimates were log-transformed to better satisfy normality and homoscedasticity assumptions, and we added 1 voxel (1 cubic mm) to all volumes before the log transformation to avoid log of zero. For each dependent variable, we fitted a model including age, sex, CoW variants, and risk factors; i.e. each model has ten risk factors, and 17 factors for each of the incomplete CoW variants including the complete CoW used as a common reference. The beta coefficients presented for these variables were not adjusted.

Post-hoc multiple comparisons of means with Dunnett contrasts were used to test whether the incomplete CoW variants had higher WMH volumes compared to the complete CoW variant (i.e. a one-sided test). This was done separately for each model. Each post-hoc comparison reports step-down Dunnett adjusted p-values relative to the conventional significance level for one-sided comparisons. The R package "multcomp" [22] was used to calculate the post-hoc comparisons with adjusted p-values based on the linear regression models. The corresponding confidence intervals constructed to calculate p-values were stochastic, making exact replication without a seed unlikely. To avoid an unwarranted increase in the probability of committing type 1 errors, at the cost of slightly increased risk of type 2 error, we corrected only for multiple tests within linear regression models as described, but not between models. We regarded the conventional $p < 0.05$ as significant.

3. Results

3.1. Study participants

Of the 1864 participants, 76 were excluded due to atrophy or image artefacts that might have led to inaccurate WMH volume estimates, then 11 were excluded due to failures in the segmentation algorithm, and at last 26 were excluded due to having a rare CoW variant (see Fig. 3). For the 1751 participants included in our analyses, mean age was 63.5 years (SD = 10.6). Men were on average 64.3 years (SD = 10.5), and women 62.8 years (SD = 10.7). Further sample characteristics of the 1751 participants are shown in Table 1.

Table 1
Characteristics of the study participants.

Variable	Unit or Factor	Measurement	Missing*	Min	Max
Age	Year	63.51 (10.63)	0	40.00	84.00
Sex	Female	938 (53.6)	0		
	Male	813 (46.4)			
Education	Up to 10 years	509 (29.7)	37		
	High school: 3+ years	471 (27.5)			
	Up to 4 years at university	340 (19.8)			
	More than 4 years at university	394 (23.0)			
SBP	mmHg	133.96 (20.79)	6	78.00	220.00
Hypertension#	No	1070 (61.3)	6		
	Yes	675 (38.7)			
Cholesterol to HDL ratio		3.67 (1.35)	7	1.28	23.00
CRP, median [IQR]	mg/L	1.02 [0.59, 2.08]	7	0.14	58.98
Smoke daily	Yes, now	222 (12.8)	18		
	Yes, previously	839 (48.4)			
	Never	672 (38.8)			
Pack years		9.39 (12.87)	71	0.00	90.00
BMI		27.15 (4.20)	1	13.90	45.90
Diabetes+	No	1587 (93.6)	55		
	Yes	109 (6.4)			
Glucose	mmol/L	5.74 (1.65)	3	2.70	19.20
Total WMH, median [95% CI]	mm^3	2113 [505, 31584]	0	0	110447
DWMH, median [95% CI]	mm^3	699 [221, 9734]	0	0	41634
PWMH, median [95% CI]	mm^3	1332 [166, 21725]	0	0	74558

Unless specified, continuous variables are given as mean (standard deviation), and categorical variables as count (percentage). Abbreviations: WMH = white matter hyperintensities, DWMH = deep white matter hyperintensities, PWMH = periventricular white matter hyperintensities, CRP = C-reactive protein, SBP = systolic blood pressure, MMS = mini mental status, BMI = body mass index, HDL = high density lipoprotein, CI = credible interval, IQR = interquartile range, and SD = standard deviation. * Missing values were imputed before analysis. # Hypertension were defined as systolic blood pressure ≥ 140 mmHg or diastolic blood pressure ≥ 90 mmHg. + Diabetes category includes both type 1 and type 2.

3.2. Deep WMH model with post-hoc multiple comparisons

There was no incomplete CoW variant with significantly higher DWMH volume compared to the complete CoW variant in the post-hoc multiple comparisons. The PcP variants were the only CoW with an adjusted p-value under 50% ($t = 2.457$, adjusted $p = 0.093$) and its unadjusted equivalent two-sided p-level was significant at 0.05 (Table 2). Altogether this suggests that the PcP variants trended to have more DWMH than the complete variant. The R^2 for the regression model was 0.167, indicating that this model did not explain DWMH well.

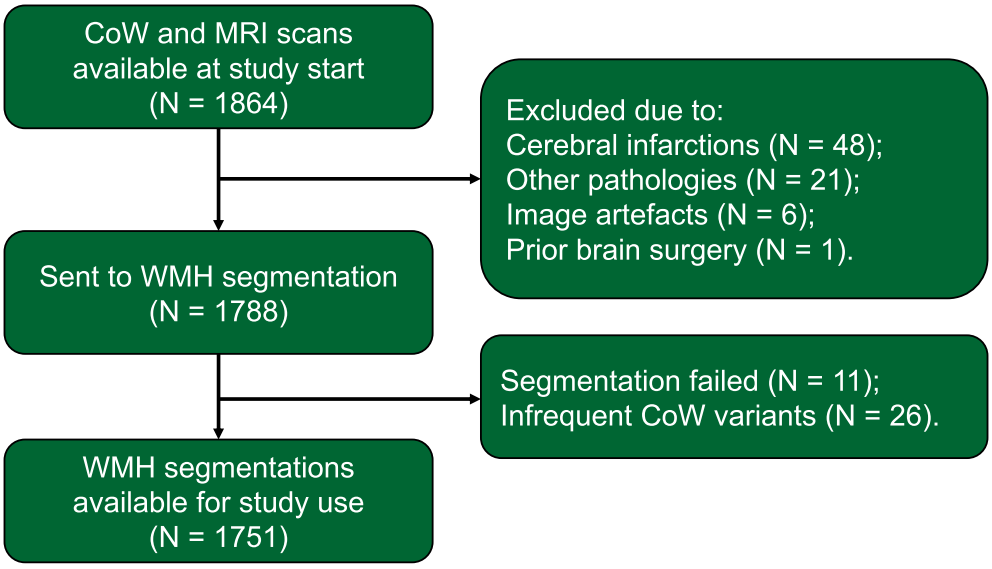

Fig. 3. Flow diagram of the sample selection process. "CoW" = Circle of Willis, "WMH" = White matter hyperintensities.

Table 2
Regression model coefficients for DWMH and PWMH. p-levels denoted by asterisk in the table are from unadjusted two-sided tests in the models included for gauging risk of type 1 error, and not results of the one-sided post-hoc analysis.

	DWMH	PWMH
Intercept	4.2089 ***	1.5267 ***
2P	0.2239	0.1304
2Pc	0.0787	−0.0072
A	0.0120	−0.0038
A2Pc	−0.2962	−0.5055 *
Ac	0.1138	−0.0132
Ac2P	0.1511	−0.0213
Ac2Pc	0.0629	−0.0585
AcP	−0.0431	−0.1081
AcPc	0.1591	−0.0477
AcPcP	−0.1860	−0.2458
AiP	−0.3697	−0.6014
AkPc	−0.1531	−0.3895
AkPcP	−0.1151	−0.2869
P	−0.1346	−0.3931 **
Pc	−0.0078	−0.0829
PcP	0.2714 *	0.1120
Age	0.0301 ***	0.0789 ***
Sex male	−0.0584	0.0641
BMI	−0.0040	0.0045
Education 2	−0.0942	−0.0821
Education 3	−0.0465	−0.0396
Education 4	−0.0921	−0.0231
Cholesterol to HDL ratio	0.0104	−0.0073
Pack year	0.0048 **	0.0057 **
CRP	0.0028	0.0191
SBP	0.0041 ***	0.0041 **
Diabetes	0.1973	0.4280 ***
Glucose	0.0284	0.0196
R^2	0.1671	0.4582

*** $p < 0.001$; ** $p < 0.01$; * $p < 0.05$.
Abbreviations: WMH = white matter hyperintensities, CRP = C-reactive protein, SBP = systolic blood pressure, BMI = body mass index, and HDL = high density lipoprotein.

3.3. Periventricular WMH model with post-hoc multiple comparisons

For the PWMH model (Table 2), no incomplete CoW variants had significantly higher PWMH volume compared to the complete CoW variant in the post-hoc multiple comparisons analysis. All adjusted *p*-values were between 0.85 and 1. In terms of the two-sided p-levels, the P and A2Pc variants had negative coefficients significant at 0.01 and 0.05, respectively, explaining why the one-sided post-hoc analysis was non-significant. The R^2 for the regression model was 0.458, and also considerably higher than for the DWMH model. This indicates that the same set of vascular risk factors and incomplete CoW variants in the regression models explained PWMH volume better than DWMH volume.

4. Discussion

In this population-based study, we examined whether participants with incomplete CoW variants had increased WMH volumes compared to those with the complete CoW. The main findings were that neither PWMH or DWMH volumes were significantly increased in participants with incomplete CoW variants relative to participants with a complete CoW when correcting for age, gender and WMH risk factors. To our knowledge, only one previous study has examined whether there is an association between the completeness of the CoW and WMH in the general population [7]. This study examined older participants from a native South American population, that have a high prevalence of small vessel disease (SVD), but failed to find any association between an incomplete CoW and increased WMH [7] and markers of SVD in general [8]. Our results, together with these findings suggest that anatomical variations in the CoW are not substantial risk factors for increased DWMH and PWMH volumes in the general population aged 40 years or older.

Our results differ from previous studies that have found an association between incomplete CoW variants and increased WMH load. Most of these studies are on patients with carotid artery stenosis [4,38,39,54]. For this patient group, there is a clear mechanism connecting the CoW anatomy and WMH, i.e., the stenosis will render the collateral capacity of the CoW important for maintaining sufficient blood flow to the brain. The association between the incompleteness of CoW and lower WMH load in atherosclerosis patients together with our negative results on generally healthy participants suggests that collateral flow in the CoW may only be protective against WMH when arteries upstream to the CoW are stenotic or occluded. However, it is difficult to firmly conclude that an incomplete CoW is a risk factor for WMH even in patients with carotid artery stenosis as some studies have failed to find such an association [29,45].

The inconsistent results on whether a complete CoW may be protective against WMH may hint of a more complex role of the CoW in the

cerebrovascular system than just having the role as a compensatory system in case of arterial occlusion. This has been suggested by previous studies [32,50]. In particular, Vrselja et al. argued that the CoW also plays a role in blood pressure dissipation, ensuring lower fluctuations in blood pressure in the downstream cerebral arteries of the CoW [50]. It is conceivable that hypoplastic segments with a diameter less than 1 mm may have an important role in dissipating fluctuations in blood pressure, but only a minor role in collateral blood flow. As greater pressure fluctuations in the blood flow are associated with WMH [33], the dampening of blood pressure fluctuations in the CoW may be just as crucial as its collateral ability. Unfortunately, we did not distinguish between missing and hypoplastic segments, similarly to most other TOF imaging studies on the CoW [7,11,26,34,39], since it is near impossible to distinguish between missing and hypoplastic segments reliably from TOF images.

As expected, some of the WMH risk factors were associated with increased DWMH and PWMH. Interestingly, diabetes was only associated with increased PWMH, lending support to the notion that DWMH and PWMH have differing aetiology [2,43]. Also, vascular risk factors, age and gender explained 45.8% of the variance in PWMH, while only 16.7% of the variance of DWMH, suggesting that PWMH is more closely associated with cerebrovascular disease than DWMH.

There are some limitations to our study warranting discussion. First, it is conceivable that other measurements of the CoW might offer greater insight into a potential connection between the CoW anatomy and WMH; e.g. considering the diameters of the arterial segments and, as already discussed, distinguishing between hypoplastic and absent segments. Second, we divided the WMH volume into deep and periventricular components which can make our study difficult to compare with other studies. Third, it is possible that partitioning the WMH volume in the individual flow territories would be more sensitivity to variations in the CoW anatomy. Still, we decided against this because flow territories depend on the CoW anatomy [48]. Fourth, we were unable to distinguish between diabetes type 1 and type 2, but most diabetes cases are generally of type 2 in a western population [53]. Fifth and last, most previous studies on the connection between WMH and CoW have grouped the anatomical variations of the CoW into broad categories (e.g. missing segments in the anterior or posterior circulation), instead of comparing unique variants as we have done. The rationale for this was that it might provide greater sensitivity, but it also complicates the comparison to previous studies.

The strengths of the study are the large cross-sectional population-based sample with reliable information on relevant risk factors. We also used a state of the art automatic WMH segmentation software to avoid WMH rater biases. Use of such automatic software has also increased the replicability of our study and allowed us to use WMH volumes instead of discrete scales, as this is found to offer greater sensitivity in correlations with clinical measures [49]. Our CoW classification also has acceptable intra and inter rater accuracy [21]. Furthermore, due to our large sample we, were able to include 17 unique CoW variants in the models without compromise in model assumptions. We applied the liberal step-down Dunnett correction for multiple tests, compared to Bonferroni, to reduce chance of type 2 errors. We also provided information about regressions' two-sided p-levels enabling some insight about chance of type 1 errors or whether our post hoc analysis had missed possible negative associations not originally hypothesized as relevant.

5. Conclusions

In this large population sample of people aged 40 and older, incomplete CoW variants are not substantial risk factors for increased DWMH and PWMH volumes.

Funding

This work was supported by two Helse Nord project grants HNF1369-17 and SFP1271-16, and computational resources from NOTUR grant #NN9562K. The funding source had no role in the study design, collection of data, analysis, interpretation of data, and in the decision to submit the article for publication.

Data availability statement

Ethical and legal restrictions prohibit the authors from making the dataset available outside The Tromsø Study database, which is available by contacting The Tromsø Study. Please see https://en.uit.no/forskning/forskningsgrupper/sub?p_document_id=453582&sub_id=669706 for detail on how to obtain access to all relevant data.

Declaration of Competing Interest

None.

Acknowledgements

We thank the participants of the Tromsø Study, the administration of the Tromsø Study, the Department of Radiology at the University Hospital North Norway and the MR imaging technologists for their contributions to the study. Special thanks to Liv Hege Johnsen for helpful discussions and assistance with the data curation process.

References

[1] N. Altaf, P.S. Morgan, A. Moody, S.T. MacSweeney, J.R. Gladman, D.P. Auer, Brain white matter hyperintensities are associated with carotid intraplaque hemorrhage, Radiology 248 (2008) 202–209, https://doi.org/10.1148/radiol.2481070300.

[2] N.J. Armstrong, K.A. Mather, M. Sargurupremraj, M.J. Knol, R. Malik, C. L. Satizabal, L.R. Yanek, W. Wen, V.G. Gudnason, N.D. Dueker, L.T. Elliott, E. Hofer, J. Bis, N. Jahanshad, S. Li, M.A. Logue, M. Luciano, M. Scholz, A.V. Smith, S. Trompet, D. Vojinovic, R. Xia, F. Alfaro-Almagro, D. Ames, N. Amin, P. Amouyel, A.S. Beiser, H. Brodaty, I.J. Deary, C. Fennema-Notestine, P.G. Gampawar, R. Gottesman, L. Griffanti, C.R. Jack, M. Jenkinson, J. Jiang, B.G. Kral, J.B. Kwok, L. Lampe, C.M. Liewald, P. Maillard, J. Marchini, M.E. Bastin, B. Mazoyer, L. Pirpamer, J. Rafael Romero, G.V. Roshchupkin, P.R. Schofield, M.L. Schroeter, D.J. Stott, A. Thalamuthu, J. Trollor, C. Tzourio, J. van der Grond, M.W. Vernooij, V.A. Witte, M.J. Wright, Q. Yang, Z. Morris, S. Siggurdsson, B. Psaty, A. Villringer, H. Schmidt, A.K. Haberg, C.M. van Duijn, J.W. Jukema, M. Dichgans, R.L. Sacco, C. B. Wright, W.S. Kremen, L.C. Becker, P.M. Thompson, T.H. Mosley, J.M. Wardlaw, M.A. Ikram, H.H.H. Adams, S. Seshadri, P.S. Sachdev, S.M. Smith, L. Launer, W. Longstreth, C. DeCarli, R. Schmidt, M. Fornage, S. Debette, P.A. Nyquist, Common genetic variation indicates separate causes for periventricular and deep white matter hyperintensities, Stroke 51 (2020) 2111–2121, https://doi.org/10.1161/STROKEAHA.119.027544.

[3] N. Cherbuin, W. Wen, P.S. Sachdev, K.J. Anstey, Fasting blood glucose levels are associated with white matter hyperintensities' burden in older individuals with and without type 2 diabetes, J. Neurol. Sci. 357 (2015), e44, https://doi.org/10.1016/j.jns.2015.08.189.

[4] Y.-M. Chuang, K.-L. Huang, Y.-J. Chang, C.-H. Chang, T.-Y. Chang, T.-C. Wu, C.-P. Lin, H.-F. Wong, S.-J. Liu, T.-H. Lee, Associations between circle of Willis morphology and white matter lesion load in subjects with carotid artery stenosis, Eur. Neurol. 66 (2011) 136–144, https://doi.org/10.1159/000329274.

[5] F.-E. de Leeuw, Prevalence of cerebral white matter lesions in elderly people: a population based magnetic resonance imaging study. The Rotterdam Scan Study, J. Neurol. Neurosurg. Psychiatry 70 (2001) 9–14, https://doi.org/10.1136/jnnp.70.1.9.

[6] S. Debette, H.S. Markus, The clinical importance of white matter hyperintensities on brain magnetic resonance imaging: systematic review and meta-analysis, BMJ 341 (2010) c3666, https://doi.org/10.1136/bmj.c3666.

[7] O.H. Del Brutto, J. Lama, Variants in the circle of Willis and white matter disease in ecuadorian mestizos, J. Neuroimaging 25 (2015) 124–126, https://doi.org/10.1111/jon.12077.

[8] O.H. Del Brutto, R.M. Mera, M. Zambrano, J. Lama, Incompleteness of the circle of Willis correlates poorly with imaging evidence of small vessel disease. A population-based study in rural Ecuador (the Atahualpa project), J. Stroke Cerebrovasc. Dis. 24 (2015) 73–77, https://doi.org/10.1016/j.jstrokecerebrovasdis.2014.07.036.

[9] D.A. Dickie, S.J. Ritchie, S.R. Cox, E. Sakka, N.A. Royle, B.S. Aribisala, Valdés Hernández, M.C. Del, S.M. Maniega, A. Pattie, J. Corley, J.M. Starr, M. E. Bastin, I.J. Deary, J.M. Wardlaw, Vascular risk factors and progression of white matter hyperintensities in the Lothian birth cohort 1936, Neurobiol. Aging 42 (2016) 116–123, https://doi.org/10.1016/j.neurobiolaging.2016.03.011.

[10] C. Dufouil, A. de Kersaint-Gilly, V. Besancon, C. Levy, E. Auffray, L. Brunnereau, A. Alperovitch, C. Tzourio, Longitudinal study of blood pressure and white matter

hyperintensities: the EVA MRI cohort, Neurology 56 (2001) 921–926, https://doi.org/10.1212/WNL.56.7.921.
[11] E. El-Barhoun, S. Gledhill, A. Pitman, Circle of Willis artery diameters on MR angiography: an Australian reference database, J. Med. Imaging Radiat. Oncol. 53 (2009) 248–260, https://doi.org/10.1111/j.1754-9485.2009.02056.x.
[12] M.S. Fernando, J.E. Simpson, F. Matthews, C. Brayne, C.E. Lewis, R. Barber, R. N. Kalaria, G. Forster, F. Esteves, S.B. Wharton, P.J. Shaw, J.T. O'Brien, P.G. Ince, White matter lesions in an unselected cohort of the elderly, Stroke 37 (2006) 1391–1398, https://doi.org/10.1161/01.STR.0000221308.94473.14.
[13] B. Fischl, D.H. Salat, E. Busa, M. Albert, M. Dieterich, C. Haselgrove, A. van der Kouwe, R. Killiany, D. Kennedy, S. Klaveness, A. Montillo, N. Makris, B. Rosen, A. M. Dale, Whole brain segmentation, Neuron 33 (2002) 341–355, https://doi.org/10.1016/S0896-6273(02)00569-X.
[14] B. Fischl, D.H. Salat, A.J.W. van der Kouwe, N. Makris, F. Ségonne, B.T. Quinn, A. M. Dale, Sequence-independent segmentation of magnetic resonance images, Neuroimage 23 (2004) S69–S84, https://doi.org/10.1016/j.neuroimage.2004.07.016.
[15] D.A. Fleischman, J. Yang, K. Arfanakis, Z. Arvanitakis, S.E. Leurgans, A.D. Turner, L.L. Barnes, D.A. Bennett, A.S. Buchman, Physical activity, motor function, and white matter hyperintensity burden in healthy older adults, Neurology 84 (2015) 1294–1300, https://doi.org/10.1212/WNL.0000000000001417.
[16] R.A.R. Gons, A.G.W. van Norden, K.F. de Laat, L.J.B. van Oudheusden, I.W.M. van Uden, M.P. Zwiers, D.G. Norris, F.-E. de Leeuw, Cigarette smoking is associated with reduced microstructural integrity of cerebral white matter, Brain 134 (2011) 2116–2124, https://doi.org/10.1093/brain/awr145.
[17] L. Griffanti, M. Jenkinson, S. Suri, E. Zsoldos, A. Mahmood, N. Filippini, C. E. Sexton, A. Topiwala, C. Allan, M. Kivimäki, A. Singh-Manoux, K.P. Ebmeier, C. E. Mackay, G. Zamboni, Classification and characterization of periventricular and deep white matter hyperintensities on MRI: A study in older adults, Neuroimage 170 (2018) 174–181, https://doi.org/10.1016/j.neuroimage.2017.03.024.
[18] L. Griffanti, G. Zamboni, A. Khan, L. Li, G. Bonifacio, V. Sundaresan, U.G. Schulz, W. Kuker, M. Battaglini, P.M. Rothwell, M. Jenkinson, BIANCA (Brain Intensity AbNormality Classification Algorithm): A new tool for automated segmentation of white matter hyperintensities, Neuroimage 141 (2016) 191–205, https://doi.org/10.1016/j.neuroimage.2016.07.018.
[19] Z.-N. Guo, X. Sun, J. Liu, H. Sun, Y. Zhao, H. Ma, B. Xu, Z. Wang, C. Li, X. Yan, H. Zhou, P. Zhang, H. Jin, Y. Yang, The impact of variational primary collaterals on cerebral autoregulation, Front. Physiol. 9 (2018), https://doi.org/10.3389/fphys.2018.00759.
[20] M. Habes, G. Erus, J.B. Toledo, T. Zhang, N. Bryan, L.J. Launer, Y. Rosseel, D. Janowitz, J. Doshi, S. Van der Auwera, B. von Sarnowski, K. Hegenscheid, N. Hosten, G. Homuth, H. Völzke, U. Schminke, W. Hoffmann, H.J. Grabe, C. Davatzikos, White matter hyperintensities and imaging patterns of brain ageing in the general population, Brain 139 (2016) 1164–1179, https://doi.org/10.1093/brain/aww008.
[21] L.B. Hindenes, A.K. Håberg, L.H. Johnsen, E.B. Mathiesen, D. Robben, T. R. Vangberg, Variations in the circle of Willis in a large population sample using 3D TOF angiography: The Tromsø Study, PLoS One 15 (2020), e0241373, https://doi.org/10.1371/journal.pone.0241373.
[22] T. Hothorn, F. Bretz, P. Westfall, Simultaneous inference in general parametric models, Biom. J. 50 (2008) 346–363, https://doi.org/10.1002/bimj.200810425.
[23] J. Jiang, T. Liu, W. Zhu, R. Koncz, H. Liu, T. Lee, P.S. Sachdev, W. Wen, UBO detector – a cluster-based, fully automated pipeline for extracting white matter hyperintensities, Neuroimage 174 (2018) 539–549, https://doi.org/10.1016/j.neuroimage.2018.03.050.
[24] K. Kamnitsas, C. Ledig, V.F.J. Newcombe, J.P. Simpson, A.D. Kane, D.K. Menon, D. Rueckert, B. Glocker, Efficient multi-scale 3D CNN with fully connected CRF for accurate brain lesion segmentation, Med. Image Anal. 36 (2017) 61–78, https://doi.org/10.1016/j.media.2016.10.004.
[25] K.S. King, R.M. Peshock, H.C. Rossetti, R.W. McColl, C.R. Ayers, K.M. Hulsey, S. R. Das, Effect of normal aging versus hypertension, abnormal body mass index, and diabetes mellitus on white matter hyperintensity volume, Stroke 45 (2014) 255–257, https://doi.org/10.1161/STROKEAHA.113.003602.
[26] M.J. Krabbe-Hartkamp, J. van der Grond, F.E. de Leeuw, J.C. de Groot, A. Algra, B. Hillen, M.M. Breteler, W.P. Mali, Circle of Willis: morphologic variation on three-dimensional time-of-flight MR angiograms, Radiology 207 (1998) 103–111, https://doi.org/10.1148/radiology.207.1.9530305.
[27] H.J. Kuijf, A. Casamitjana, D.L. Collins, M. Dadar, A. Georgiou, M. Ghafoorian, D. Jin, A. Khademi, J. Knight, H. Li, X. Llado, J.M. Biesbroek, M. Luna, Q. Mahmood, R. McKinley, A. Mehrtash, S. Ourselin, B.-Y. Park, H. Park, S.H. Park, S. Pezold, E. Puybareau, J. De Bresser, L. Rittner, C.H. Sudre, S. Valverde, V. Vilaplana, R. Wiest, Y. Xu, Z. Xu, G. Zeng, J. Zhang, G. Zheng, R. Heinen, C. Chen, W. van der Flier, F. Barkhof, M.A. Viergever, G.J. Biessels, S. Andermatt, M. Bento, M. Berseth, M. Belyaev, M.J. Cardoso, Standardized assessment of automatic segmentation of white matter hyperintensities and results of the WMH segmentation challenge, IEEE Trans. Med. Imaging 38 (2019) 2556–2568, https://doi.org/10.1109/TMI.2019.2905770.
[28] H. Li, G. Jiang, J. Zhang, R. Wang, Z. Wang, W.-S. Zheng, B. Menze, Fully convolutional network ensembles for white matter hyperintensities segmentation in MR images, Neuroimage 183 (2018) 650–665, https://doi.org/10.1016/j.neuroimage.2018.07.005.
[29] H. Li, Y. Xiong, G. Xu, R. Zhang, W. Zhu, Q. Yin, M. Ma, X. Fan, F. Yang, W. Liu, Z. Duan, X. Liu, The circle of Willis and White matter lesions in patients with carotid atherosclerosis, J. Stroke Cerebrovasc. Dis. 24 (2015) 1749–1754, https://doi.org/10.1016/j.jstrokecerebrovasdis.2015.03.048.
[30] I. Njølstad, E.B. Mathiesen, H. Schirmer, D.S. Thelle, The Tromsø study 1974–2016: 40 years of cardiovascular research, Scand. Cardiovasc. J. 50 (2016) 276–281, https://doi.org/10.1080/14017431.2016.1239837.
[31] P.A. Nyquist, M. Bilgel, R. Gottesman, L.R. Yanek, T.F. Moy, L.C. Becker, J. L. Cuzzocreo, J. Prince, B.A. Wasserman, D.M. Yousem, D.M. Becker, B.G. Kral, D. Vaidya, Age differences in periventricular and deep white matter lesions, Neurobiol. Aging 36 (2015) 1653–1658, https://doi.org/10.1016/j.neurobiolaging.2015.01.005.
[32] R. Pascalau, V.A. Padurean, D. Bartoș, A. Bartoș, B.A. Szabo, The geometry of the circle of Willis anatomical variants as a potential cerebrovascular risk factor, Turk. Neurosurg. (2018), https://doi.org/10.5137/1019-5149.JTN.21835-17.3.
[33] S. Purkayastha, O. Fadar, A. Mehregan, D.H. Salat, N. Moscufo, D.S. Meier, C. R. Guttmann, N.D. Fisher, L.A. Lipsitz, F.A. Sorond, Impaired cerebrovascular hemodynamics are associated with cerebral white matter damage, J. Cereb. Blood Flow Metab. 34 (2014) 228–234, https://doi.org/10.1038/jcbfm.2013.180.
[34] C. Qiu, Y. Zhang, C. Xue, S. Jiang, W. Zhang, MRA study on variation of the circle of Willis in healthy Chinese male adults, Biomed. Res. Int. 2015 (2015) 8, https://doi.org/10.1155/2015/976340.
[35] M.F. Rachmadi, M.C. del Valdés-Hernández, M.L.F. Agan, C. Di Perri, T. Komura, Segmentation of white matter hyperintensities using convolutional neural networks with global spatial information in routine clinical brain MRI with none or mild vascular pathology, Comput. Med. Imaging Graph. 66 (2018) 28–43, https://doi.org/10.1016/j.compmedimag.2018.02.002.
[36] E. Rostrup, A.A. Gouw, H. Vrenken, E.C.W. van Straaten, S. Ropele, L. Pantoni, D. Inzitari, F. Barkhof, G. Waldemar, The spatial distribution of age-related white matter changes as a function of vascular risk factors—results from the LADIS study, Neuroimage 60 (2012) 1597–1607, https://doi.org/10.1016/j.neuroimage.2012.01.106.
[37] D.J. Ryan, S. Byrne, R. Dunne, M. Harmon, J. Harbison, White matter disease and an incomplete circle of Willis, Int. J. Stroke 10 (2015) 547–552, https://doi.org/10.1111/ijs.12042.
[38] L. Saba, E. Raz, G. Fatterpekar, R. Montisci, M. di Martino, P.P. Bassareo, M. Piga, Correlation between leukoaraiosis volume and circle of Willis variants, J. Neuroimaging 25 (2015) 226–231, https://doi.org/10.1111/jon.12103.
[39] L. Saba, R. Sanfilippo, M. Porcu, P. Lucatelli, R. Montisci, F. Zaccagna, J.S. Suri, M. Anzidei, M. Wintermark, Relationship between white matter hyperintensities volume and the circle of Willis configurations in patients with carotid artery pathology, Eur. J. Radiol. 89 (2017) 111–116, https://doi.org/10.1016/j.ejrad.2017.01.031.
[40] C.L. Satizabal, Y.C. Zhu, B. Mazoyer, C. Dufouil, C. Tzourio, Circulating IL-6 and CRP are associated with MRI findings in the elderly: the 3C-Dijon Study, Neurology 78 (2012) 720–727, https://doi.org/10.1212/WNL.0b013e318248e50f.
[41] P. Schmidt, C. Gaser, M. Arsic, D. Buck, A. Förschler, A. Berthele, M. Hoshi, R. Ilg, V.J. Schmid, C. Zimmer, B. Hemmer, M. Mühlau, An automated tool for detection of FLAIR-hyperintense white-matter lesions in multiple sclerosis, Neuroimage 59 (2012) 3774–3783, https://doi.org/10.1016/j.neuroimage.2011.11.032.
[42] N. Takaya, C. Yuan, B. Chu, T. Saam, N.L. Polissar, G.P. Jarvik, C. Isaac, J. McDonough, C. Natiello, R. Small, M.S. Ferguson, T.S. Hatsukami, Presence of intraplaque hemorrhage stimulates progression of carotid atherosclerotic plaques, Circulation 111 (2005) 2768–2775, https://doi.org/10.1161/CIRCULATIONAHA.104.504167.
[43] V.H. ten Dam, D.M.J. van den Heuvel, A.J.M. de Craen, E.L.E.M. Bollen, H. M. Murray, R.G.J. Westendorp, G.J. Blauw, M.A. van Buchem, Decline in total cerebral blood flow is linked with increase in periventricular but not deep white matter hyperintensities, Radiology 243 (2007) 198–203, https://doi.org/10.1148/radiol.2431052111.
[44] S. Valverde, M. Cabezas, E. Roura, S. González-Villà, D. Pareto, J.C. Vilanova, L. Ramió-Torrentà, À. Rovira, A. Oliver, X. Lladó, Improving automated multiple sclerosis lesion segmentation with a cascaded 3D convolutional neural network approach, Neuroimage 155 (2017) 159–168, https://doi.org/10.1016/j.neuroimage.2017.04.034.
[45] J. van der Grond, A.F. van Raamt, Y. van der Graaf, W.P.T.M. Mali, R.H. C. Bisschops, A fetal circle of Willis is associated with a decreased deep white matter lesion load, Neurology 63 (2004) 1452–1456, https://doi.org/10.1212/01.WNL.0000142041.42491.F4.
[46] E.J. van Dijk, M.M.B. Breteler, R. Schmidt, K. Berger, L.-G. Nilsson, M. Oudkerk, A. Pajak, S. Sans, M. de Ridder, C. Dufouil, R. Fuhrer, S. Giampaoli, L.J. Launer, A. Hofman, The association between blood pressure, hypertension, and cerebral white matter lesions: cardiovascular determinants of dementia study, Hypertension 44 (2004) 625–630, https://doi.org/10.1161/01.HYP.0000145857.98904.20.
[47] E.J. van Dijk, N.D. Prins, H.A. Vrooman, A. Hofman, P.J. Koudstaal, M.M. B. Breteler, Progression of cerebral small vessel disease in relation to risk factors and cognitive consequences, Stroke 39 (2008) 2712–2719, https://doi.org/10.1161/STROKEAHA.107.513176.
[48] P.J. van Laar, J. Hendrikse, X. Golay, H. Lu, M.J.P. Van Osch, J. Van Der Grond, In vivo flow territory mapping of major brain feeding arteries, Neuroimage 29 (2006) 136–144, https://doi.org/10.1016/j.neuroimage.2005.07.011.
[49] E.C.W. van Straaten, F. Fazekas, E. Rostrup, P. Scheltens, R. Schmidt, L. Pantoni, D. Inzitari, G. Waldemar, T. Erkinjuntti, R. Mäntylä, L.-O. Wahlund, F. Barkhof, Impact of white matter hyperintensities scoring method on correlations with clinical data, Stroke 37 (2006) 836–840, https://doi.org/10.1161/01.STR.0000202585.26325.74.
[50] Z. Vrselja, H. Brkic, S. Mrdenovic, R. Radic, G. Curic, Function of circle of Willis, J. Cereb. Blood Flow Metab. 34 (2014) 578–584, https://doi.org/10.1038/jcbfm.2014.7.

[51] J.M. Wardlaw, M.C. Valdés Hernández, S. Muñoz-Maniega, What are white matter hyperintensities made of? Relevance to vascular cognitive impairment, J. Am. Heart Assoc. 4 (2015), e001140, https://doi.org/10.1161/JAHA.114.001140.
[52] P. Wijesinghe, H.W.M. Steinbusch, S.K. Shankar, T.C. Yasha, K.R.D. De Silva, Circle of Willis abnormalities and their clinical importance in ageing brains: a cadaveric anatomical and pathological study, J. Chem. Neuroanat. 106 (2020) 101772, https://doi.org/10.1016/j.jchemneu.2020.101772.
[53] G. Xu, B. Liu, Y. Sun, Y. Du, L.G. Snetselaar, F.B. Hu, W. Bao, Prevalence of diagnosed type 1 and type 2 diabetes among US adults in 2016 and 2017: population based study, BMJ (2018), https://doi.org/10.1136/bmj.k1497 k1497.
[54] H. Ye, X. Wu, J. Yan, J. Wang, J. Qiu, Y. Wang, Completeness of circle of Willis and white matter hyperintensities in patients with severe internal carotid artery stenosis, Neurol. Sci. 40 (2019) 509–514, https://doi.org/10.1007/s10072-018-3683-9.
[55] O.A. Zaninovich, W.L. Ramey, C.M. Walter, T.M. Dumont, Completion of the circle of Willis varies by gender, age, and indication for computed tomography angiography, World Neurosurg. 106 (2017) 953–963, https://doi.org/10.1016/j.wneu.2017.07.084.
[56] C. Zhou, C. Yuan, R. Li, W. Wang, C. Li, X. Zhao, Association between incomplete circle of Willis and carotid vulnerable atherosclerotic plaques, Arterioscler. Thromb. Vasc. Biol. 38 (2018) 2744–2749, https://doi.org/10.1161/ATVBAHA.118.311797.

Paper III

Appendix A – Fundamentals of MR imaging

MR utilises radio frequency (RF) waves and a strong magnetic field created by a superconductive magnet to create images. MR is therefore non-invasive and harmless for participants without any ferromagnetic implants, and for participants that do not experience discomfort (e.g. claustrophobia) from laying in a narrow space.

Broadly speaking, using a strong stationary magnetic field, RF pulses are used to excite hydrogen protons (predominantly from water in biological imaging), and a subsequent relaxation with release of RF creates signals that can be reconstructed to MR images. The protons of hydrogens are practical targets as they are abundant in biological tissue, and different tissue types have different water density and composition, affecting the proton relaxation rates, and subsequently yielding varying signal strengths for different tissue types.

In order to excite protons with RF pulses, one must use RF waves with the Larmor frequency which is the resonance frequency for a given magnetic field strength. With appropriate RF pulses a transfer of energy from the RF to the proton occur due to resonance. The excited protons will then relax to their ground state mainly via two mechanisms, the spin-lattice relaxation, commonly called T1 relaxation, and the spin-spin relaxation, usually called T2 relaxation. The speed of these two relaxation processes, together with the proton density, mainly determine differences in signal intensity for various tissue types, and lays the foundation for the usefulness of MRI for discerning various tissue types and changes in composition of biological tissue. By changing the imaging parameters, it is also possible to adjust MR images so that the contrast mainly reflects the T1 or T2 relaxation times.

Image formation in MRI is a complicated process, for which a detailed description would be outside the scope of the current thesis. However, in the simple case of 2D imaging, i.e. where one slice is acquired at a time, spatial gradients are used to spatially encode the signals. Here

spatial gradients refer to an additional magnetic field generated by the scanner that can vary along an arbitrary direction within the scanner bore. First the “slice select” gradient allows for selective excitation of a particular image slice. Next, using two additional magnetic gradient fields in succession, the phase encoding gradient and the frequency encoding gradient (orthogonal to each other and to the slice select gradient), it is possible to spatially encode the RF signals. The signal is discretely sampled into a pre-defined image array representing the spatial frequencies of the image slice, which is often called the k-space. A Fourier transform of k-space produces the MR image. As k-space is complex-valued, most MR images are the magnitude of the Fourier transform of k-space, but in some instances, the phase contains useful information such as in imaging of flow.

Appendix B – Supplementary table from Paper I

Table 5. *Overview of rare Circle of Willis variants.*

Variant:	Number (Percentage of total)
Ar	9 (0.5)
AlPl	7 (0.4)
AlPcrPl	5 (0.3)
ArPcr	5 (0.3)
Ar2P	4 (0.2)
ArPr	4 (0.2)
Al	3 (0.2)
AlPcr	3 (0.2)
ArPcrPl	3 (0.2)
AlPcl	2 (0.1)
2AAc2Pc	1 (0.1)
2MAlPcr	1 (0.1)
AcPlB	1 (0.1)
AcPrB	1 (0.1)
AlPclPr	1 (0.1)
AlPr	1 (0.1)
ArAc2Pc	1 (0.1)
Il	1 (0.1)
Il2Pc	1 (0.1)
IlPcr	1 (0.1)
Ir	1 (0.1)
IrAr	1 (0.1)
Ml2Pc	1 (0.1)
MrAr	1 (0.1)

PclPrB	1 (0.1)

Each variant's name is put together by the missing segments with the following notation: 2A = Bilateral anterior cerebral artery, Ac = Anterior communicating artery, 2Pc = Bilateral posterior communicating artery, 2M = Bilateral middle cerebral artery, A = Anterior cerebral artery, Pc = Posterior communicating artery, P = Posterior cerebral artery, B = Basilar artery, 2P = Bilateral posterior cerebral artery, I = Internal carotid artery, M = Middle cerebral artery, while the suffixes "r" and "l" denote right and left lateralization of arteries.

Appendix C – Supplementary table from Paper III

Table 6. *Demographic characteristics divided by the different Circle of Willis variants. Default analysis of variance test (ANOVA) were used on continuous variables, while the default Pearson's Chi-squared goodness of fit test were used on categorical variables.*

	O (N=221)	Ac (N=49)	AcPc (N=107)	Ac2Pc (N=173)	AcPcP (N=38)	Pc (N=364)	2Pc (N=517)	PcP (N=114)	P (N=84)	Total (N=1667)	p value
AGE											< 0.001
Mean (SD)	61.335 (10.701)	61.327 (11.402)	63.542 (10.208)	65.457 (9.882)	65.289 (8.627)	61.676 (10.826)	64.352 (10.315)	64.816 (11.642)	65.714 (10.056)	63.463 (10.607)	
Range	40.000 - 84.000	40.000 - 84.000	40.000 - 84.000	40.000 - 84.000	43.000 - 84.000	40.000 - 84.000	40.000 - 84.000	41.000 - 84.000	44.000 - 84.000	40.000 - 84.000	
SEX											0.082
Female	133 (60.2%)	30 (61.2%)	57 (53.3%)	101 (58.4%)	20 (52.6%)	200 (54.9%)	251 (48.5%)	54 (47.4%)	46 (54.8%)	892 (53.5%)	
Male	88 (39.8%)	19 (38.8%)	50 (46.7%)	72 (41.6%)	18 (47.4%)	164 (45.1%)	266 (51.5%)	60 (52.6%)	38 (45.2%)	775 (46.5%)	
BMI											0.188
N-Miss	0	0	0	0	0	0	1	0	0	1	
Mean (SD)	26.591 (4.261)	26.796 (4.282)	27.158 (4.069)	27.252 (3.998)	26.571 (4.382)	27.301 (4.240)	27.369 (4.190)	26.588 (4.150)	26.409 (4.410)	27.088 (4.203)	
Range	16.577 - 42.305	18.229 - 41.500	20.336 - 40.805	17.829 - 40.266	17.767 - 38.269	14.846 - 43.290	13.898 - 43.999	17.020 - 37.753	18.210 - 45.901	13.898 - 45.901	
CHOL. HDL											0.128
N-Miss	1	0	0	2	0	0	1	1	1	6	
Mean (SD)	3.527 (1.319)	3.760 (1.743)	3.735 (1.289)	3.818 (1.959)	3.806 (1.476)	3.641 (1.187)	3.723 (1.295)	3.494 (1.166)	3.352 (1.067)	3.659 (1.362)	
Range	1.393 - 8.372	2.077 - 14.000	1.850 - 7.778	1.686 - 23.000	1.548 - 8.125	1.783 - 10.111	1.364 - 8.721	1.278 - 7.250	1.794 - 6.900	1.278 - 23.000	
SBP											0.021
N-Miss	3	0	1	0	0	1	1	0	0	6	
Mean (SD)	128.952 (19.489)	131.122 (18.146)	133.995 (22.967)	134.009 (21.221)	134.263 (24.427)	132.482 (20.539)	134.869 (19.993)	137.022 (21.437)	133.577 (20.215)	133.384 (20.611)	
Range	88.500 - 187.000	88.000 - 175.500	89.500 - 208.500	82.000 - 186.000	87.500 - 193.500	78.000 - 198.500	81.500 - 206.000	91.000 - 220.000	96.500 - 213.500	78.000 - 220.000	
DBP											0.390
N-Miss	3	0	1	0	0	1	1	0	0	6	
Mean (SD)	74.002 (9.463)	72.490 (8.952)	74.849 (10.170)	75.168 (10.186)	75.395 (11.302)	75.610 (10.211)	75.236 (9.781)	75.952 (9.029)	74.494 (9.567)	75.058 (9.859)	
Range	51.000 - 103.000	50.500 - 89.000	50.500 - 103.000	53.000 - 104.500	57.000 - 104.500	49.500 - 109.000	44.500 - 112.000	44.000 - 99.000	54.500 - 99.000	44.000 - 112.000	
HYPERTENSION											0.024
N-Miss	3	0	1	0	0	1	1	0	0	6	
No	161 (73.9%)	34 (69.4%)	68 (64.2%)	102 (59.0%)	22 (57.9%)	217 (59.8%)	319 (61.8%)	64 (56.1%)	51 (60.7%)	1038 (62.5%)	
Yes	57 (26.1%)	15 (30.6%)	38 (35.8%)	71 (41.0%)	16 (42.1%)	146 (40.2%)	197 (38.2%)	50 (43.9%)	33 (39.3%)	623 (37.5%)	
SMOKE											0.293
N-Miss	2	1	1	2	0	3	5	3	2	19	
No	193 (88.1%)	40 (83.3%)	88 (83.0%)	147 (86.0%)	31 (81.6%)	319 (88.4%)	441 (86.1%)	104 (93.7%)	74 (90.2%)	1437 (87.2%)	
Yes	26 (11.9%)	8 (16.7%)	18 (17.0%)	24 (14.0%)	7 (18.4%)	42 (11.6%)	71 (13.9%)	7 (6.3%)	8 (9.8%)	211 (12.8%)	
	O (N=221)	**Ac (N=49)**	**AcPc (N=107)**	**Ac2Pc (N=173)**	**AcPcP (N=38)**	**Pc (N=364)**	**2Pc (N=517)**	**PcP (N=114)**	**P (N=84)**	**Total (N=1667)**	**p value**

Abbreviations: BMI = body mass index, CHOL. HDL = cholesterol to high density lipoprotein ratio, SD = standard deviation, SBP = systolic blood pressure, DBP = diastolic blood pressure. Circle of Willis variant component abbreviations: O = complete variant, Ac = anterior communicating artery, Pc = posterior communicating artery, P = posterior cerebral artery, "2" = prefix that signifies that both segments of the label prefixed are missing.